Master's thesis

NTNU
Norwegian University of Science and Technology
Faculty of Natural Sciences
Department of Physics

Anne Louise Kristoffersen

Magnon Condensation in Magnetic Insulators

Master's thesis in Applied Physics and Mathematics
Supervisor: Alireza Qaiumzadeh
June 2023

NTNU
Norwegian University of
Science and Technology

QuSpin

Anne Louise Kristoffersen

Magnon Condensation in Magnetic Insulators

Master's thesis in Applied Physics and Mathematics
Supervisor: Alireza Qaiumzadeh
June 2023

Norwegian University of Science and Technology
Faculty of Natural Sciences
Department of Physics

NTNU
Norwegian University of
Science and Technology

Abstract

Bose-Einstein condensation as a theoretical concept was suggested a century ago, but is a relatively new research field experimentally. It gained attention after Ketterle *et al.* and Cornell *et al.* realised the first condensates in 1995. The condensates were formed of weakly interacting, real atomic gases. Magnons, which are quasiparticle bosonic excitations of a magnetically ordered system, were proposed by Felix Bloch in 1936. In 2006 Demokritov *et al.* found evidence of Bose-Einstein condensation of magnons at room temperature for the first time.

To explain the physics leading to a magnon condensate in *ferromagnetic* insulators, the dipolar interaction between the spins is essential, although it is weak. To realise a BEC, there needs to be a repulsive effective interaction between the magnons, which the direct exchange interaction and Zeeman coupling are unable to provide on their own. Part II of this work will revisit the calculations leading to the prediction of Bose-Einstein condensation of magnons in yttrium-iron garnet. To obtain this complete analysis of the stability, we have closely followed the work done by Kopietz, Li and Demokritov. We find a term in the interaction potential that was missing in the literature.

Conclusive evidence of Bose-Einstein condensation of magnons in *antiferromagnetic* insulators has not yet been found. We perform similar calculations as for the ferromagnetic system, to predict the theoretical existence of such condensates. We found that there are combinations of parameters for the system that facilitates condensation of magnons in antiferromagnetic insulators at non-zero momenta. When the interactions between the magnons in the condensates are repulsive, we found that the intervalley scattering, namely between the two types of magnons, dominates the interaction potential. We believe that our analysis can be of use for determining parameters in future experiments, where the goal is to observe condensation of magnons.

Sammendrag

Bose-Einstein kondensasjon er et forskningsfelt som har fått økt oppmerksomhet etter at Ketterle *et al.* og Cornell *et al.*, i 1995, fremstilte et kondensat for første gang. Begge gruppene laget kondensatet av reelle materialpartikler, nærmere bestemt svakt vekselvirkende atomgasser. Magnoner er bosoniske eksitasjoner av et magnetisk ordnet system. De ble foreslått for første gang av Felix Bloch i 1936. I 2006 fremstilte Demokritov *et al.* de første kondensatene av magnoner ved romtemperatur .

Magnetisk dipolvekselvirkning er svært viktig ved fremstilling av et kondensat av magnoner, selv om den er svak. For å kunne ha et stabilt kondensat, må potenisalet mellom bestanddelene være frastøtende. Den sterkere Heisenberg vekselvirkningen og Zeemankoblingen vil ikke gi potenisalet de nødvendige egenskapene. Spesialiseringsprosjektet analyserer stabliteten til et kondensat av magnoner i ferromagnetiske isolatorer, spesifikt for en tynn film av yttrium-jern granat. Vi har fulgt arbeidet til Kopietz , Li og Demokritov i denne fullstendige analysen av stabiliteten. Vi fant et ledd i vekselvirkningspotensialet som ikke var beskrevet i litteraturen.

Endelige bevis for Bose-Einstein kondensasjon av magnoner i antiferromagnetiske isolatorer er ennå ikke funnet. Vi utfører analyser for et antiferromagnetisk system, analogt med analysene som allerede er utført for ferromagnetiske systemer. Vi har funnet kombinasjoner av parametere for systemet som underbygger teorien om at det er mulig for magnoner, med impuls forskjellig fra null, å kondensere i antiferromagnetiske isolatorer. Vi fant også at med disse parameterne vil mellomdals-spredning, altså spredning mellom de to typene antiferromagnetiske magnoner, dominere vekselvirkningspotensialet. Vi tror dette kan være nyttig for å bestemme parametere for eksperimenter i antiferromagnetiske systemer, hvor man ønsker å finne kondensasjon av magnoner.

Preface

This master's thesis is written is the last semester of the five-year programme Master of Science in Applied Physics and Mathematics at the Norwegian University of Science and Technology (NTNU), during the spring of 2023. This work is a continuation of the specialisation project carried out in the autumn of 2022.

Firstly, I want to thank my supervisor Alireza Qaiumzadeh for giving me this truly exciting project, and for excellent guidance throughout the last year. I also want to thank Therese Frostad for insightful discussions. Furthermore, I want to thank QuSpin for providing such a great and inspiring work environment. A special thanks to the other master's student in the study hall for the incredible social environment, and helpful academic conversations.

Additionally, I want to thank my family, friends and Morten for being so patient and supportive through my years at NTNU. Especially, I want to thank my father for his dedication to helping me, and reading through this thesis multiple times.

Anne Louise Kristoffersen

Anne Louise Kristoffersen
Trondheim, Norway
June, 2023

Disclaimer

This work consists of three parts. Part I consists of work done mainly in the autumn of 2022, but with some modifications done in the spring of 2023. Particularly, section 2.5 has been significantly extended.

Part II is the work done in autumn of 2022, in TFY4510 Physics Specialisation Project, which is credited 15 ECTS. Although it has already been graded, it is profoundly relevant for the master's thesis. We will frequently refer to the work done in the specialisation project.

The remaining, and most important, sections of the master's thesis, TFY4900 - Physics Master's Thesis, which is credited 30 ECTS, are found in Part III. The parts that have already been graded are marked with a star, "*".

Table of Contents

List of Figures

Conventions and Abbreviations

To increase readability, we specify the conventions that are used throughout the thesis,

x	Scalar
$\mathbf{x}$	Vector of scalars
$\hat{\mathbf{x}}$	Unit vector, $\hat{\mathbf{x}} = \mathbf{x}/\lvert\mathbf{x}\rvert$
x	Single operator
$\vec{x}$	Vector of operators
X	Matrix.

The difference in scalar and single operator will be clear from the context. Specific symbols will be introduced throughout the text.

The notation $\{a, b\}^n$ denotes a product of any combination of a and b, n times.

In Part II, we will mainly be working in three spatial dimensions (or quasi 2D). In Part III, we will consider a spin chain model in one dimension.

Throughout Part III, we will mainly use i for sublattice A, and j for sublattice B. However, for interactions between different lattice sites, we will use i for the lattice point, and j for the nearest neighbours.

Commonly used abbreviations are

BEC	Bose-Einstein condensation/condensate
FMI	ferromagnetic insulator
AFMI	antiferromagnetic insulator
DMI	Dzyaloshinskii-Moriya interaction
YIG	yttrium-iron garnet
BLS	Brillouin light scattering
1BZ	First Brillouin zone.

Part I

Preliminaries

Chapter 1

Introduction

1.1 Background on the field*

In three dimensions, all particles can be classified as either bosons or fermions. Fermions cannot have all their quantum numbers identical, such as energy level, while their wavefunctions overlap. Bosons, on the other hand, can [1]. Bose-Einstein condensate (BEC) is a new state of matter for bosonic particles [2]. This state is obtained when the spatial extension of the wave functions for these particles becomes large. For a gas of real particles this happens when the gas is cooled to very low temperatures. The single particle wavefunctions will then overlap, and the particles in the condensate can be described with one macroscopic wave function [3].

This state of matter was first proposed by Bose and Einstein. Bose treated light as indistinguishable particles and obtained the same results as Planck for the radiated energy density of a black body, without mixing classical and quantum mechanics. He sent his work to Einstein, who was impressed and published it in *Zeitschrift für Physik* in 1924, on Bose's behalf [4]. In 1925 he published an article based on Bose's work, proposing the new state of matter for atoms, Bose-Einstein condensate [5, 6].

After around 70 years, in 1995, two different groups managed to create and observe a BEC experimentally for the first time. One with Eric Cornell at the University of Colorado at Boulder [7, 8], and the other with Wolfgang Ketterle at MIT [3, 9]. Cornell and his group created a condensate of rubidium atoms, while Ketterle and his group used sodium atoms. They were awarded the Nobel Prize in Physics for their work in 2001. The main reason for the long time between the founding of the theory, and the experimental proof was the difficulties of cooling the gas sufficiently [3].

More than 90 years ago, in 1930, Felix Bloch introduced the idea of a spin wave [10]. Intuitively, one might think that a single spin-flip would be the lowest excited energy eigenstate of a ferromagnetically ordered system. However, this is not correct. A magnon, which is a quantised spin wave, is the lowest excitation [11]. The spins at all lattice sites deviate from the quantisation axis in a way such that the deviations total to a spin flip [12, 13].

After the discovery of particle BEC, there have been numerous discoveries of quasi-particle BEC. Some examples are BEC of photons [14], excitons [15, 16] and exciton-polaritons [17]. In 2006 Demokritov *et al.* published an article with experimental results that proved the existence of a BEC of magnons at room temperature [18]. The dispersion relation for a BEC of magnons in some ferromagnetic insulator (FMI) has two minima and thus two condensates, an example being yttrium-iron garnet (YIG). Six years after the discovery of the condensate, in 2012, Demokritov and his group also proved the coherence of the condensates [19].

Recent publications present a promising application of magnon BEC, namely qubits for use in quantum computers. Superconducting qubits, made of Cooper-pairs, have been of great interest. However, they have shown weakness due to decoherence effects caused by Coulomb interactions. Magnons, which are electrically neutral, could therefore be a promising candidate for stable qubits [20, 21].

1.2 Purpose of thesis

An important requirement for the existence of a Bose-Einstein condensate is the presence of a repulsive interaction between the constituents of the condensate [22, 2]. This ensures the stability of the condensate. The purpose of Part II, the specialisation project report, was to rederive a full analysis of the stability of a BEC of magnons in a FMI, specifically YIG.

In the master's thesis, mainly Part III, the goal is to investigate how the stability of BEC of magnons in an antiferromagnetic insulator (AFMI) depend on the various interactions in the system.

1.3 Structure of thesis

The structure of the thesis is as follows. In Chapter 2 we introduce various interactions that are relevant to magnetic spin systems. We present a more detailed explanation of the new state of matter, known as the Bose-Einstein condensate, in Chapter 3. In Chapter 4, the first chapter of Part II, we perform a Holstein-Primakoff transformation for the interactions in a ferromagnetic thin film insulator with a cubic lattice. A physical realisation of such a system is YIG. Next, we carry out a Bogoliubov transformation to diagonalise the non-interacting Hamiltonian. In Chapter 5 we perform the majority of the stability analysis. The dipolar interaction is crucial to the stability of the condensate, which we show in Chapter 6. In Chapter 7 we conclude the ferromagnetic part.

In Chapter 8, the first of Part III, we present some relevant background on antiferromagnetic systems. In general, we will not repeat theory from Part II, but some topics will be elaborated on. Concerning the criteria for condensate formation, we also refer to Part II, but emphasise that the crucial property that must be satisfied is a repulsive effective interaction between the magnons. In Chapter 9 we perform similar steps as in Chapter 4. The results, are found in Chapter 10. The discussion of the antiferromagnetic part is found in Chapter 11. A summary of Part III and the main work of the master's thesis, is found in Chapter 12. Further work is proposed in Chapter 13.

In Appendix A we elaborately show that there is a term missing in the energy function for the magnon condensate in YIG, in the literature such as in Demokritovs work in [23]. In Appendix B we have included additional figures for the discussion.

Chapter 2

Spintronics

In this section we will introduce the idea of spin and explain how it connects to magnetisation. Then we will introduce the various interactions that take place in a magnetic system. All interactions are introduced with their Hamiltonian, which is the relevant description for this thesis. We assume a system at half-filling, which means that there is one electron at each lattice site on average.

2.1 Spin and magnetisation*

Spin, $\mathbf{S}$, is a form of angular momentum. It has a physical appearance similar to a particle spinning about its centre of mass, but unlike orbital angular momentum, $\mathbf{L}$, this angular momentum actually has nothing to do with spinning motion in space. Spin is an intrinsic form of angular momentum [1]. From the Dirac equation, which is a relativistic wave equation, it can be shown that $\mathbf{L}$ is not a conserved quantity. However, if the particles are allowed to carry an appropriate intrinsic angular momentum, $\mathbf{S}$, then the total angular momentum $\mathbf{J} = \mathbf{L} + \mathbf{S}$ will be a conserved quantity [24].

If a classical, charged particle is actually spinning, it creates a magnetic dipole with an associated magnetic dipole moment, $\mathbf{m}$. A quantum particle with spin also has a magnetic dipole moment. For electrons, this takes the form $\mathbf{m} \approx \gamma_e \mathbf{S}$, where γ_e is the gyromagnetic ratio for the electron. Generally, the operator is $\vec{m} = \gamma_S \vec{S} + \gamma_L \vec{L}$ [25]. But because the orbital angular momentum generally is quenched by the crystal field, the operator is approximated by $\vec{m} \approx \gamma_e \vec{S}$ [12]. In this thesis, we will assume that the length of magnetic moments is constant, $|\mathbf{m}| = 1$.

Different materials will have different types of total magnetisation. They can be divided into five categories: diamagnetic, paramagnetic, ferrimagnetic, ferromagnetic and antiferromagnetic [13]. In the last three types, the spins are ordered. In this thesis, we will first look at ferromagnetic systems, and then focus on antiferromag-

netic systems. Ferromagnetic materials have a non-zero net magnetisation as most spins orient themselves along the same axis, even in the absence of an external magnetic field. Antiferromagnetic materials will usually have no net magnetisation, as neighbouring spins cancel each other (in square and cubic lattices). A ferromagnetic system in a cubic lattice is illustrated in Figure 2.1(a), and an antiferromagnetic system in Figure 2.1(b).

When the temperature of a (anti)ferromagnetic material is above the critical tem-

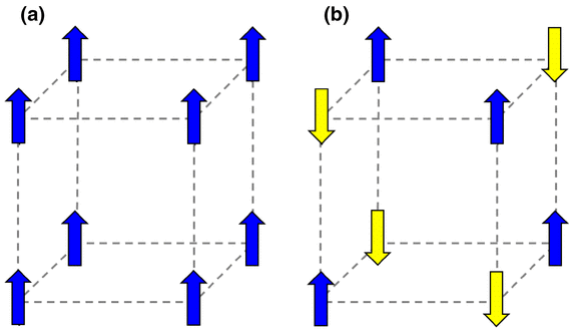

Figure 2.1: (a) Ferromagnetic spin ordering, (b) antiferromagnetic spin ordering. The figure is from [26].

perature, the thermal energy is stronger than the coupling between the spins. When this occurs, the spin orientations are randomised. This is the paramagnetic phase. As the materials are cooled down, and the material is cooled below the critical temperature , the spins start to order. This is a phase transition, with the order parameter being the magnetisation for ferromagnetic systems and staggered magnetisation, also known as Nèel-vector, for antiferromagnetic systems and the control parameter being the temperature. This is of second order, which means that it is a continuous transition [27].

This phase transition is illustrated in Figure 2.2(a) for ferromagnetic and Figure 2.2(b) for antiferromagnetic systems. The magnetisation as a function of temperature is denoted by $m(T)$, and $n(T)$ is the staggered magnetisation as a function of temperature. The saturation (staggered) magnetisation is m_S (n_S), which is reached at zero temperature. When the (staggered) magnetisation is saturated, all the dipoles have aligned as energetically preferred. Then it is not possible to further increase the (staggered) magnetisation.

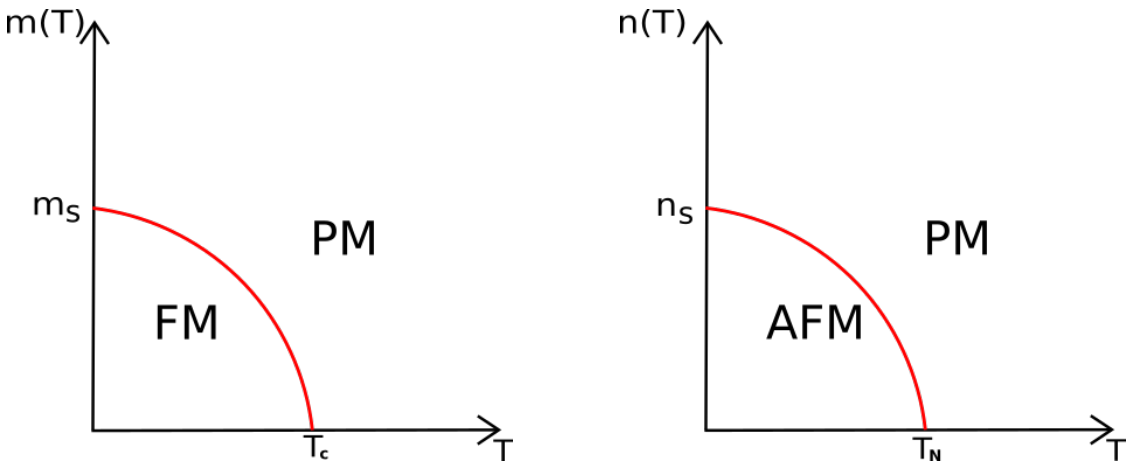

(a) (b)

Figure 2.2: (a) Phase transition from paramagnetic to ferromagnetic phase. (b) Phase transition from paramagnetic to antiferromagnetic phase.

2.2 Direct exchange interaction*

As the systems temperature decreases to below the critical temperature, the direct exchange interaction will be the most important one. The system will not have enough thermal energy for the spins to break the preferred ordering. The critical temperature is the Curie-temperature, T_C, for ferromagnetic systems and Nèel-temperature, T_N, for antiferromagnetic systems [27]. Although this is the strongest interaction, it is short-ranged. To a good approximation, the spins interact only with their nearest neighbours. This is the Heisenberg model [13].

In ferromagnetic ordered systems, the direct exchange interaction originates from the Coulomb force. For antiferromagnetic ordered systems this interaction comes from the kinetic energy of electrons, and their tendency to hop [12, 28].

This Hamiltonian can be expanded to cover the interaction between spins at all lattice sites i, and all nearest neighbours at lattice sites j

$$H_{\text{ex}} = -J \sum_{\langle i,j \rangle} \vec{S}_i \cdot \vec{S}_j. \tag{2.1}$$

Note that since i and j are nearest neighbours, denoted by $\langle i, j \rangle$, this sum excludes $i = j$. Minimising the energy corresponding to this Hamiltonian, leads to the different ordering of ferromagnetic and antiferromagnetic systems. To minimise for a positive J, the spins will be parallel, which is the defining trait of ferromagnetism. To minimise for a negative J, the spins will be antiparallel, hence giving antiferromagnetism.

2.3 Dipolar interaction*

A magnetic dipole has a magnetic field. The dipolar interaction describes how one magnetic dipole is affected by the magnetic field from another. The magnetic field from one magnetic dipole $\mathbf{m}$ is $\mathbf{B}_{\text{dip}} = 1/4\pi[3\mathbf{r}(\mathbf{m}\cdot\mathbf{r})/r^5 - \mathbf{m}/r^3]$, where $\mathbf{r}$ is the distance from the dipole. The energy stored in the interaction between the two magnetic moments is $U_{\text{dip}} = -\mathbf{m}\cdot\mathbf{B}_{\text{dip}}$ [29].

This gives an energy between two magnetic dipoles, $\mathbf{m}_1$, $\mathbf{m}_2$, of

$$U_{\text{dip}} = \frac{1}{r^3}[\mathbf{m}_1\cdot\mathbf{m}_2 - 3(\mathbf{m}_1\cdot\hat{\mathbf{r}})(\mathbf{m}_2\cdot\hat{\mathbf{r}})]. \tag{2.2}$$

The Hamiltonian describing the dipolar interaction between N spins is

$$H_{\text{dip}} = -\frac{1}{2}\sum_{ij}\sum_{\alpha\beta} D_{ij}^{\alpha\beta} S_i^\alpha S_j^\beta, \tag{2.3}$$

where i and j are lattice sites and $i \neq j$ [30]. Here, $\alpha, \beta = \{x, y, z\}$. The dipolar tensor is denoted by D. It contains the interaction strength, and its elements are defined as

$$D_{ij}^{\alpha\beta} = (1-\delta_{ij})\frac{\mu^2}{|\mathbf{R}_{ij}|}\left[3\hat{R}_{ij}^\alpha \hat{R}_{ij}^\beta - \delta^{\alpha\beta}\right], \tag{2.4}$$

with μ being the magnetic moment associated with the spin, and $\mathbf{R}_{ij} = \mathbf{r}_i - \mathbf{r}_j$ is the vector from lattice site i to j [31]. The length of the unit vector $\hat{\mathbf{R}}$ in the α-direction is denoted by $\hat{R}_i^\alpha$.

Note that there is no restriction on i and j. This is a long-ranged interaction, meaning that one spin couples to all other spins in the lattice. Inserting approximate values, we can see that it will also be weak compared to the direct exchange for small spatial separations [32].

As we will see later, this is an important contribution in ferromagnetic insulators. When an antiferromagnetic insulator has a square bipartite lattice, it will have vanishing magnetic dipolar interaction. Therefore, this interaction mainly manifests in ferromagnetic systems.

2.4 Magnetic anisotropy*

There is a variety of types of magnetic anisotropy effects, however we will look at the *magneto-crystalline anisotropy*. This effect originates from the coupling between the relativistic spin-orbit coupling and the electric charge density [27].

The geometry of the system thus plays a role in the spin-configuration. The direct exchange interaction imposes a preferred parallel or antiparallel spin alignment,

however all quantisation axes are equivalent. Anisotropy will provide the system with a preferred quantisation axis.

A good approximation to crystalline anisotropy is the single-ion anisotropy. In most materials it is the most important anisotropy mechanism [27].

The Hamiltonian for this type of anisotropy is

$$\begin{aligned} H_{\text{ani}} &= -K_{\text{easy}}(\vec{S}_i \cdot \hat{\mathbf{e}}_{\text{easy}})^2 + K_{\text{hard}}(\vec{S}_i \cdot \hat{\mathbf{e}}_{\text{hard}})^2 \\ &= \pm|K_{\text{ani}}| \sum_i (\vec{S}_i \cdot \hat{\mathbf{e}})^2, \end{aligned} \tag{2.5}$$

where $K_{\text{easy}} \geq 0$ and $K_{\text{hard}} \geq 0$ are the anisotropy strengths for the easy and hard axes, respectively [33]. Correspondingly, $\hat{\mathbf{e}}_{\text{easy/hard}}$ is the direction of the easy/hard axis. Aligning along the easy axis will minimise the energy.

Also note that in Eq. (2.5), the sum over i is over the total lattice, meaning both sublattices. In this thesis, our material does not have a hard axis, so we will use a single-ion anisotropy with an easy axis.

2.5 Zeeman coupling

When an external magnetic field, $\mathbf{h}$, is applied to a magnetic system, the spins in the system couple to the field. This is called the Zeeman coupling. If the system has degenerate energy levels, applying $\mathbf{h}$ to the system will split the levels. We will see this effect in section 10.2.
The coupling only involves interaction between the magnetic field and individual spins. There is no interaction between spins at different lattice sites.

We choose to orient the magnetic field along the $\hat{\mathbf{z}}$-direction, $\mathbf{h} = h\hat{\mathbf{z}}$. This gives us a simple expression for the Hamiltonian

$$\begin{aligned} H_{\text{Zee}} &= -\mu \sum_i \mathbf{h} \cdot \vec{S}_i \\ &= -\mu \sum_i h S_i^z. \end{aligned} \tag{2.6}$$

Note that in both the ferromagnetic and antiferromagnetic case, the sum over i runs over the total lattice. This means that both sublattices in the AFMI are indexed by i.

The antiparallel ordering of our antiferromagnetic system analysed in Part III, is caused by the direct exchange interaction between the nearest neighbouring spins. However, if we impose magnetic anisotropy, and an external magnetic field that is stronger than the critical field, $\mathbf{h}_{\text{c}} = h_{\text{c}}\hat{\mathbf{z}}$, the antiparallel ordering starts to break down. This is known as the spin-flop transition, where the Zeeman coupling, rather

than the direct exchange interaction, dominates the energy minimisation [34, 35]. The spins antiparallel to the $\hat{\mathbf{z}}$-axis start to rotate towards the positive $\hat{\mathbf{z}}$-axis.

Although we have not yet presented the dispersion relations, we will briefly describe how the critical field, $\mathbf{h}_\mathrm{c}$, is found. By inspecting Eq. (10.20), we have at $k = 0$

$$\omega_H^\mathrm{c} = \mu h_\mathrm{c} \geq \sqrt{(\omega_E + \omega_A)^2 - \omega_E^2} \approx \sqrt{2\omega_E\omega_A}, \tag{2.7}$$

where $\omega_E = 2JS$ and $\omega_A = K_z S$, gives dispersion relations with negative energy. To obtain the form of $\mathbf{h}_\mathrm{c}$ in Eq. (2.7) we utilised the fact that the magnetic anisotropy is much smaller than the direct exchange interaction.

2.6 Dzyaloshinskii–Moriya interaction*

When the spin-orbit coupling is treated perturbatively, the Dzyaloshinskii–Moriya interaction (DMI) emerges from the expansion [27, 36]. It is an antisymmetric exchange interaction. DMI competes with the much stronger direct exchange interaction [37]. To exist, there needs to be a local environment with absence of inversion symmetry [27].

DMI is heavily affected by the crystal lattice, and the symmetry determines whether it is a nearest neighbour or a next nearest neighbour exchange interaction. We will therefore present the Hamiltonian for a general lattice.

The Hamiltonian for the DMI between spins $\vec{S}_i$, $\vec{S}_j$ is

$$H_\mathrm{DMI} = \sum_{i,j} \mathbf{D}_{ij} \cdot (\vec{S}_i \times \vec{S}_j), \tag{2.8}$$

where $\mathbf{D}_{ij} = -\mathbf{D}_{ji}$ is the DM-vector, and i and j being lattice sites. The sum excludes $i = j$. The DM-vector, which will be specified for each system, defines the type of interaction. To minimise the energy from this interaction, the spins will be tilted towards the direction of $\mathbf{D}_{ij}$. Note that this $\mathbf{D}$ is not the same as in Eq. (2.4).

The cross product in (2.8) competes with the dot product in (2.1). To obtain the lowest energy possible caused by DMI, spins $\vec{S}_i$, $\vec{S}_j$ would have to be orthogonal. The direct exchange interaction is stronger than DMI, and will therefore be more energetically important. Although it is weak, DMI will sometimes give a small, finite magnetisation in antiferromagnets, and a small but finite Néel-vector in ferromagnets. In a typical magnetic material, DMI usually tilts the spin of the order of 1°[12]. This interaction is fundamental for the creation of skyrmions, which originates from the magnetic frustration caused by the competition between DMI and direct exchange interaction [38].

Chapter 3

Bose-Einstein Condensation of Particles and Quasiparticles*

The bosons involved in this condensate occupy the quantum-mechanical ground state. To achieve this condensation for real particles, a gas must be cooled very close to $T = 0$ K, while keeping the particle density, n, small [39]. As the gas is cooled to such low temperatures, the individual particle wave functions begin to overlap, and the system collapses to one single quantum state, that can be described with one collective wave function. The condensate can be modelled both as interacting and non-interacting.

To estimate the critical temperature T_C, at which the wavefunctions begin to overlap, we can set the average interparticle spacing $1/n^{1/3}$, equal to the thermal de Broglie wavelength. We then find that T_C is proportional to $n^{2/3}/m$.

Bogoliubov founded a theory, which considers perturbations from the non-interacting systems. The theory predicts a finite pressure of the particles at zero temperature. From thermodynamics, we have the requirement that the partial derivative of density with respect to pressure, $\partial n/\partial P$, is positive [40, 41]. As a consequence of this, Bogoliubovs theory finds that the interaction amplitude needs to be positive. Thus, to have a stable condensate, we need a repulsive interaction between the particles. This is an important result when we try to prove the existence of magnon BEC theoretically.

The experimental results of Demokritov *et al.* [42], which proved the existence of a BEC of magnons, was done in yttrium-iron garnet, YIG. This is a much-investigated material in this field. A great advantage of YIG, is that the Gilbert damping. Another crucial advantage is that magnons in YIG have a long lifetime, τ_{life} [39].

By long lifetime we mean long relative to the thermalisation time, τ_{th}. The thermalisation time is the time needed for the magnons to distribute their energy and fall into the lowest energy level - thus forming the condensate. Therefore, it is important that $\tau_{\text{life}} \gg \tau_{\text{th}}$. The magnon-phonon coupling does not conserve the number of magnons, which is why the magnons have a limited lifetime. In YIG $\tau_{\text{th}} \approx 100$ ns and $\tau_{\text{life}} \approx 1$ ms [23]. This means that a magnon BEC is not truly in equilibrium, but rather in a state of quasi-equilibrium. However, as long as $\tau_{\text{life}} \gg \tau_{\text{th}}$ this is not a problem [23].

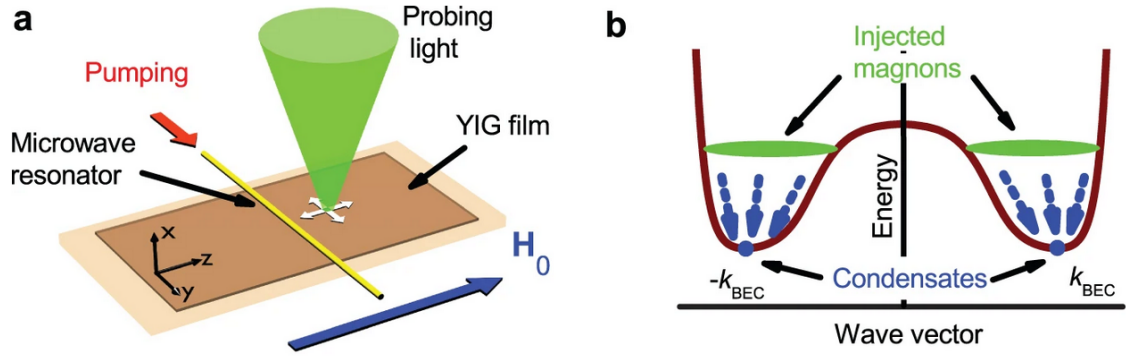

Figure 3.1: (a) The setup in Demokritov *et al.*'s experiment that showed the existence of magnon BEC. (b) Shows the magnon dispersion relation as a function of k_z. The illustration also shows how the magnons thermalise into the wave vectors $\pm k_{\text{BEC}}$, in which the energy function has its minima. H_0 is the applied external magnetic field. The figure is from [43].

Contrary to atomic BECs, which exist at temperatures of the order of nanokelvins [3], magnon BECs can be found at room temperature. We argued above that T_C is proportional to $n^{2/3}/m$. For an atomic gas, the density cannot be too high, as that would cause the system to condense to a liquid or solid state. This problem does not apply to magnons. Furthermore, the mass of magnons is significantly lower than for real particles. It is the combination of a higher density and a lower mass that allows a magnon BEC to exist at much higher temperatures than an atomic BEC.

To observe the condensate, Demokritov and others use Brillouin Light Scattering (BLS) to image it [18, 44]. BLS outputs an intensity, which is proportional to the number of magnons. Their procedure of creating a magnon BEC also requires an in-plane magnetic field and microwave radiation [23]. Microwave radiation is used for parametric pumping of magnons into the system. We base our analysis on these magnons.

Parametric pumping is one of several techniques used to create magnons. The chemical potential of magnons under normal circumstances is zero. For a BEC to be realisable, there is a certain critical value for the chemical potential [18]. Therefore, there is a need to alter the chemical potential from zero, to its critical value. This can be done by e.g. parametric pumping [18, 45].

Figure 3.1 is from Demokritov *et al.*'s set-up in 2006 [43]. Figure 3.1a) shows the experimental set-up. Magnons are pumped into the film by the microwave resonator. The probing light is used to image the BEC. Figure 3.1b) shows the magnon dispersion relation for k_z, $\theta = 0$. It also shows the process of thermalisation of the magnons. They are injected at a certain momentum, $\boldsymbol{k} > \boldsymbol{k}_{\mathrm{BEC}}$ and end up in $\pm\boldsymbol{k}_{\mathrm{BEC}}$.

Part II

Ferromagnetic System

Chapter 4

Bosonisation of Ferromagnetic System*

So far, all the Hamiltonians have been presented with spin operators. These operators follow a commutation relation of $[S_i^\alpha, S_j^\beta] = i\varepsilon_{\alpha\beta\gamma} S_i^\gamma \delta_{ij}$, where α, β is x, y, z, i and j denote lattice sites and $\varepsilon_{\alpha\beta\gamma}$ is the Levi-Civita tensor. This commutation relation makes the forthcoming computations complicated. We will perform a Holstein-Primakoff transformation to obtain a Hamiltonian expressed in bosonic operators $a_i^\dagger, a_i$, that instead follow the simple commutation relation $[a_i, a_j^\dagger] = \delta_{ij}$. This procedure is known as a bosonisation of the Hamiltonian.

The first step is to introduce two new operators, S^+, S^-, the spin raising and lowering operators, respectively. These are defined as

$$\begin{aligned} S_i^z &= S - a_i^\dagger a_i \\ S_i^+ &= S_i^x + iS_i^y \\ S_i^- &= (S_i^+)^\dagger = S_i^x - iS_i^y, \end{aligned} \tag{4.1}$$

where S is the total spin.

From these we see that we can express S_i^x, S_i^y as

$$\begin{aligned} S_i^x &= \frac{1}{2}(S_i^+ + S_i^-) \\ S_i^y &= \frac{1}{2i}(S_i^+ - S_i^-). \end{aligned} \tag{4.2}$$

We assume that our system exhibits a large degree of order, and that it is quantised along the z-axis. By assuming that the spins only deviate a small amount from the quantisation axis, we can introduce the Holstein-Primakoff transformation. The

transformation is defined as

$$\begin{aligned} S_i^z &= S - a_i^\dagger a_i \\ S_i^+ &= \sqrt{2S}\sqrt{1 - \frac{a_i^\dagger a_i}{2S}}\, a_i \\ S_i^- &= \sqrt{2S}\, a_i^\dagger \sqrt{1 - \frac{a_i^\dagger a_i}{2S}}. \end{aligned} \tag{4.3}$$

If we now can assume that S is large, $S \gg \langle a_i^\dagger a_i \rangle$, we can utilise the approximation $\sqrt{1-x} \approx 1 - x/2$. In YIG, $S \approx 14.2$, which means this approximation is valid [31]. By also including S_i^z from Eq. (4.1), we obtain the full expression for the transformation we will be using

$$\begin{aligned} S_i^z &= S - a_i^\dagger a_i \\ S_i^+ &\approx \sqrt{2S}\,(1 - \frac{1}{4S} a_i^\dagger a_i)\, a_i \\ S_i^- &\approx \sqrt{2S}\, a_i^\dagger\, (1 - \frac{1}{4S} a_i^\dagger a_i). \end{aligned} \tag{4.4}$$

4.1 Direct exchange interaction

We now want to rewrite the direct exchange interaction Hamiltonian in our new basis, Eq. (4.4). Before substituting the transformation operators, we expand the dot product in Eq. (2.1). We then insert the operators in Eq. (4.2), which gives the resulting bosonised Hamiltonian

$$H_{\text{ex}}^s = -\frac{J}{2} \sum_{\langle i,j \rangle} \big[S_i^z S_j^z + \frac{1}{2} \big(S_i^+ S_j^- + S_i^- S_j^+ \big) \big].$$

After inserting the transformation in Eq. (4.4), the resulting Hamiltonian is

$$\begin{aligned} H_{ex}^b = &-JNzS^2/2 - SJ/2 \sum_{\langle i,j \rangle} \big[-a_i^\dagger a_i - a_j^\dagger a_j + a_i a_j^\dagger + a_i^\dagger a_j \big] \\ &-J/2 \sum_{\langle i,j \rangle} \big[a_i^\dagger a_i a_j^\dagger a_j - \frac{1}{2} a_i a_j^\dagger a_j^\dagger a_j - \frac{1}{2} a_i^\dagger a_i a_i a_j^\dagger \big], \end{aligned} \tag{4.5}$$

where z is the number of nearest neighbours.

The first term in the first line in Eq. (4.5) is just a constant, which we can absorb in a reference energy. The sum in the first line is the non-interacting Hamiltonian, $H_{\text{ex}}^{b,2}$. It is called non-interacting as it is $\mathcal{O}(a^2)$.

The sum in the second line is the interacting Hamiltonian, $H_{\text{ex}}^{b,4}$. The first term in this sum is a density term. The last two terms express hopping processes. E.g., the

last term in this sum shows a boson being created at lattice site j, two bosons being destructed at lattice-site i and a boson being created at i.

This Hamiltonian is not diagonal, as it contains terms of the type $a_i^\dagger a_j$. Applying a Fourier transform will diagonalise it. We introduce the Fourier transformed bosonic operators, $a_{\mathbf{k}}, a_{\mathbf{k}}^\dagger$. A boson with momentum $\mathbf{k}$ will be destructed by $a_{\boldsymbol{k}}$, while $a_{\boldsymbol{k}}^\dagger$ creates a boson with momentum $\mathbf{k}$. The inverse Fourier transforms take the form

$$\begin{aligned} a_i &= \sum_{\mathbf{k}} a_{\mathbf{k}}\, \mathrm{e}^{i\mathbf{k}\cdot\vec{r}_i} \\ a_i^\dagger &= \sum_{\mathbf{k}} a_{\mathbf{k}}^\dagger\, \mathrm{e}^{-i\mathbf{k}\cdot\vec{r}_i}. \end{aligned} \tag{4.6}$$

An important detail here, is that we assume three spatial dimensions. The x-direction of the film is extremely short, relative to the y and z-directions. Reference [31] shows we can approximate the system as periodic in all directions, and then set k_x to zero - the lowest magnon band. This is the uniform mode approximation, and it allows us to work with a system that is effectively two-dimensional.

Inserting Eq. (4.6) into $H_{\mathrm{ex}}^{b,2} = -SJ/2 \sum_{\langle i,j\rangle} \left[-a_i^\dagger a_i - a_j^\dagger a_j + a_j a_j^\dagger + a_i^\dagger a_j\right]$, we obtain

$$\begin{aligned} H_{\mathrm{ex}}^{b,2} = \text{-SJ}/2\big[&-2 \sum_{\mathbf{k_1},\mathbf{k_2}} \sum_j \delta(\mathbf{k_2}-\mathbf{k_1}) a_{\mathbf{k_1}}^\dagger a_{\mathbf{k_2}} \\ &+ \sum_{\mathbf{k_1},\mathbf{k_2}} \delta(\mathbf{k_2}-\mathbf{k_1}) a_{\mathbf{k_1}}^\dagger a_{\mathbf{k_2}} \sum_{\boldsymbol{\delta}} \mathrm{e}^{-i\mathbf{k_1}\cdot\boldsymbol{\delta}} \\ &+ \sum_{\mathbf{k_1},\mathbf{k_2}} \delta(\mathbf{k_1}-\mathbf{k_2}) a_{\mathbf{k_1}}^\dagger a_{\mathbf{k_2}} \sum_{\boldsymbol{\delta}} \mathrm{e}^{i\mathbf{k_2}\cdot\boldsymbol{\delta}}\big] \end{aligned} \tag{4.7}$$

$$\begin{aligned} &= -SJz\left[\sum_{\mathbf{k}} a_{\mathbf{k}}^\dagger a_{\mathbf{k}} + \sum_{\mathbf{k}} \gamma(\mathbf{k}) a_{\mathbf{k}}^\dagger a_{\mathbf{k}}\right] \\ &= -SJz \sum_{\mathbf{k}} \big[1+\gamma(\mathbf{k})\big] a_{\mathbf{k}}^\dagger a_{\mathbf{k}}, \end{aligned} \tag{4.8}$$

where we have defined $\gamma(\mathbf{k}) = 1/z \sum_{\boldsymbol{\delta}} \mathrm{e}^{i\mathbf{k}\cdot\boldsymbol{\delta}}$. The sum over $\boldsymbol{\delta}$ is the sum over the vectors from a lattice site, to its nearest neighbours. The number of nearest neighbours on this specific lattice is represented by z, and we have utilised the fact that $\gamma(-\mathbf{k}) = \gamma(\mathbf{k})$ in a square (cubic) lattice. We notice that by just inserting the Fourier transformed operators, we have diagonalised the Hamiltonian.

We insert the same transformation (Eq. (4.6)) into the interacting Hamiltonian,

$H_{\text{ex}}^{b,4}$, and obtain

$$
\begin{aligned}
H_{\text{ex}}^{b,4} = -\frac{J}{2}\sum_{i,\boldsymbol{\delta}}\Bigg[&\frac{1}{N^2}\sum_{\mathbf{k}_1,\ldots,\mathbf{k}_4} a^\dagger_{\mathbf{k}_1}a_{\mathbf{k}_2}a^\dagger_{\mathbf{k}_3}a_{\mathbf{k}_4}\mathrm{e}^{i(-\mathbf{k}_1+\mathbf{k}_2-\mathbf{k}_3+\mathbf{k}_4)\cdot\mathbf{r}_i}\,\mathrm{e}^{i(\mathbf{k}_4-\mathbf{k}_3)\cdot\boldsymbol{\delta}} \\
&+\frac{1}{2}\frac{1}{N^2}\sum_{\mathbf{k}_1,\ldots,\mathbf{k}_4} a_{\mathbf{k}_1}a^\dagger_{\mathbf{k}_2}a^\dagger_{\mathbf{k}_3}a_{\mathbf{k}_4}\mathrm{e}^{i(\mathbf{k}_1-\mathbf{k}_2-\mathbf{k}_3+\mathbf{k}_4)\cdot\mathbf{r}_i}\,\mathrm{e}^{i(\mathbf{k}_4-\mathbf{k}_2-\mathbf{k}_3)\cdot\boldsymbol{\delta}} \\
&+\frac{1}{2}\frac{1}{N^2}\sum_{\mathbf{k}_1,\ldots,\mathbf{k}_4} a^\dagger_{\mathbf{k}_1}a_{\mathbf{k}_2}a_{\mathbf{k}_3}a^\dagger_{\mathbf{k}_4}\mathrm{e}^{i(-\mathbf{k}_1+\mathbf{k}_2+\mathbf{k}_3-\mathbf{k}_4)\cdot\mathbf{r}_i}\,\mathrm{e}^{-i\mathbf{k}_4\cdot\boldsymbol{\delta}}\Bigg] \qquad (4.9)\\
= -\frac{Jz}{2}\Bigg[&\frac{1}{N}\sum_{\mathbf{k}_1,\mathbf{k}_2,\mathbf{k}_3} a^\dagger_{\mathbf{k}_1}a_{\mathbf{k}_2}a^\dagger_{\mathbf{k}_3}a_{\mathbf{k}_1+\mathbf{k}_3-\mathbf{k}_2}\,\gamma(\mathbf{k}_1-\mathbf{k}_2) \\
&-\frac{1}{2}\frac{1}{N}\sum_{\mathbf{k}_1,\mathbf{k}_2,\mathbf{k}_3} a_{\mathbf{k}_1}a^\dagger_{\mathbf{k}_2}a^\dagger_{\mathbf{k}_3}a_{\mathbf{k}_2+\mathbf{k}_3-\mathbf{k}_1}\,\gamma(\mathbf{k}_1) \\
&-\frac{1}{2}\frac{1}{N}\sum_{\mathbf{k}_1,\mathbf{k}_2,\mathbf{k}_3} a^\dagger_{\mathbf{k}_1}a_{\mathbf{k}_2}a_{\mathbf{k}_3}a^\dagger_{\mathbf{k}_2+\mathbf{k}_3-\mathbf{k}_1}\,\gamma(\mathbf{k}_2+\mathbf{k}_3-\mathbf{k}_1)\Bigg]. \qquad (4.10)
\end{aligned}
$$

In Eq. (4.10), the first sum represents that a boson with momentum $\mathbf{k}_1+\mathbf{k}_3-\mathbf{k}_2$ is destructed, a boson with momentum $\mathbf{k}_3$ is created, one with momentum $\mathbf{k}_2$ is destructed and one with momentum $\mathbf{k}_1$ is created. The same reasoning applies to the second and third sums. In all these sums, the number of bosons is conserved, as well as the momentum. Every term has an equal amount of destruction and creation operators.

As mentioned, $\gamma(\mathbf{k}_1-\mathbf{k}_2)$ is a form factor. It depends on the number of nearest neighbours, as well as the geometry of the lattice. It will be different for a square and e.g. a honeycomb lattice. We can utilise the geometry of the square lattice, in which for every neighbour, the lattice has another neighbour in the opposite direction. This geometry ensures that $\gamma(\mathbf{k})$ will always be real. That is not true in general, and not for e.g. the honeycomb lattice.

By performing the Holstein-Primakoff transformation, we introduced new bosonic operators, which significantly simplified the calculations. By Fourier transforming the new bosonic operators, we have diagonalised the Hamiltonian for the direct exchange interaction.

4.2 Zeeman coupling

We will assume an external field parallel with the quantisation axis, $\mathbf{h} \parallel \hat{\mathbf{z}}$. When inserting the transformation in Eq. (4.1) into the spin Hamiltonian in Eq. (2.6), we

get the bosonised Hamiltonian

$$\begin{aligned} H^s_{\text{Zee}} &= -\sum_i \mu h S^z_i \\ H^b_{\text{Zee}} &= -\sum_i \mu h (S - a^\dagger_i a_i) \\ &= -\mu h N S + \mu h \sum_{\mathbf{k}} a^\dagger_{\mathbf{k}} a_{\mathbf{k}}. \end{aligned} \tag{4.11}$$

The first term is a constant, and can be absorbed into a reference energy. The Hamiltonian for the Zeeman coupling was already diagonal, but we have now written it with operators that are more convenient to work with.

4.3 Dipolar interaction

As already written in Eq. (2.3), the Hamiltonian describing the dipolar interaction is

$$H^s_{\text{dip}} = -\frac{1}{2}\sum_{i,j}\sum_{\alpha,\beta} D^{\alpha\beta}_{ij} S^\alpha_i S^\beta_j. \tag{4.12}$$

We want this Hamiltonian to be expressed in the bosonic operators in Eq. (4.1) as well. We insert (4.2) and S^z_i from Eq. (4.1). When doing this, we get some terms $\mathcal{O}(a^1)$ and $\mathcal{O}(a^3)$. These will all have an off-diagonal matrix-element as coefficient. It can be shown that off-diagonal elements of the $\mathbf{D}_{ij}$-matrix are all zero in a thin film [31].

We then obtain a bosonic dipole Hamiltonian

$$H^b_{\text{dip}} = H^{b,2}_{\text{dip}} + H^{b,4}_{\text{dip}} \tag{4.13}$$

$$\begin{aligned} H^{b,2}_{\text{dip}} = \frac{1}{4}\sum_{i,j} S\big[&-(D^{xx}_{ij} + D^{yy}_{ij})\, a^\dagger_i a^\dagger_j + (-D^{xx}_{ij} - D^{yy}_{ij})\, a_i a^\dagger_j \\ &+ (-D^{xx}_{ij} - D^{yy}_{ij})\, a^\dagger_i a_j + (-D^{xx}_{ij} + D^{yy}_{ij})\, a_i a_j \\ &+ 2\, D^{zz}_{ij}\, a^\dagger_i a_i + 2\, D^{zz}_{ij}\, a^\dagger_j a_j \big] \end{aligned} \tag{4.14}$$

$$\begin{aligned} H^{b,4}_{\text{dip}} = \frac{1}{2}\frac{1}{8}\sum_{i,j}\Big\{ &\ 2(D^{xx}_{ij} + D^{yy}_{ij})\big[a^\dagger_i a_i a_i a^\dagger_j + a_j a^\dagger_i a^\dagger_i a_i + 4 a^\dagger_i a_i a^\dagger_j a_j\big] \\ &+2(D^{xx}_{ij} - D^{yy}_{ij})\big[a^\dagger_j a^\dagger_i a^\dagger_i a_j + a^\dagger_i a_i a_i a_j\big]\Big\}. \end{aligned} \tag{4.15}$$

We now define new coefficients

$$\begin{aligned} A_{ij} &= S\left[\delta_{ij}\sum_n D^{zz}_{in} - \frac{D^{xx}_{ij} + D^{yy}_{ij}}{2}\right] \\ B_{ij} &= -S/2\big[D^{xx}_{ij} - D^{yy}_{ij}\big]. \end{aligned} \tag{4.16}$$

These coefficients are defined such that when inserting them back into the sums, we change the sums to include $i = j$.

By cleaning up Eq. (4.14) and inserting coefficients in Eq. (4.16), we obtain a simple Hamiltonian

$$H_{\text{dip}}^{b,2} = \frac{1}{2}\sum_{ij}\Big[A_{ij}a_i^\dagger a_j + B_{ij}a_i a_j + B_{ij}^* a_i^\dagger a_j^\dagger\Big]. \tag{4.17}$$

We now want to express the interaction in momentum space. We obtain this by inserting the inverse Fourier transform of $a_i, a_i^\dagger$, Eq. (4.6) and of $D_{ij}^{\alpha\beta}, A_{ij}$ and B_{ij}

$$\begin{aligned} A_{ij} &= \sum_{\mathbf{k}} A_{\mathbf{k}}\, \mathrm{e}^{-i\,\mathbf{k}\cdot\mathbf{r}_{ij}} \\ B_{ij} &= \sum_{\mathbf{k}} B_{\mathbf{k}}\, \mathrm{e}^{-i\,\mathbf{k}\cdot\mathbf{r}_{ij}} \\ D_{ij}^{\alpha\beta} &= \sum_{\mathbf{k}} D_{\mathbf{k}}^{\alpha\beta}\, \mathrm{e}^{-i\,\mathbf{k}\cdot\mathbf{r}_{ij}}. \end{aligned} \tag{4.18}$$

As previously stated, since we study a thin film, we only need $D_{ij}^{\alpha\alpha}$. The Fourier transformed coefficients in Eq. (4.18) are

$$\begin{aligned} A_{\mathbf{k}} &= \frac{\Delta}{3} - \frac{S}{2}(D_{\mathbf{k}}^{xx} + D_{\mathbf{k}}^{yy}) \\ B_{\mathbf{k}} &= -\frac{S}{2}(D_{\mathbf{k}}^{xx} - D_{\mathbf{k}}^{yy}) \\ D_{\mathbf{k}}^{xx} &= \frac{4\pi\mu^2}{a^3}\big[\frac{1}{3} - f_{\mathbf{k}}\big] \\ D_{\mathbf{k}}^{yy} &= \frac{4\pi\mu^2}{a^3}\big[\frac{1}{3} + \sin^2\theta_{\mathbf{k}}(f_{\mathbf{k}} - 1)\big] \\ D_{\mathbf{k}}^{zz} &= \frac{4\pi\mu^2}{a^3}\big[\frac{1}{3} + \cos^2\theta_{\mathbf{k}}(f_{\mathbf{k}} - 1)\big], \end{aligned} \tag{4.19}$$

where $\Delta = 4\pi\mu^2/a^3 = 4\pi M_s$, with M_s being the saturation magnetisation. The angle between $\mathbf{k}$ and the external magnetic field, $\mathbf{h}$, is denoted by $\theta_{\mathbf{k}}$. For later convenience, we will present the variables A_k and B_k when the direct exchange interaction and Zeeman coupling are included as well

$$\begin{aligned} A_{\mathbf{k}} &= h + JS[4 - 2\cos(k_y a) - 2\cos(k_z a)] \\ &\quad + \frac{\Delta}{3} - \frac{S}{2}(D_{\mathbf{k}}^{xx} + D_{\mathbf{k}}^{yy}) \end{aligned} \tag{4.20}$$

$$\begin{aligned} B_{\mathbf{k}} &= -\frac{S}{2}(D_{\mathbf{k}}^{xx} - D_{\mathbf{k}}^{yy}) \\ D_{\mathbf{k}}^{xx} &= \frac{4\pi\mu^2}{a^3}\left[\frac{1}{3} - f_{\mathbf{k}}\right] \\ D_{\mathbf{k}}^{yy} &= \frac{4\pi\mu^2}{a^3}\left[\frac{1}{3} + \sin^2\theta_{\mathbf{k}}(f_{\mathbf{k}} - 1)\right] \\ D_{\mathbf{k}}^{zz} &= \frac{4\pi\mu^2}{a^3}\left[\frac{1}{3} + \cos^2\theta_{\mathbf{k}}(f_{\mathbf{k}} - 1)\right]. \end{aligned} \tag{4.21}$$

As we would intuitively have thought, B_k in Eq. (4.21) is zero in the absence of the dipolar interaction. Inspecting Eq. (4.17) and Eq. (4.8), we see that there are only diagonal terms emerging from the direct exchange interaction and Zeeman coupling.

The momentum space $H^{b,2}_{\text{dip}}$ reads

$$H^{b,2}_{\text{dip}} = \frac{1}{2}\sum_{\mathbf{k}}\left[2A_{\mathbf{k}}a^\dagger_{\mathbf{k}}a_{\mathbf{k}} + B^*_{\mathbf{k}}a^\dagger_{\mathbf{k}}a^\dagger_{-\mathbf{k}} + B_{\mathbf{k}}a_{-\mathbf{k}}a_{\mathbf{k}}\right] \tag{4.22}$$

$$= \sum_{\mathbf{k}} \vec{a}^{\,\dagger}_{\mathbf{k}} H_{\mathbf{k}} \vec{a}_{\mathbf{k}}, \tag{4.23}$$

where $\vec{a}_{\mathbf{k}}$ and $H_{\mathbf{k}}$ are defined as

$$\vec{a}_{\mathbf{k}} = \begin{pmatrix} a_{\mathbf{k}} \\ a^\dagger_{-\mathbf{k}} \end{pmatrix}, \qquad H_{\mathbf{k}} = \begin{pmatrix} A_{\mathbf{k}} & B_{\mathbf{k}} \\ B^*_{\mathbf{k}} & A_{\mathbf{k}} \end{pmatrix}. \tag{4.24}$$

We now want to apply the same procedure that we used for $H^{b,2}_{\text{dip}}$, to $H^{b,4}_{\text{dip}}$. Inserting Eqs. (4.6) into eq (4.15) we obtain

$$\begin{aligned} H^{b,4}_{\text{dip}} = \frac{1}{2}\frac{1}{8}\frac{2}{N^{3/2}}\Bigg\{\Bigg[&4\sum_{\mathbf{k}_1,\ldots,\mathbf{k}_4}\left(D^{xx}_{\mathbf{k}_3-\mathbf{k}_4} + D^{yy}_{\mathbf{k}_3-\mathbf{k}_4}\right) a^\dagger_{\mathbf{k}_1}a_{\mathbf{k}_2}a^\dagger_{\mathbf{k}_3}a_{\mathbf{k}_4}\,\delta(\mathbf{k}_4+\mathbf{k}_2-\mathbf{k}_1-\mathbf{k}_3) \\ &+\sum_{\mathbf{k}_1,\ldots,\mathbf{k}_4}\left(D^{xx}_{\mathbf{k}_4} + D^{yy}_{\mathbf{k}_4}\right) a_{\mathbf{k}_1}a^\dagger_{\mathbf{k}_2}a_{\mathbf{k}_3}a^\dagger_{\mathbf{k}_4}\,\delta(\mathbf{k}_2+\mathbf{k}_3-\mathbf{k}_1-\mathbf{k}_4) \\ &+\sum_{\mathbf{k}_1,\ldots,\mathbf{k}_4}\left(D^{xx}_{\mathbf{k}_1} + D^{yy}_{\mathbf{k}_1}\right) a_{\mathbf{k}_1}a^\dagger_{\mathbf{k}_2}a^\dagger_{\mathbf{k}_3}a_{\mathbf{k}_4}\,\delta(\mathbf{k}_1+\mathbf{k}_4-\mathbf{k}_2-\mathbf{k}_3)\Bigg] \\ +\Bigg[&\sum_{\mathbf{k}_1,\ldots,\mathbf{k}_4}\left(D^{xx}_{\mathbf{k}_1} - D^{yy}_{\mathbf{k}_1}\right) a^\dagger_{\mathbf{k}_1}a^\dagger_{\mathbf{k}_2}a^\dagger_{\mathbf{k}_3}a_{\mathbf{k}_4}\,\delta(\mathbf{k}_4-\mathbf{k}_3-\mathbf{k}_2-\mathbf{k}_1) \\ &+\sum_{\mathbf{k}_1,\ldots,\mathbf{k}_4}\left(D^{xx}_{\mathbf{k}_4} - D^{yy}_{\mathbf{k}_4}\right) a^\dagger_{\mathbf{k}_1}a_{\mathbf{k}_2}a_{\mathbf{k}_3}a_{\mathbf{k}_4}\,\delta(\mathbf{k}_4+\mathbf{k}_3+\mathbf{k}_2-\mathbf{k}_1)\Bigg]\Bigg\}. \end{aligned} \tag{4.25}$$

After performing one of the $\mathbf{k}_i$ sums, taking advantage of the δ-functions and renaming the momenta, $H^{b,4}_{\text{dip}}$ will be

$$\begin{aligned} H^{b,4}_{\text{dip}} = \frac{1}{2}\frac{1}{8}\frac{2}{N}\sum_{\mathbf{k},\mathbf{q},\mathbf{q}'}\Bigg\{&2(D^{xx}_{\mathbf{k}} + D^{yy}_{\mathbf{k}})\left[a^\dagger_{\mathbf{q}+\mathbf{k}}a_{\mathbf{q}}a^\dagger_{\mathbf{q}'-\mathbf{k}}a_{\mathbf{q}'} + \text{h.c.}\right] \\ &+(D^{xx}_{\mathbf{q}} + D^{yy}_{\mathbf{q}})\left[a_{\mathbf{q}}a^\dagger_{\mathbf{q}+\mathbf{k}}a^\dagger_{\mathbf{q}'-\mathbf{k}}a_{\mathbf{q}'} + \text{h.c.}\right] \\ &+(D^{xx}_{\mathbf{k}} - D^{yy}_{\mathbf{k}})\left[a^\dagger_{\mathbf{q}+\mathbf{q}'+\mathbf{k}}a_{\mathbf{q}}a_{\mathbf{q}'}a_{\mathbf{k}} + \text{h.c.}\right]\Bigg\}, \end{aligned} \tag{4.26}$$

where h.c. denotes the Hermitian conjugate of the preceding terms within the parenthesis.

We have now expressed the full dipolar Hamiltonian in momentum space. In doing this, we have obtained some terms which do not conserve the number of magnons. The last line in Eq. (4.26) annihilates three bosons, while it only creates one. We note that even though the number of magnons are not conserved, the momentum is.

Defining three new functions, $f_1(\mathbf{k}), f_2(\mathbf{k}), f_3(\mathbf{k})$ we can write Eq. (4.26) more compactly as

$$H_{\text{dip}}^{b,4} = \frac{1}{2}\frac{1}{8}\frac{2}{N}\,4 \sum_{\mathbf{k},\mathbf{q},\mathbf{q}'} \Big\{ \big[f_3(\mathbf{k}) - 2f_1(\mathbf{q})\big] \left[a^\dagger_{\mathbf{q}+\mathbf{k}} a_{\mathbf{q}} a^\dagger_{\mathbf{q}'-\mathbf{k}} a_{\mathbf{q}'} + \text{h.c.}\right] \\ + 2f_2(\mathbf{k}) \left[a^\dagger_{\mathbf{q}+\mathbf{q}'+\mathbf{k}} a_{\mathbf{q}} a_{\mathbf{q}'} a_{\mathbf{k}} + \text{h.c.}\right] \Big\}, \tag{4.27}$$

where the functions are defined as

$$\begin{aligned} f_1(k) &= \frac{\hbar\gamma 2\pi M_s}{S}\big[(1 - f_{\mathbf{k}})\sin^2\theta + f_{\mathbf{k}}\big]/4 \\ f_2(k) &= \frac{\hbar\gamma 2\pi M_s}{S}\big[(1 - f_{\mathbf{k}})\sin^2\theta - f_{\mathbf{k}}\big]/4 \\ f_3(k) &= \frac{\hbar\gamma 2\pi M_s}{S}(1 - f_{\mathbf{k}})\cos^2\theta. \end{aligned} \tag{4.28}$$

Chapter 5

Stability Analysis of Ferromagnetic System*

5.1 Bogoliubov transformation

As we see in Eq. (4.17), $H^{b,2}_{\text{dip}}$ is not diagonal, since it still has terms of the type $a^\dagger_{\mathbf{k}} a^\dagger_{\mathbf{k}}$ and $a_{\mathbf{k}}\, a_{\mathbf{k}}$. To diagonalise it, we will perform a Bogoliubov transformation. We diagonalise the Hamiltonian to find the eigenstates of the non-interacting Hamiltonian. The interacting Hamiltonian is perceived as a small perturbation to the exact solvable system, the non-interacting Hamiltonian.

As we are working with operators, and vectors of operators, we need to be careful when diagonalising the Hamiltonian. We cannot diagonalise it carelessly, as that will not guarantee that the eigenvectors are bosonic. That is why we need to do a Bogoliubov transformation [46].

We define a matrix, U, for the Bogoliubov transformation [30]. The matrix and its inverse is

$$U = \begin{pmatrix} u_{\mathbf{k}} & v_{\mathbf{k}} \\ v^*_{\mathbf{k}} & u_{\mathbf{k}} \end{pmatrix}, \quad U^{-1} = \begin{pmatrix} u_{\mathbf{k}} & -v_{\mathbf{k}} \\ -v^*_{\mathbf{k}} & u_{\mathbf{k}} \end{pmatrix} \tag{5.1}$$

where $u_{\mathbf{k}}$ and $v_{\mathbf{k}}$ are the Bogoliubov coefficients. We note from the matrices that $u_{\mathbf{k}}$ is a real number, whereas $v_{\mathbf{k}}$ can be complex.

We now define two new bosonic operators, $\alpha_{\mathbf{k}}, \alpha^\dagger_{\mathbf{k}}$

$$\begin{pmatrix} \alpha_{\mathbf{k}} \\ \alpha^\dagger_{-\mathbf{k}} \end{pmatrix} = \begin{pmatrix} u_{\mathbf{k}} & v_{\mathbf{k}} \\ v^*_{\mathbf{k}} & u_{\mathbf{k}} \end{pmatrix} \begin{pmatrix} a_{\mathbf{k}} \\ a^\dagger_{-\mathbf{k}} \end{pmatrix}, \tag{5.2}$$

$$\begin{pmatrix} a_{\mathbf{k}} \\ a^\dagger_{-\mathbf{k}} \end{pmatrix} = \begin{pmatrix} u_{\mathbf{k}} & -v_{\mathbf{k}} \\ -v^*_{\mathbf{k}} & u_{\mathbf{k}} \end{pmatrix} \begin{pmatrix} \alpha_{\mathbf{k}} \\ \alpha^\dagger_{-\mathbf{k}} \end{pmatrix}. \tag{5.3}$$

We require these new operators to follow the same bosonic commutation relation as for $a_{\mathbf{k}}, a_{\mathbf{k}}^\dagger$, meaning that $[\alpha_{\mathbf{k}}, \alpha_{\mathbf{k}'}] = [\alpha_{\mathbf{k}}^\dagger, \alpha_{\mathbf{k}'}^\dagger] = 0$, and $[\alpha_{\mathbf{k}}, \alpha_{\mathbf{k}'}^\dagger] = \delta_{\mathbf{k},\mathbf{k}'}$. From the first two commutators we find that $u_{-\mathbf{k}} = u_{\mathbf{k}}$ and $v_{-\mathbf{k}} = v_{\mathbf{k}}$. From the commutator $[\alpha_{\mathbf{k}}, \alpha_{\mathbf{k}'}^\dagger] = \delta_{\mathbf{k},\mathbf{k}'}$ we find that

$$u_{\mathbf{k}}^2 - |v_{\mathbf{k}}|^2 = 1. \tag{5.4}$$

We want to find restrictions on $u_{\mathbf{k}}$ and $v_{\mathbf{k}}$ so that $H_{\text{dip}}^{b,2}$ becomes diagonal. This can be done by inserting Eq. (5.3) into Eq. (4.23). We then require that $U^\dagger H U$ is diagonal, by setting off-diagonal elements to zero.

We then obtain the following expressions for $u_{\mathbf{k}}, v_{\mathbf{k}}$

$$u_{\mathbf{k}} = \sqrt{\frac{A_{\mathbf{k}} + \varepsilon_{\mathbf{k}}}{2\varepsilon_{\mathbf{k}}}}\,, \qquad v_{\mathbf{k}} = \frac{B_{\mathbf{k}}}{|B_{\mathbf{k}}|}\sqrt{\frac{A_{\mathbf{k}} - \varepsilon_{\mathbf{k}}}{2\varepsilon_{\mathbf{k}}}}, \tag{5.5}$$

where $\varepsilon_{\mathbf{k}} = \sqrt{A_{\mathbf{k}}^2 - |B_{\mathbf{k}}|^2}$.
This results in a Hamiltonian that is diagonal in the new operators $\alpha, \alpha^\dagger$

$$H_{\text{dip}}^{b,2} = \sum_{\mathbf{k}} \left[\varepsilon_{\mathbf{k}} \alpha_{\mathbf{k}}^\dagger \alpha_{\mathbf{k}} + \frac{\varepsilon_{\mathbf{k}} - A_{\mathbf{k}}}{2} \right]. \tag{5.6}$$

The dispersion relation, $\varepsilon_{\mathbf{k}}$ can be plotted by inserting typical values for YIG, e.g. from [45].

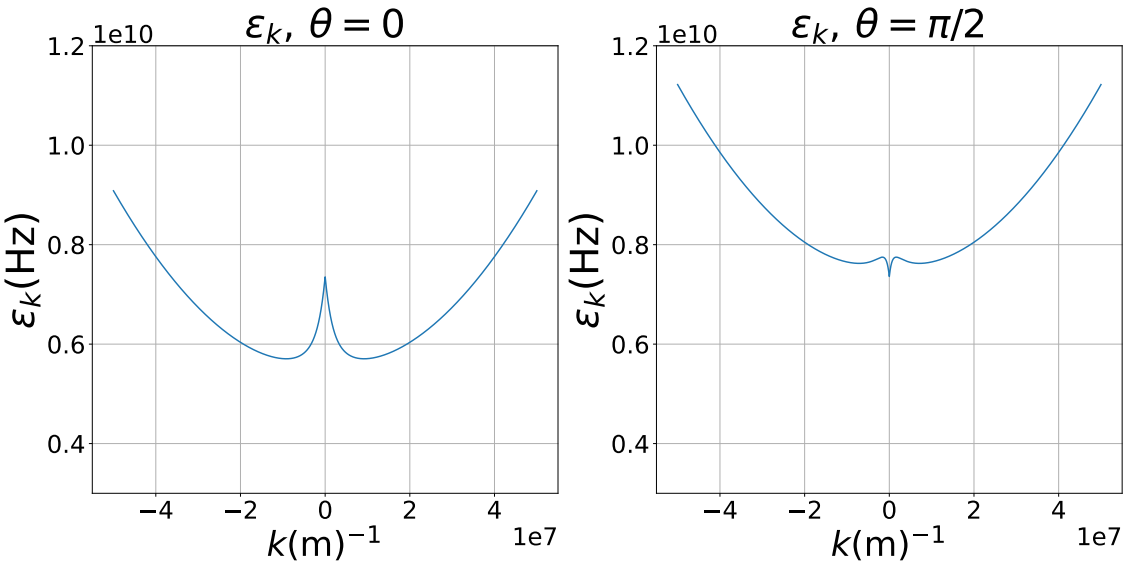

(a)

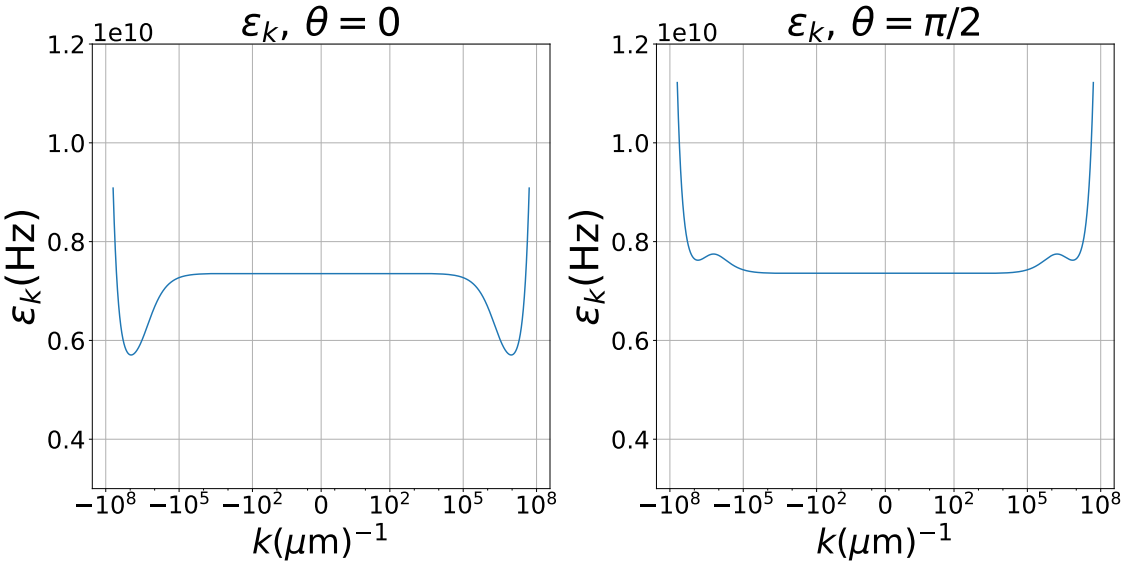

(b)

Figure 5.1: (a) ε_k plotted as a function of k_z, ($\theta = 0$) and as a function of k_y, ($\theta = \pi/2$). (b) same plots as (a)) but with logarithmic k-axis.

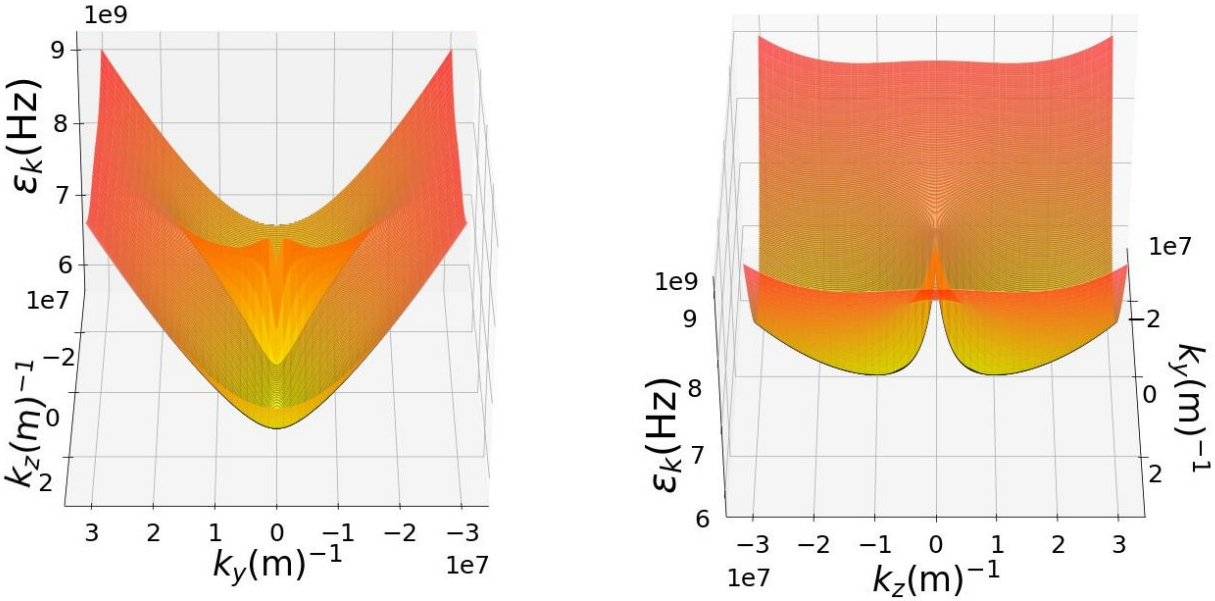

Figure 5.2: Surface plot of ε_k as a function of k_y and k_z.

Figure 5.1(a) shows the two-dimensional slice of the dispersion relation for the direct exchange interaction, Zeeman coupling and dipolar interaction, ε_k, plotted with $\theta = 0$ and $\theta = \pi/2$. For both angles we see two symmetric minima. In Figure 5.1(b), we see two-dimensional slices of ε_k plotted with logarithmic k-axis. We recognise the shape of ε_k from other works, such as [18]. In Figure 5.2 we have plotted the same ε_k in three dimensions. We can recognise that a two-dimensional slice has the same shape of ε_k when $\theta = \{0, \pi/2\}$ as in Figure 5.1(a). The anisotropy of the dispersion relation is due to the dipolar interaction.

By looking at the dispersions, we see that there are two energy minima for the magnons. We know that the condensation takes place in these two minima. We therefore choose to only look at these two momenta, $\pm\mathbf{Q}$. To achieve this, we let the sum pick out momenta such that all creation and destruction operators have momenta $\mathbf{k} = \pm\mathbf{Q}$. We define $\omega_m = \gamma 4\pi M_s$. The resulting Bose-Einstein condensate Hamiltonian is

$$\begin{aligned} H_Q = &-\left[a^\dagger_{\mathbf{Q}} a^\dagger_{\mathbf{Q}} a_{\mathbf{Q}} a_{\mathbf{Q}} + a^\dagger_{-\mathbf{Q}} a^\dagger_{-\mathbf{Q}} a_{-\mathbf{Q}} a_{-\mathbf{Q}}\right]\left[\frac{DQ^2}{2S} + \frac{\hbar\omega_m}{4S} F_Q\right]/N \\ &- a^\dagger_{-\mathbf{Q}} a^\dagger_{\mathbf{Q}} a_{-\mathbf{Q}} a_{\mathbf{Q}}\left[-4\frac{DQ^2}{2S} + \frac{\hbar\omega_m}{8S} 8F_Q - \frac{\hbar\omega_m}{2S} 2(1 - F_{2Q})\right]/N \\ &- \left[a^\dagger_{\mathbf{Q}} a_{\mathbf{Q}} a_{\mathbf{Q}} a_{-\mathbf{Q}} + a^\dagger_{-\mathbf{Q}} a_{-\mathbf{Q}} a_{-\mathbf{Q}} a_{\mathbf{Q}} + \text{h.c.}\right]\frac{3\hbar\omega_m}{8S} F_Q/N. \end{aligned} \tag{5.7}$$

5.2 Hamiltonian at the minima

We now want to express the Hamiltonian, H_Q, in the new basis, Eq. (5.2). Inserting Eq. (5.3) into Eq. (5.7), we obtain

$$\begin{aligned} H_Q = A\big[&\alpha^\dagger_{\mathbf{Q}}\alpha^\dagger_{\mathbf{Q}}\alpha_{\mathbf{Q}}\alpha_{\mathbf{Q}} + \alpha^\dagger_{-\mathbf{Q}}\alpha^\dagger_{-\mathbf{Q}}\alpha_{-\mathbf{Q}}\alpha_{-\mathbf{Q}}\big] \\ &+ 2B\,\alpha^\dagger_{\mathbf{Q}}\alpha^\dagger_{-\mathbf{Q}}\alpha_{\mathbf{Q}}\alpha_{-\mathbf{Q}} \\ &+ C\big[\alpha^\dagger_{\mathbf{Q}}\alpha_{\mathbf{Q}}\alpha_{\mathbf{Q}}\alpha_{-\mathbf{Q}} + \alpha^\dagger_{-\mathbf{Q}}\alpha_{-\mathbf{Q}}\alpha_{-\mathbf{Q}}\alpha_{\mathbf{Q}} + \text{h.c.}\big] \\ &+ D\big[\alpha_{-\mathbf{Q}}\alpha_{\mathbf{Q}}\alpha_{\mathbf{Q}}\alpha_{-\mathbf{Q}} + \text{h.c.}\big]. \end{aligned} \tag{5.8}$$

The coefficients A, B, C, D are functions of the Bogoliubov coefficients, and take the form

$$\begin{aligned} A &= -\frac{\hbar\omega_m}{4SN}\big[(\alpha_1-\alpha_3)F_Q - 2\alpha_2(1-F_{2Q})\big] - \frac{\mathcal{D}Q^2}{2SN}(\alpha_1-4\alpha_2) \\ B &= \frac{\hbar\omega_m}{2SN}\big[(\alpha_1-\alpha_2)(1-F_{2Q}) - (\alpha_1-\alpha_3)F_Q\big] + \frac{\mathcal{D}Q^2}{SN}(\alpha_1-2\alpha_2) \\ C &= -\left[\frac{\hbar\omega_m}{8SN}\big[(3\alpha_1+3\alpha_2-4\alpha_3)F_Q + \frac{8}{3}\alpha_3(1-F_{2Q})\big] + \frac{\mathcal{D}Q^2}{SN}\frac{\alpha_3}{3}\right] \\ D &= \frac{\hbar\omega_m}{4SN}\big[(\alpha_3-3\alpha_2)F_Q + 2\alpha_2(a-F_{2Q})\big] + \frac{\mathcal{D}Q^2}{2SN}\alpha_2, \end{aligned} \tag{5.9}$$

where $\alpha_1 = u_Q^4 + 4u_Q^2v_Q^2 + v_Q^4$, $\alpha_2 = 2u_Q^2v_Q^2$, $\alpha_3 = 3u_Qv_Q(u_Q^2+v_Q^2)$. When performing these calculations, we inspect B_Q and its phase. From Eq. (5.5) we know v_Q's phase is determined by B_Q's phase. It turns out B_Q and v_Q are both real, which allowed for significant simplification of the expression.

The constant $\mathcal{D}$ is defined as $\mathcal{D} = 2JSa^2$. In calculating the expression in Eq. (5.8) we have also utilised the fact that $H^{b,2}_{\text{dip}}$ in Eq. (4.17) is $\mathcal{O}(S^1)$, while H^4 is $\mathcal{O}(S^0)$. When inserting the commutation relations $[\alpha_{\mathbf{Q}}, \alpha^\dagger_{\mathbf{Q}}] = 1$, some terms that are $\mathcal{O}(\alpha^2)$ emerge. We can neglect those terms, as H^2 is one order of magnitude larger than the newly emerged $\mathcal{O}(\alpha^2)$ terms.

Comparing with the work of Demokritov *et al.* [23], we have identical expressions for A, B, D. The coefficient C however, has the opposite sign. Tracing this backwards through the calculations, we can see that it emerges from the definitions of $B_{\mathbf{k}}$. Our definition in Eq. (4.19) is identical to Kopietz' [31], which has the opposite sign of Demokritov's. This also manifests in $f_2(\mathbf{k})$ in Eq. (4.28), and the sign of the last line in Eq. (5.7).

We note that a new type of term has appeared in the Bogoliubov transformed Hamiltonian, Eq. (4.15). The last two terms only destruct, while the Hermitian conjugate only creates magnons. These terms obviously do not conserve the number of magnons, however they do conserve momenta.

5.3 Energy function for the Bose-Einstein condensate

As this Hamiltonian describes the magnons with momenta corresponding to the BEC, we want to approximate $\alpha_{\pm\mathbf{Q}}$ with a macroscopic field, utilising a Madelung transformation. The field we insert into Eq. (5.8) is $\langle\alpha_{\pm\mathbf{Q}}\rangle = \sqrt{N_{\pm\mathbf{Q}}}\exp(i\phi_{\pm})$. The number of magnons in $\mathbf{k} = +\mathbf{Q}$ is $N_{+\mathbf{Q}}$, and correspondingly for $N_{-\mathbf{Q}}$. The phase of the magnon condensate in $\mathbf{k} = +\mathbf{Q}$ is ϕ_+, and correspondingly for ϕ_-. This results in the interaction potential

$$\mathcal{V}_4 = \frac{1}{2}N_c^2\big[(A+B)-(B+D\,\cos 2\Phi-A)(\delta/N_c)^2+D\,\cos 2\Phi+2C\sqrt{1-(\delta/N_c)^2}\cos\Phi\big]. \tag{5.10}$$

Here we have defined three new numbers, N_c, Φ and δ. N_c is the total number of condensed magnons, $N_c = N_{+\mathbf{Q}} + N_{-\mathbf{Q}}$, which can be tuned and kept constant [23]. The total phase for the two condensates is $\Phi = \phi_+ + \phi_-$. The difference in the number of magnons in the two condensates is $\delta = N_{+\mathbf{Q}} - N_{-\mathbf{Q}}$.

Comparing with Eq. 10 in [23], we see that there is an extra term in our calculations, $D\cos(2\Phi)$. In Appendix A we have rigorously shown that this term should be present. As the extra term is a function of Φ, it could alter the phase diagram.

5.4 Curvature of the potential

As we now have our interaction potential in Eq. (5.10), we can inspect the possibilities for the existence of a BEC. We know that $\mathcal{V}_4$ needs to be a repulsive potential. We therefore look for extremum points, and determine if they are minima or maxima.

The process of determining such points is to first differentiate $\mathcal{V}_4$ with respect to δ and Φ. We then set the expression to zero and solve for the respective variable

$$\begin{aligned}\frac{\partial\mathcal{V}_4}{\partial\delta} &= \frac{1}{2}N_c^2\Big[(B+D\,\cos(2\Phi)-A)(2\delta/N_c^2) - \frac{2C\delta}{N_c^2\sqrt{1-(\delta/N_c)^2}}\cos(2\Phi)\Big] = 0\\ \frac{\partial\mathcal{V}_4}{\partial\Phi} &= \frac{1}{2}N_c^2\big[2D\,\sin(2\Phi)(\delta/N_c)^2 - 2D\,\sin(2\Phi) - 2C\sqrt{1-(\delta/N_c)^2}\sin(\Phi)\big] = 0.\end{aligned} \tag{5.11}$$

This yields six extremum points

$$\begin{aligned}
&\text{i) } (\delta/N_c)^2 = 0, \Phi = 0 \\
&\text{ii) } (\delta/N_c)^2 = 0, \Phi = \pi \\
&\text{iii) } (\delta/N_c)^2 = 1 - \left[\frac{C\,\cos(\Phi)}{A - B - D\,\cos(2\Phi)}\right]^2, \Phi = 0 \\
&\text{iv) } (\delta/N_c)^2 = 1 - \left[\frac{C\,\cos(\Phi)}{A - B - D\,\cos(2\Phi)}\right]^2, \Phi = \pi \\
&\text{v) } (\delta/N_c)^2 = 0, \Phi = \arccos\left[\frac{C\sqrt{1-(\delta/N_c)^2}}{((\delta/N_c)^2 - 1)D}\right] \\
&\text{vi) } (\delta/N_c)^2 = 1 - \left[\frac{C\,\cos(\Phi)}{A - B - D\,\cos(2\Phi)}\right]^2, \Phi = \arccos\left[\frac{C\sqrt{1-(\delta/N_c)^2}}{((\delta/N_c)^2 - 1)D}\right]
\end{aligned} \tag{5.12}$$

To check if any of these extrema could be minima, we need to find the second derivatives

$$\begin{aligned}
\frac{\partial^2 \mathcal{V}_4}{\partial \delta^2} &= \frac{1}{2}N_c^2\left[(A - B - D\,\cos(2\Phi))(2/N_c^2) - \frac{2C\,\cos(\Phi)}{N_c^2(1-(\delta/N_c)^2)^{3/2}}\right] \\
\frac{\partial^2 \mathcal{V}_4}{\partial \Phi^2} &= \frac{1}{2}N_c^2\left[4D\,cos(2\Phi)(\delta/N_c)^2 - 4D\,\cos(2\Phi) - 2C\sqrt{1-(\delta/N_c)^2}\cos(\Phi)\right] \\
\frac{\partial^2 \mathcal{V}_4}{\partial \delta \partial \Phi} &= \frac{\partial^2 \mathcal{V}_4}{\partial \Phi \delta} = \frac{1}{2}N_c^2\left[4D\,\sin(2\Phi)(\delta/N_c^2) + \frac{2C\delta}{\sqrt{1-(\delta/N_c)^2}}\sin(\Phi)\right].
\end{aligned} \tag{5.13}$$

If a point is a minimum, there are three criteria it needs to fulfil: a) $\partial^2\mathcal{V}_4/\partial\delta^2 > 0$, b) $\partial^2\mathcal{V}_4/\partial\Phi^2 > 0$ and c) $(\partial^2\mathcal{V}_4/\partial\delta^2)\,(\partial^2\mathcal{V}_4/\partial\Phi^2) - (\partial^2\mathcal{V}_4/\partial\delta\partial\Phi)^2 > 0$ when evaluated at the point in question [47].

Extremum point i)

We look at the two first extrema, to see if we can consider restrictions that satisfy the criteria for a minimum. We start by checking the point $(\delta/N_c)^2 = 0, \Phi = 0$

$$\begin{aligned}
\frac{\partial^2 \mathcal{V}_4}{\partial \delta^2} &= \frac{1}{2}N_c^2\left[(A - B - D)(2/N_c^2) - 2C/N_c^2\right] \\
&= A - B - D - C \\
\frac{\partial^2 \mathcal{V}_4}{\partial \Phi^2} &= \frac{1}{2}N_c^2\left[-4D - 2C\right] \\
\frac{\partial^2 \mathcal{V}_4}{\partial \delta \Phi} &= 0.
\end{aligned}$$

To be a minimum we need, a) $\left[A - B - D - C\right]\left[-4D - 2C\right]2/N_c^2 > 0$, b) $A - B - D - C > 0$ and c) $\left[-4D - 2C\right] > 0$ to be fulfilled.

Extremum point ii)

The next extremum point is $(\delta/N_c)^2 = 0, \Phi = \pi$

$$\begin{aligned}\frac{\partial^2 \mathcal{V}_4}{\partial \delta^2} &= \frac{1}{2} N_c^2 \big[(A - B - D)(2/N_c^2) + 2C/N_c^2\big] \\ &= A - B - D + C \\ \frac{\partial^2 \mathcal{V}_4}{\partial \Phi^2} &= \frac{1}{2} N_c^2 \big[2C - 4D\big] \\ \frac{\partial^2 \mathcal{V}_4}{\partial \delta \Phi} &= 0.\end{aligned}$$

To be a minimum we need a) $\big[A{-}B{-}D{+}C\big]\big[2C{-}4D\big]2/N_c^2 > 0$, b) $A{-}B{-}D{+}C > 0$ and c) $\big[2C - 4D\big] > 0$ to be fulfilled.

We know that A, B, C and D are functions of the external magnetic field, $\mathbf{h}$, and the thickness, d, of the film. These are parameters that can be tuned. If our system satisfies the restrictions in either of the two extrema, we have found conditions under which a stable BEC can exist.

The important thing to note here is that the ability to tune the coefficients A, B, C and D comes from $\mathbf{h}$ and d. These emerge from the Zeeman coupling and dipolar interaction, respectively. Therefore we see that the dipolar interaction is important, and not negligible although of small value. In section 6.2 we have elaborately shown that the direct exchange interaction and Zeeman coupling cannot create a stable BEC. When extremum point i) and ii) are tuned to be minima, they will be symmetric condensates. δ, the difference in the number of magnon in the two condensates, is zero in both cases. As mentioned before, δ has a well-established way of being measured, namely BLS. The difference in phase between the two condensates, Φ, is zero in the first minimum and π in the second. The experimental aspects of the difference in the phases is discussed in section 6.1.

Chapter 6

Discussion*

6.1 Phase of the condensate

The two varying quantities in magnon BEC are $\delta = N_+ - N_-$ and $\Phi = \phi_+ - \phi_-$. Since δ is the difference in the number of magnons in the two coherent condensates, this is a physical, and more importantly, measurable quantity. Experimentally, the condensates are imaged using Brillouin Light Scattering, BLS. This method measures an intensity from the condensates, which is proportional to the number of magnons in the condensate. This has been done e.g. in reference [19].

The difference in phase, Φ, is however more complicated. One possible approach to quantify it, is to measure a persistent spin-current [48]. This idea is borrowed from superconductors. The corresponding order parameter is Δ. As in our case, this order parameter also has a phase, $\Delta \sim \exp(i\phi)$. A Josephson junction can be created between two superconductors. These superconductors must have the same Δ. This is a material dependent constant, thus meaning that they are made of the same material. Sandwiched in between these, we place a normal metal/material. If these two otherwise identical superconductors have different phases, $\phi_1 \neq \phi_2$ there will flow a charge current through the normal metal/material.

The idea, then, is to create a similar setup, but exchanging the superconductors with ferromagnetic insulators. The relevant set-up is then two ferromagnetic insulators separated by a normal metal/material. The setup is illustrated in Figure 6.1. In both of the ferromagnetic insulators, there will be two coherent condensates. If the Φs are different, a persistent spin current could flow. A more detailed explanation can be found in e.g. [48].

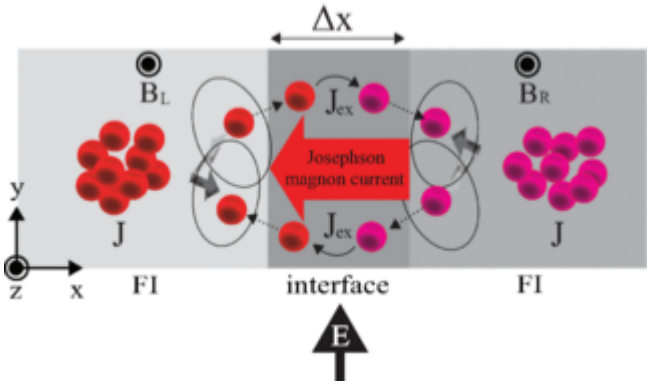

Figure 6.1: Two ferromagnetic insulators on either side of a normal metal. A magnon BEC exists in both insulators. A persistent spin-current flows from one FMI to the other. The figure is from [48].

6.2 Importance of the dipolar interaction

As mentioned earlier in the report, the dipolar interaction was needed to explain the formation of a condensate in a ferromagnetic system. We will now present the reason why the direct exchange interaction and Zeeman coupling alone are insufficient to explain the formation of a stable BEC.

We start by looking at the coefficients in Eq. (4.21). Since we only want to include the direct exchange interaction and Zeeman coupling, we set the terms emerging only from the dipolar interaction to zero

$$\begin{aligned} A_{\boldsymbol{k}} &= h + JS[4 - 2\cos(k_y a) - 2\cos(k_z a)] \\ B_{\boldsymbol{k}} &= 0 \\ D^{xx}_{\boldsymbol{k}} &= 0 \\ D^{yy}_{\boldsymbol{k}} &= 0 \\ D^{zz}_{\boldsymbol{k}} &= 0. \end{aligned} \tag{6.1}$$

(6.2)

To obtain the modified Bogoliubov transformation, we insert these values into u_k and v_k in Eq. (5.5). Since $B_k = 0$, we see that the modified coefficients are now $u_k = 1$ and $v_k = 0$. We could equally well have argued this by intuition, as the direct exchange interaction Hamiltonian is diagonal. The Bogoliubov transformation thus reduces to just the identity transformation.

We also know that the terms proportional to F_Q in Eq. (5.9) stem from the dipolar interaction. Thus, we set these to zero as well. The coefficients in Eq. (5.9) reduce to

$$\begin{aligned} A &= -\frac{\mathcal{D}Q^2}{2SN} \\ B &= \frac{\mathcal{D}Q^2}{SN} \\ C &= 0 \\ D &= 0. \end{aligned} \tag{6.3}$$

Now we do the same transformation as in the case including the dipolar interaction, $a_{\pm\boldsymbol{Q}} = \sqrt{N_{\pm\boldsymbol{Q}}}\exp(i\phi_\pm)$. This gives us

$$\begin{aligned} \mathcal{V}_4 &= A\big[N_{+\boldsymbol{Q}}^2\exp(-2i\phi_+ + 2i\phi_+) + N_{-\boldsymbol{Q}}^2\exp(-2i\phi_- + 2i\phi_-)\big] \\ &\quad + 2B\,N_{+\boldsymbol{Q}}N_{-\boldsymbol{Q}}\exp(-i\phi_+ + i\phi_+)\exp(-i\phi_- + i\phi_-) \\ &= A\frac{1}{2}\big[N_c^2 + \delta^2\big] + 2B\,\frac{1}{4}\big[N_c^2 - \delta^2\big] \\ \mathcal{V}_4 &= \frac{1}{2}N_c^2\big[(A+B) + (A-B)(\delta/N_c)^2\big]. \end{aligned} \tag{6.4}$$

To determine if this system qualifies for BEC, we need to find some minima in the energy/potential. As before, we start by differentiating $\mathcal{V}_4$ with respect to δ and setting the derivative equal to zero

$$\frac{\partial\mathcal{V}_4}{\partial\delta} = \frac{1}{2}N_c^2(A-B)\,2\delta/N_c^2 = 0. \tag{6.5}$$

Eq. (6.5) is fulfilled when $\delta = 0$, which is the extremum point. We now need to check if this extremum point is a maximum, minimum or saddle point. The second derivative of $\mathcal{V}_4$ is

$$\begin{aligned} \frac{\partial^2\mathcal{V}_4}{\partial\delta^2} &= A - B \\ &= -\frac{\mathcal{D}Q^2}{2SN} - \frac{\mathcal{D}Q^2}{SN} \\ &= -\frac{3\mathcal{D}Q^2}{2SN} < 0, \end{aligned} \tag{6.6}$$

where we inserted values for A and B from Eq. (6.3). Since all the constants in the last line in Eq. (6.6) are positive, we know that the total term is always less than zero. Therefore, the second derivative of $\mathcal{V}_4$ is always less than zero, and thus the potential does not have a minimum. This means that there cannot exist a Bose-Einstein condensate of magnons. As we know, such a condensate does exist. This means that we have not successfully explained the system. The missing part is the dipolar interaction.

Chapter 7

Summary and Outlook*

7.1 Summary

In the specialisation project report, we have presented a full analysis of the stability of a magnon BEC in a ferromagnetic insulator. By performing three consecutive transformations, namely the Holstein-Primakoff, Fourier and Bogoliubov transformations, we produced a bosonic Hamiltonian describing the magnetic system. By omitting other momenta than $\pm\boldsymbol{k}_{\mathrm{BEC}}$, we obtained the Hamiltonian describing only the condensate. Inserting the condensate fields, we found the potential function, which we used in our analysis to find potential minima. By tuning the external magnetic field and the thickness of the film, we can tune the parameters such that we obtain a minimum in the potential.

In Part III, we will shift the focus to stability analysis of BEC of magnons in antiferromagnetic insulators.

Part III

Antiferromagnetic System

Chapter 8

Introduction to Antiferromagnetic System

8.1 The antiferromagnetic system

Most of the work done in the master's thesis is presented in Part III (although some sections of Part I also belong to it). In Part II, we investigated the stability of a Bose-Einstein condensate in a ferromagnetic system. Now, the goal is to carry out a similar analysis for an antiferromagnetic system. This is a more difficult task, as the relevant interactions are considerably more complicated due to the bipartite lattice. However, it is also more interesting and rewarding, since much less is known about Bose-Einstein condensation of magnons in antiferromagnetic systems.

We include the direct exchange interaction, magnetic anisotropy, Zeeman coupling and DMI in our system. These interactions were all introduced in Chapter 2. In Part II, we gave an introduction to Bose-Einstein condensates, and the history of the field. We will therefore not repeat that material here, but rather encourage the reader to consult Chapters 1 and 3.

In Chapter 2, Figure 2.1(b), we showed a cubic, bipartite lattice. In the next section, we will elaborate on the dimensionality of our system. However, we always divide the total lattice into two sublattices, A and B. In sublattice A the quantisation axis is along the positive $\hat{\mathbf{z}}$-axis. The spins on sublattice B are aligned antiparallel to the $\hat{\mathbf{z}}$-axis.

In the ferromagnetic case, we included the long-range dipolar interaction. However, we have no significant contribution from this interaction in the antiferromagnetic case. As stated in section 2.3, the dipolar interaction vanishes in the square (cubic) bipartite antiferromagnetic case, due to the dipoles cancelling. The DMI, on the other hand, is non-vanishing for the antiferromagnetic system. We assume a system

similar to those of ref. [49, 50] which has already been investigated experimentally.

For the direct exchange interaction, we include only nearest neighbour interactions, meaning between the two sublattices. The magnetic anisotropy is modelled by on-site anisotropy, which means that there is no interaction between different lattice sites. The same also applies for the Zeeman coupling. The DMI, however, is an inter-site interaction. For the DMI as well, we only look at distances up to nearest neighbours. There are many possible configurations of the DMI, however we will use a uniform DMI. This means that all DM-vectors are parallel. We decided on this configurations based on the properties that this DMI gives the dispersion relations, as elaborated on in ref. [50].

In the ferromagnetic case, there is only one species of magnons. In antiferromagnetic systems on the other hand, there are two species. They are right-handed and left-handed magnons, also referred to as clockwise and counter-clockwise, respectively. As we will see, without an external field to couple the spins to, or without DMI, the two magnon species are degenerate in energy.

After performing a Bogoliubov transformation, the magnons are represented in a diagonal basis. This representation is the one we will use in our investigations. We will find that there are two regions in k-space where the condensates can form, one for each species. We will see that there are terms in the Hamiltonian that cause an oscillation of magnons between the two condensates. This includes a transfer of angular momentum, which was not necessary for the ferromagnetic case. However, this is explained by the spin-orbit coupling (SOC) that also gives rise to the DMI.

We observed in Part II that the interactions between the magnons determine whether there can exist a stable condensate. This is also the case for antiferromagnetic systems. We will see that the interaction between the magnons can be tuned with magnetic anisotropy and DMI. This can be done by doping for the anisotropy, and by applying an external electric field for the DMI.

The main reason for including DMI in our system is that we want to obtain dispersion relations similar to those in ref. [50]. As mentioned, the DMI will shift the dispersion relations and their minima, and thus the momenta at which the condensations occur. This is known as non-reciprocal magnons. The shift causes the condensates to be more easily observed experimentally.

When a magnetic field pulse with energy equal to the gap is applied to the system, magnons at $k = 0$ are excited. This is known as antiferromagnetic resonance (AFMR). To be able to observe the condensates, we need to experimentally observe the constituent magnons. Thus, we need to be able to distinguish the magnons in the condensates, from those that are not part of them [51]. Therefore it is interesting

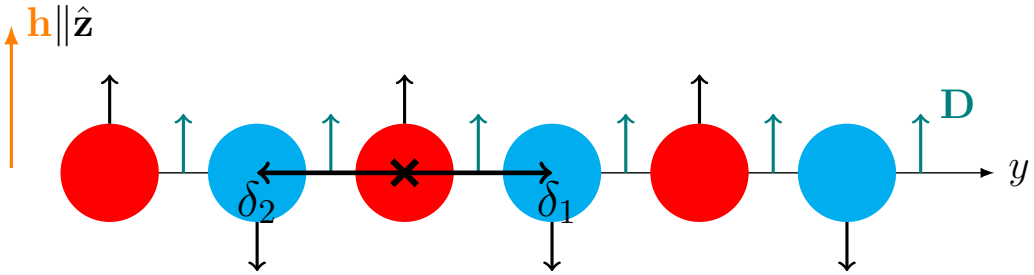

Figure 8.1: Antiferromagnetic 1D spin chain showing orientation of external magnetic field and DMI. The nearest neighbour vectors $\boldsymbol{\delta}_1$ and $\boldsymbol{\delta}_2$ are also shown.

to include DMI, since the resulting system possess the above-mentioned shift away from $k = 0$.

8.2 Dimensionality and symmetry

Real-world physical systems are usually three-dimensional. Yet, some systems are two-dimensional to a good approximation. An example was the YIG film mentioned in Part II. Furthermore, physical systems may sometimes be well described with a model of lower dimension. In this part we will look at a one-dimensional bosonic system. Ref. [52] argues that since we do not have long-range interactions, reducing the dimensionality from 3D to 1D can be done without significantly changing the underlying physics of this system.

Having decided on the dimensionality and the interactions included, we now present an illustration of the resulting system and its interactions in Figure 8.1. Throughout our calculations, we will mostly use a wave vector $\mathbf{k} = (0, k, 0)$. We are thus looking at a 1D spin chain. Note the directions of the $\boldsymbol{\delta}_i$ in Figure 8.1. This will be of great significance in section 9.4.

Like dimensionality, symmetry also effects the way physical systems behave, and some properties can be determined just from symmetry considerations. A famous example is Noëthers theorem [53]. Symmetry is an extensive subject, and we will only mention a few results, directly relevant to this work. First, we note that in the context of spin system, the DMI can only exist if spatial inversion symmetry is broken.

Furthermore, it is relevant to mention the Mermin-Wagner theorem [54, 27]. It states that for one and two-dimensional systems, long-range order cannot exist at finite temperature if the system has a continuous symmetry and short-ranged interactions. Any fluctuation, thermal or quantum mechanical, will disrupt the long-range order of the system. Consequently, we can conclude that the 1D and 2D Heisenberg model, which has a continuous rotation symmetry, must have a critical temperature equal to zero. This is not necessarily the case if we include interactions that break the continuous symmetry.

Finally, Goldstone's theorem [55, 56] asserts that if a continuous symmetry is spontaneously broken in the ground state, then there exist gapless excitations. These are known as Goldstone bosons in general, and as magnons in the case of ferromagnets and antiferromagnets.

Chapter 9

Bosonisation of Antiferromagnetic System

To perform calculations in our current basis will be difficult. The spin operators' commutator is $[S_i^\alpha, S_j^\beta] = i\varepsilon_{\alpha\beta\gamma} S_i^\gamma \delta_{ij}$. The analysis is considerably simplified by a bosonisation procedure, resulting in commutators that maps to a number, as opposed to an operator. We utilise a Holstein-Primakoff transformation, which transforms the spin operators to bosonic operators that have simpler commutation relations on the form $[a_i, a_j^\dagger] = [b_i, b_j^\dagger] = \delta_{ij}$, $[a_i, b_j^\dagger] = 0$, and all others equal to zero.

In an antiferromagnetic system, the bosonisation procedure will be analogous to the ferromagnetic case. However, we now have two sublattices. The Holstein-Primakoff transformation for the up-spins, sublattice A, will be identical to the one applied for a ferromagnetic system, as we assume that the spins are quantised parallel to the $\hat{\mathbf{z}}$-axis. In sublattice B we obtain an adjusted transformation, as we assume that the spins are quantised antiparallel to the $\hat{\mathbf{z}}$-axis. The spin raising and lowering operators for sublattice A are

$$\begin{aligned} S_i^+ &= S_i^x + iS_i^y \\ S_i^- &= (S_i^+)^\dagger = S_i^x - iS_i^y. \end{aligned} \tag{9.1}$$

We introduce the same raising and lowering operators as before, adjusted for sublattice B

$$\begin{aligned} S_j^+ &= S_j^x + iS_j^y \\ S_j^- &= (S_j^+)^\dagger = S_j^x - iS_j^y. \end{aligned} \tag{9.2}$$

We see that we can express $S_{i/j}^x$ and $S_{i/j}^y$ in terms of the raising and lowering operators as

$$\begin{aligned} S_{i/j}^x &= \frac{1}{2}(S_{i/j}^+ + S_{i/j}^-) \\ S_{i/j}^y &= \frac{1}{2i}(S_{i/j}^+ - S_{i/j}^-). \end{aligned} \tag{9.3}$$

As we have two sublattices, one aligning parallel to the $\hat{\mathbf{z}}$-axis, and one aligning antiparallel to the $\hat{\mathbf{z}}$-axis, the Holstein-Primakoff transformation differs for the two sublattices. For sublattice A, the Holstein-Primakoff transformation is

$$\begin{aligned} S_i^z &= S - a_i^\dagger a_i \\ S_i^+ &= \sqrt{2S}\sqrt{1-\frac{a_i^\dagger a_i}{2S}}\,a_i \approx \sqrt{2S}\,(1-\frac{1}{4S}a_i^\dagger a_i)\,a_i \\ S_i^- &= \sqrt{2S}\,a_i^\dagger\sqrt{1-\frac{a_i^\dagger a_i}{2S}} \approx \sqrt{2S}\,a_i^\dagger\,(1-\frac{1}{4S}a_i^\dagger a_i). \end{aligned} \tag{9.4}$$

For sublattice B, the Holstein-Primakoff transformation is

$$\begin{aligned} S_j^z &= -S + b_j^\dagger b_j \\ S_j^+ &= \sqrt{2S}\,b_j^\dagger\sqrt{1-\frac{b_j^\dagger b_j}{2S}} \approx \sqrt{2S}\,b_j^\dagger\,(1-\frac{1}{4S}b_j^\dagger b_j) \\ S_j^- &= \sqrt{2S}\sqrt{1-\frac{b_j^\dagger b_j}{2S}}\,b_j \approx \sqrt{2S}\,(1-\frac{1}{4S}b_j^\dagger b_j)\,b_j. \end{aligned} \tag{9.5}$$

Note the asymmetry in S_i^z and S_j^z in Eq. (9.4) and (9.5). Also observe from $S_{i/j}^z$ in Eqs. (9.4) and (9.5), that $2S$ is the maximum number of bosons on each lattice site. To approximate the square roots in Eq. (9.4) and Eq. (9.5) we utilised the assumption that $\langle a_i^\dagger a_i\rangle/2S \ll 1$. We thus use the same first order approximation for the square root as in the ferromagnetic case, namely $\sqrt{1-x}\approx 1-x/2$. Note that the average $\langle a_i^\dagger a_i\rangle$ is the actual mean number of bosons in the system at a given temperature. Thus it includes both the thermal average and the quantum average. The majority of these magnons are pumped in, as described in Chapter 3.

9.1 Direct exchange interaction

To bosonise the interaction, we start by expanding the dot product in Eq. (2.1) . We obtain two double sums, the first being a sum over sublattice A, with neighbours in sublattice B. The other sum is over sublattice B with neighbours in sublattice A.

$$\begin{aligned} H_{\text{ex}} &= J\sum_{\langle ij\rangle}\left[\frac{1}{2}S_i^+S_j^- + \frac{1}{2}S_i^-S_j^+ + S_i^zS_j^z\right] \\ &= J\sum_{\substack{i\in A\\ j\in B}}\left[\frac{1}{2}S_i^+S_j^- + \frac{1}{2}S_i^-S_j^+ + S_i^zS_j^z\right] + J\sum_{\substack{i\in B\\ j\in A}}\left[\frac{1}{2}S_i^+S_j^- + \frac{1}{2}S_i^-S_j^+ + S_i^zS_j^z\right]. \end{aligned} \tag{9.6}$$

Note that because of the commutativity of the dot product, seen in Eq. (2.1), the sums are identical. Because of this property, we can swap places of the operators

and rename the dummy indices i,j. We thus obtain a Hamiltonian with only one double sum

$$\begin{aligned} H_{\text{ex}} = 2J \sum_{\substack{\langle ij \rangle \\ i\in A \\ j\in B}} \big[& -S^2 + S\big[a_i b_j + a_i^\dagger b_j^\dagger + b_j^\dagger b_j + a_i^\dagger a_i\big] \\ & - \frac{1}{4}\big[a_i b_j^\dagger b_j b_j + a_i^\dagger a_i a_i b_j + a_i^\dagger b_j^\dagger b_j^\dagger b_j + a_i^\dagger a_i^\dagger a_i b_j^\dagger + 4 a_i^\dagger a_i b_j^\dagger b_j\big]\big]. \end{aligned}$$

We have disregarded terms $\mathcal{O}(\{a,b\}^6)$, due to the smallness of their expectation values.

We now define the interacting and non-interacting Hamiltonian for the direct exchange interaction

$$\begin{aligned} H_{\text{ex}}^0 &= -JS^2 Nz \\ H_{\text{ex}}^2 &= 2SJ \sum_{\substack{i\in A \\ j\in B}} \big[a_i b_j + a_i^\dagger b_j^\dagger + b_j^\dagger b_j + a_i a_i^\dagger\big] \\ H_{\text{ex}}^4 &= -\frac{1}{2} J \sum_{\substack{i\in A \\ j\in B}} \big[a_i b_j^\dagger b_j b_j + a_i^\dagger a_i a_i b_j + a_i^\dagger b_j^\dagger b_j^\dagger b_j + a_i^\dagger a_i^\dagger a_i b_j^\dagger + 4 a_i^\dagger a_i b_j^\dagger b_j\big], \end{aligned} \tag{9.7}$$

where N is the number of lattice points on the total lattice, and z is the number of nearest neighbours.

The first line in Eq. (9.7), H_{ex}^0, is just a constant. We absorb it into the reference energy. The second line, H_{ex}^2 is the non-interacting part, as it is $\mathcal{O}(\{a,b\}^2)$. We see that it is not diagonal, since it contains terms of the form $a_i b_j$ and $a_i^\dagger b_j^\dagger$. The last line, H_{ex}^4, is the interacting part. The last term in the interacting part is a density term. Note that the other terms do not conserve the number of bosons.

We will apply a Fourier transformation, which will give us the Hamiltonian in momentum space, while also diagonalising the non-interacting Hamiltonian for the direct exchange interaction.

For sublattice A we insert the inverse Fourier transforms

$$\begin{aligned} a_i &= \frac{1}{\sqrt{N/2}} \sum_{\mathbf{k}} a_{\mathbf{k}}\, \mathrm{e}^{-i\mathbf{k}\cdot r_i} \\ a_i^\dagger &= \frac{1}{\sqrt{N/2}} \sum_{\mathbf{k}} a_{\mathbf{k}}^\dagger\, \mathrm{e}^{i\mathbf{k}\cdot r_i}, \end{aligned} \tag{9.8}$$

where N is the number of lattice points on the total lattice, and $N/2$ is the number of lattice points on each sublattice. The position vector $\mathbf{r}_i$ is generally three-dimensional, however it is reduced to $\mathbf{r}_i = (0, y_i, 0)$ for our calculations on a 1D spin chain.

Similarly, for sublattice B, we have the inverse Fourier transforms

$$b_j = \frac{1}{\sqrt{N/2}} \sum_{\mathbf{k}} b_{\mathbf{k}} \, \mathrm{e}^{-i\mathbf{k}\cdot r_j}$$
$$b_j^\dagger = \frac{1}{\sqrt{N/2}} \sum_{\mathbf{k}} b_{\mathbf{k}}^\dagger \, \mathrm{e}^{i\mathbf{k}\cdot r_j}, \tag{9.9}$$

where, in a similar manner, $\mathbf{r}_j = (0, y_j, 0)$ for the 1D spin chain. Note that since the lattice constant on each sublattice is now twice that of the total lattice, the first Brillouin zone (1BZ) is halved.

We start by expressing the non-interacting Hamiltonian in momentum space. By inserting the transformations in Eq. (9.8) and (9.9) into the non-interacting Hamiltonian in Eq. (9.7), and performing the sums over i and j, we obtain

$$H_{\mathrm{ex}}^2 = 2SJ\Bigg[z \sum_{\mathbf{k}_1\mathbf{k}_2} \delta(\mathbf{k}_1 - \mathbf{k}_2) \, a_{\mathbf{k}_1} a_{\mathbf{k}_2}^\dagger + z \sum_{\mathbf{k}_1\mathbf{k}_2} \delta(\mathbf{k}_1 - \mathbf{k}_2) \, b_{\mathbf{k}_1}^\dagger b_{\mathbf{k}_2}$$
$$+ \sum_{\mathbf{k}_1\mathbf{k}_2} \delta(\mathbf{k}_1 + \mathbf{k}_2) \, \gamma(\mathbf{k}_2) \, a_{\mathbf{k}_1} b_{\mathbf{k}_2} + \sum_{\mathbf{k}_1\mathbf{k}_2} \delta(\mathbf{k}_1 + \mathbf{k}_2) \, \gamma(\mathbf{k}_2) \, a_{\mathbf{k}_1}^\dagger b_{\mathbf{k}_2}^\dagger \Bigg], \tag{9.10}$$

where $\gamma(k) = \sum_\delta \mathrm{e}^{ik\cdot\delta}$, and δ are the vectors from a lattice site to its neighbours. As mentioned in Part II, $\gamma(k)$ is often referred to as the *form factor*. In three dimensions, the δ-sum, over a cubic lattice, is extended to include six nearest neighbours. In our 1D spin chain model, there are two nearest neighbours, and we obtain a contribution of $2\cos(k_x) + 2\cos(k_z)\big|_{k_x=k_z=0} = 4$ to the reference energy.

We can now perform one of the k-sums in each double sum. We then find

$$H_{\mathrm{ex}}^2 = 2SJ \sum_{\mathbf{k}} z[a_{\mathbf{k}}^\dagger a_{\mathbf{k}} + b_{\mathbf{k}}^\dagger b_{\mathbf{k}}] + 2[a_{\mathbf{k}} b_{-\mathbf{k}} + a_{\mathbf{k}}^\dagger b_{-\mathbf{k}}^\dagger] \cos(k), \tag{9.11}$$

where we have utilised that $\cos(k)$ is an even function.

Later, we will gather the bosonic operators in vectors and express the Hamiltonian as a quadratic form. Therefore, we rewrite the Hamiltonian in a symmetric form by using the commutation relations $[a_i, a_j^\dagger] = \delta_{ij}, [b_i, b_i^\dagger] = \delta_{ij}$, at an appropriate stage in the calculations. We will refer to this as the expanded Hamiltonian This will be useful when we diagonalise the non-interacting Hamiltonian through a Bogoliubov transformation in section 10.1. We present it here for later use

$$H_{\mathrm{ex}}^2 = SJ \sum_{\mathbf{k}} z\big[[a_{\mathbf{k}}^\dagger a_{\mathbf{k}} + a_{\mathbf{k}} a_{\mathbf{k}}^\dagger + b_{\mathbf{k}}^\dagger b_{\mathbf{k}} + b_{\mathbf{k}} b_{\mathbf{k}}^\dagger]$$
$$+2[a_{\mathbf{k}} b_{-\mathbf{k}} + b_{-\mathbf{k}} a_{\mathbf{k}} + a_{\mathbf{k}}^\dagger b_{-\mathbf{k}}^\dagger + b_{-\mathbf{k}}^\dagger a_{\mathbf{k}}^\dagger] \cos(k)\big]. \tag{9.12}$$

We now look at the interaction Hamiltonian in Eq. (9.7). We once again insert the

inverse Fourier transformations from Eq. (9.8) and (9.9), into H_{ex}^4. We find

$$\begin{aligned} H_{\text{ex}}^4 = 2J(-\frac{1}{4})\frac{1}{(N/2)} &\sum_{\mathbf{k}_1\ldots\mathbf{k}_4} a_{\mathbf{k}_1} b_{\mathbf{k}_2}^\dagger b_{\mathbf{k}_3} b_{\mathbf{k}_4}\, \delta(\mathbf{k}_2 - \mathbf{k}_1 - \mathbf{k}_3 - \mathbf{k}_4) \sum_\delta \mathrm{e}^{i(\mathbf{k}_2-\mathbf{k}_3-\mathbf{k}_4)\cdot\delta} \\ &+ \sum_{\mathbf{k}_1\ldots\mathbf{k}_4} a_{\mathbf{k}_1}^\dagger a_{\mathbf{k}_2} a_{\mathbf{k}_3} b_{\mathbf{k}_4}\, \delta(\mathbf{k}_1 - \mathbf{k}_2 - \mathbf{k}_3 - \mathbf{k}_4) \sum_\delta \mathrm{e}^{-i\mathbf{k}_4\cdot\delta} \\ &+ \sum_{\mathbf{k}_1\ldots\mathbf{k}_4} a_{\mathbf{k}_1}^\dagger b_{\mathbf{k}_2}^\dagger b_{\mathbf{k}_3}^\dagger b_{\mathbf{k}_4}\, \delta(\mathbf{k}_1 + \mathbf{k}_2 + \mathbf{k}_3 - \mathbf{k}_4) \sum_\delta \mathrm{e}^{i(\mathbf{k}_2+\mathbf{k}_3-\mathbf{k}_4)\cdot\delta} \\ &+ \sum_{\mathbf{k}_1\ldots\mathbf{k}_4} a_{\mathbf{k}_1}^\dagger a_{\mathbf{k}_2}^\dagger a_{\mathbf{k}_3} b_{\mathbf{k}_4}^\dagger\, \delta(\mathbf{k}_1 + \mathbf{k}_2 + \mathbf{k}_4 - \mathbf{k}_3) \sum_\delta \mathrm{e}^{i\mathbf{k}_4\cdot\delta} \\ &+4 \sum_{\mathbf{k}_1\ldots\mathbf{k}_4} a_{\mathbf{k}_1}^\dagger a_{\mathbf{k}_2} b_{\mathbf{k}_3}^\dagger b_{\mathbf{k}_4}\, \delta(\mathbf{k}_1 + \mathbf{k}_3 - \mathbf{k}_2 - \mathbf{k}_4) \sum_\delta \mathrm{e}^{i(\mathbf{k}_3-\mathbf{k}_4)\cdot\delta}. \end{aligned} \tag{9.13}$$

Performing one of the k-sums and renaming the indices, we obtain

$$\begin{aligned} H_{\text{ex}}^4 = 4J(-\frac{1}{4})\frac{1}{(N/2)} \sum_{\mathbf{k},\mathbf{q},\mathbf{q}'} \cos(k)[&a_{\mathbf{k}} b_{\mathbf{k}+\mathbf{q}+\mathbf{q}'} b_{\mathbf{q}} b_{\mathbf{q}'} + a_{\mathbf{k}+\mathbf{q}+\mathbf{q}'} a_{\mathbf{q}} b_{\mathbf{k}} + \text{h.c.} \\ &+4a_{\mathbf{q}-\mathbf{k}}^\dagger a_{\mathbf{q}} b_{\mathbf{q}'+\mathbf{k}}^\dagger b_{\mathbf{q}'}], \end{aligned}$$

where h.c. denotes the Hermitian conjugates of the terms in front of it.

9.2 Magnetic anisotropy

The magnetic anisotropy was first introduced in Eq. (2.5). As mentioned, we assume on-site, easy-axis anisotropy along the $\hat{\mathbf{z}}$-axis, $\hat{\mathbf{e}}_{\text{easy}} \parallel \hat{\mathbf{z}}$. We now split the sum for our two sublattices. We obtain

$$H_{\text{ani}} = -K_z \sum_i (S_i^z)^2 - K_z \sum_j (S_j^z)^2, \tag{9.14}$$

where the i-sum runs over sublattice A, while the j-sum runs over sublattice B.

We now insert the Holstein-Primakoff transformation given in Eqs. (9.4) and (9.5). The transformed Hamiltonian is then

$$H_{\text{ani}} = -K_z \sum_i \left[S^2 - 2Sa_i^\dagger a_i + a_i^\dagger a_i a_i^\dagger a_i\right] - K_z \sum_j \left[S^2 - 2Sb_j^\dagger b_j + b_j^\dagger b_j b_j^\dagger b_j\right]. \tag{9.15}$$

The first term in each sum is just a constant, which we absord into the reference energy. The second term is the non-interacting Hamiltonian, while the last term is the interaction Hamiltonian.

We can split Eq. (9.15) into a Hamiltonian for the non-interacting part, H_{ani}^2 and a

Hamiltonian for the interaction part H^4_{ani}

$$H^2_{\text{ani}} = 2SK_z\Big[\sum_i a_i^\dagger a_i + \sum_j b_j^\dagger b_j\Big]$$
$$H^4_{\text{ani}} = -K_z\Big[\sum_i a_i^\dagger a_i a_i^\dagger a_i + \sum_j b_j^\dagger b_j b_j^\dagger b_j\Big]. \tag{9.16}$$

As for the direct exchange interaction, we want to insert the inverse Fourier transformations into Eqs. (9.8) and (9.9) to bring the Hamiltonian to momentum space. We start by considering the non-interacting Hamiltonian

$$H^2_{\text{ani}} = 2SK_z \sum_{\mathbf{k}} \big[a_{\mathbf{k}}^\dagger a_{\mathbf{k}} + b_{\mathbf{k}}^\dagger b_{\mathbf{k}}\big]. \tag{9.17}$$

For later convenience, we introduce the expanded H^2_{ani} which is useful for matrix-notation. In addition to an extra term for the reference energy arising from the commutation relations, the expanded non-interacting Hamiltonian is

$$H^2_{\text{ani}} = SK_z \sum_{\mathbf{k}} \big[a_{\mathbf{k}}^\dagger a_{\mathbf{k}} + a_{\mathbf{k}} a_{\mathbf{k}}^\dagger + b_{\mathbf{k}}^\dagger b_{\mathbf{k}} + b_{\mathbf{k}} b_{\mathbf{k}}^\dagger\big]. \tag{9.18}$$

We find the interaction Hamiltonian the same way, namely by inserting the inverse Fourier-transformations in Eqs. (9.8) and (9.9), into H^4_{ani}, giving

$$\begin{aligned} H^4_{\text{ani}} &= -K_z \frac{1}{(N/2)}\Big[\sum_{\mathbf{k}_1\ldots\mathbf{k}_4} a_{\mathbf{k}_1}^\dagger a_{\mathbf{k}_2} a_{\mathbf{k}_3}^\dagger a_{\mathbf{k}_4} \delta(\mathbf{k}_1 + \mathbf{k}_3 - \mathbf{k}_2 - \mathbf{k}_4) \\ &\qquad + \sum_{\mathbf{k}_1\ldots\mathbf{k}_4} b_{\mathbf{k}_1}^\dagger b_{\mathbf{k}_2} b_{\mathbf{k}_3}^\dagger b_{\mathbf{k}_4} \delta(\mathbf{k}_1 + \mathbf{k}_3 - \mathbf{k}_2 - \mathbf{k}_4)\Big] \\ &= -K_z \frac{1}{(N/2)} \sum_{\mathbf{k}\mathbf{q}\mathbf{q}'} \big[a_{\mathbf{q}-\mathbf{k}}^\dagger a_{\mathbf{q}} a_{\mathbf{q}'+\mathbf{k}}^\dagger a_{\mathbf{q}'} + b_{\mathbf{q}-\mathbf{k}}^\dagger b_{\mathbf{q}} b_{\mathbf{q}'+\mathbf{k}}^\dagger b_{\mathbf{q}'}\big]. \end{aligned} \tag{9.19}$$

We see that the expressions for the magnetic anisotropy, Eqs. (9.17) and (9.19) are quite simple.

9.3 Zeeman coupling

To bosonise the Zeeman coupling, we insert the Holstein-Primakoff transformation in Eqs. (9.4) and (9.5) into Eq. (2.6)

$$H_{\text{Zee}} = -\mu h \sum_{i\in A} \big[S - a_i^\dagger a_i\big] - \mu h \sum_{j\in B} \big[-S + b_j^\dagger b_j\big], \tag{9.20}$$

where i sums over sublattice A, and j over sublattice B. An important note here is that the Zeeman coupling does not contribute to the interaction Hamiltonian, it

is purely non-interacting. Note also that we do not obtain a contribution to the reference energy, as the terms $\mathcal{O}(S)$ cancel.

We insert the inverse Fourier transforms in Eqs. (9.8) and (9.9) to obtain

$$H_{\text{Zee}} = -g_{\text{e}}\mu_{\text{B}}h\sum_{\mathbf{k}}\left[b_{\mathbf{k}}^{\dagger}b_{\mathbf{k}} - a_{\mathbf{k}}^{\dagger}a_{\mathbf{k}}\right]. \tag{9.21}$$

Again we introduce the expanded Hamiltonian, which will prove convenient when we write the total non-interacting Hamiltonian in matrix notation

$$H_{\text{Zee}} = -\frac{\mu h}{2}\sum_{\mathbf{k}}\left[b_{\mathbf{k}}^{\dagger}b_{\mathbf{k}} + b_{\mathbf{k}}b_{\mathbf{k}}^{\dagger} - a_{\mathbf{k}}^{\dagger}a_{\mathbf{k}} - a_{\mathbf{k}}a_{\mathbf{k}}^{\dagger}\right]. \tag{9.22}$$

9.4 Dzyaloshinskii-Moriya interaction

By inspecting Figure 3 and arguments in [[50], we use a DM-vector that is parallel to the $\hat{\mathbf{z}}$-axis. We see from the reference that to obtain the system we desire, the DM-vector needs to be uniform, rather than staggered. This will ensure that the clockwise and anti-clockwise magnon bands split, and are no longer degenerate in energy. Uniform DMI means that the DM-vector is parallel to the $\hat{\mathbf{z}}$-axis at every lattice point.

The DMI in this setup is carried by nearest neighbour interactions. As usual, we will denote this by $\langle ij\rangle$, where i denotes the lattice point and j the nearest neighbours. By letting the DM-vector be parallel to the $\hat{\mathbf{z}}$-axis, $\mathbf{D}_{ij} = D\nu_{ij}\hat{\mathbf{z}}$, Eq. (2.8) expands to

$$H_{\text{DMI}} = D\sum_{\langle ij\rangle}\nu_{ij}\left[\vec{S}_i \times \vec{S}_j\right]_z, \tag{9.23}$$

where in the double sum, i runs over the total lattice, while j runs over the nearest neighbours of a lattice point. ν_{ij} is inserted to conserve the DM-vector's antisymmetry, namely $\mathbf{D}_{ij} = -\mathbf{D}_{ji}$. The symmetry of ν is then $\nu_{ij} = -\nu_{ji}$.

We divide the the double sum in Eq. (9.23) into two double sums, one where we sum over sublattice A, with neighbours in sublattice B and vice versa. Explicitly, we use i as the lattice index, and j for the nearest neighbours in both double sums

$$H_{\text{DMI}} = \frac{D}{2i}\sum_{\substack{\langle ij\rangle \\ i\in A \\ j\in B}}\nu_{ij}\left[S_i^- S_j^+ - S_i^+ S_j^-\right] + \frac{D}{2i}\sum_{\substack{\langle ij\rangle \\ i\in B \\ j\in A}}\nu_{ij}\left[S_i^- S_j^+ - S_i^+ S_j^-\right]. \tag{9.24}$$

We now insert the Holstein-Primakoff transformation in Eqs. (9.1) and (9.2) into H_{DMI}, which gives

$$\begin{aligned}H_{\mathrm{DMI}} =&\frac{D}{2i}\sum_{\substack{\langle ij\rangle\\ i\in A\\ j\in B}}\nu_{ij}\,2S\big[a_i^\dagger b_j^\dagger-\frac{1}{4S}\big[a_i^\dagger b_j^\dagger b_j^\dagger b_j+a_i^\dagger a_i^\dagger a_i b_j^\dagger\big]-a_i b_j+\frac{1}{4S}\big[a_i b_j^\dagger b_j b_j+a_i^\dagger a_i a_i b_j\big]\big]\\ &+\frac{D}{2i}\sum_{\substack{\langle ij\rangle\\ i\in B\\ j\in A}}\nu_{ij}\,2S\big[b_i a_j-\frac{1}{4S}[b_i a_j^\dagger a_j a_j+b_i^\dagger b_i b_i a_j]-b_i^\dagger a_j^\dagger+\frac{1}{4S}\big[b_i^\dagger a_j^\dagger a_j^\dagger a_j+b_i^\dagger b_i^\dagger b_i a_j^\dagger\big]\big].\end{aligned} \tag{9.25}$$

We should note here that both a- and b-operators have i and j as indices.

We divide H_{DMI} into a non-interacting Hamiltonian and an interacting Hamiltonian,

$$\begin{aligned}H^2_{\mathrm{DMI}} =& \frac{D}{2i}\sum_{\substack{\langle ij\rangle\\ i\in A\\ j\in B}}\nu_{ij}\,2S\left[a_i^\dagger b_j^\dagger-a_i b_j\right]+\frac{D}{2i}\sum_{\substack{\langle ij\rangle\\ i\in B\\ j\in A}}\nu_{ij}\,2S\left[b_i a_j-b_i^\dagger a_j^\dagger\right]\\ H^4_{\mathrm{DMI}} =& \frac{D}{2i}\sum_{\substack{\langle ij\rangle\\ i\in A\\ j\in B}}\left[-\frac{1}{4S}\big[a_i^\dagger b_j^\dagger b_j^\dagger b_j+a_i^\dagger a_i^\dagger a_i b_j^\dagger\big]+\frac{1}{4S}\big[a_i b_j^\dagger b_j b_j+a_i^\dagger a_i a_i b_j\big]\right]\\ &+\sum_{\substack{\langle ij\rangle\\ i\in B\\ j\in A}}\left[-\frac{1}{4S}\big[b_i a_j^\dagger a_j a_j+b_i^\dagger b_i b_i a_j\big]+\frac{1}{4S}\big[b_i^\dagger a_j^\dagger a_j^\dagger a_j+b_i^\dagger b_i^\dagger b_i a_j^\dagger\big]\right].\end{aligned} \tag{9.26}$$

We start by investigating the non-interacting Hamiltonian, H^2_{DMI}. We insert the inverse Fourier transform of the operators from Eqs. (9.8) and (9.9). The non-interacting Hamiltonian then becomes

$$\begin{aligned}H^2_{\mathrm{DMI}} =& \frac{D}{2i}\sum_{i\in A}2S\frac{1}{N/2}\Bigg[\sum_{\mathbf{k}_1\mathbf{k}_2}a^\dagger_{\mathbf{k}_1}b^\dagger_{\mathbf{k}_2}\mathrm{e}^{i(\mathbf{k}_1+\mathbf{k}_2)\cdot\mathbf{r}_i}\sum_\delta\nu_{i,i+\delta}\,\mathrm{e}^{i\mathbf{k}_2\cdot\delta}\\ &\qquad-\sum_{\mathbf{k}_1\mathbf{k}_2}a_{\mathbf{k}_1}b_{\mathbf{k}_2}\mathrm{e}^{-i(\mathbf{k}_1+\mathbf{k}_2)\cdot\mathbf{r}_i}\sum_\delta\nu_{i,i+\delta}\,\mathrm{e}^{-i\mathbf{k}_2\cdot\delta}\Bigg]\\ &+\frac{D}{2i}\sum_{i\in B}2S\frac{1}{N/2}\Bigg[\sum_{\mathbf{k}_1\mathbf{k}_2}b_{\mathbf{k}_1}a_{\mathbf{k}_2}\mathrm{e}^{-i(\mathbf{k}_1+\mathbf{k}_2)\cdot\mathbf{r}_i}\sum_\delta\nu_{i,i+\delta}\,\mathrm{e}^{-i\mathbf{k}_2\cdot\delta}\\ &\qquad-\sum_{\mathbf{k}_1\mathbf{k}_2}b^\dagger_{\mathbf{k}_1}a^\dagger_{\mathbf{k}_2}\mathrm{e}^{i(\mathbf{k}_1+\mathbf{k}_2)\cdot\mathbf{r}_i}\sum_\delta\nu_{i,i+\delta}\,\mathrm{e}^{i\mathbf{k}_2\cdot\delta}\Bigg].\end{aligned} \tag{9.27}$$

Collecting terms gives

$$\begin{aligned}H^2_{\mathrm{DMI}} =&\frac{D}{2i}2S\sum_{\mathbf{k}}a^\dagger_{\mathbf{k}}b^\dagger_{-\mathbf{k}}\sum_\delta\nu_{i,i+\delta}\big(\mathrm{e}^{-i\mathbf{k}\cdot\delta}-\mathrm{e}^{i\mathbf{k}\cdot\delta}\big)\\ &+\frac{D}{2i}2S\sum_{\mathbf{k}}b_{-\mathbf{k}}a_{\mathbf{k}}\sum_\delta\nu_{i,i+\delta}\big(\mathrm{e}^{-i\mathbf{k}\cdot\delta}-\mathrm{e}^{i\mathbf{k}\cdot\delta}\big).\end{aligned} \tag{9.28}$$

Note that the last part of both lines in Eq. (9.28) is a sine function. Without $\nu_{i,i+\delta}$ this sum would be zero. However, because of the definitions of δ in Figure 8.1 we see that for δ_2, the $\nu_{i,i+\delta_2}$ becomes negative. This ensures a non-zero, non-interacting Hamiltonian for DMI

$$H^2_{\mathrm{DMI}} = -D4S \sum_{\mathbf{k}} \left[a^\dagger_{\mathbf{k}} b^\dagger_{-\mathbf{k}} + a_{\mathbf{k}} b_{-\mathbf{k}} \right] \sin(k). \tag{9.29}$$

We present the expanded H^2_{DMI}, which will be useful later.

$$H^2_{\mathrm{DMI}} = -D2S \sum_{\mathbf{k}} \left[a^\dagger_{\mathbf{k}} b^\dagger_{-\mathbf{k}} + a^\dagger_{\mathbf{k}} b^\dagger_{-\mathbf{k}} + a_{\mathbf{k}} b_{-\mathbf{k}} + a_{\mathbf{k}} b_{-\mathbf{k}} \right]. \tag{9.30}$$

We now turn to the interaction part of the Hamiltonian, H^4_{DMI} in Eq. (9.26). Inserting the inverse Fourier transforms of the operators brings it to momentum space

$$\begin{aligned}
H^4_{\mathrm{DMI}} = \frac{D}{2i} \sum_{i\in A} \frac{1}{(N/2)^2} \Bigg\{ -\frac{1}{2} \Bigg[& \sum_{\mathbf{k}_1 \ldots \mathbf{k}_4} a^\dagger_{\mathbf{k}_1} b^\dagger_{\mathbf{k}_2} b^\dagger_{\mathbf{k}_3} b_{\mathbf{k}_4} \mathrm{e}^{i(\mathbf{k}_1+\mathbf{k}_2+\mathbf{k}_3-\mathbf{k}_4)\cdot \mathbf{r}_i} \sum_\delta \nu_{i,i+\delta} \mathrm{e}^{i(\mathbf{k}_2+\mathbf{k}_3-\mathbf{k}_4)\cdot\delta} \\
& + \sum_{\mathbf{k}_1 \ldots \mathbf{k}_4} a^\dagger_{\mathbf{k}_1} a^\dagger_{\mathbf{k}_2} a_{\mathbf{k}_3} b^\dagger_{\mathbf{k}_4} \mathrm{e}^{i(\mathbf{k}_1+\mathbf{k}_2+\mathbf{k}_4-\mathbf{k}_3)\cdot \mathbf{r}_i} \sum_\delta \nu_{i,i+\delta} \mathrm{e}^{i\mathbf{k}_4\cdot\delta} \Bigg] \\
+ \frac{1}{2} \Bigg[& \sum_{\mathbf{k}_1 \ldots \mathbf{k}_4} a_{\mathbf{k}_1} b^\dagger_{\mathbf{k}_2} b_{\mathbf{k}_3} b_{\mathbf{k}_4} \mathrm{e}^{i(\mathbf{k}_2-\mathbf{k}_1-\mathbf{k}_3-\mathbf{k}_4)\cdot \mathbf{r}_i} \sum_\delta \nu_{i,i+\delta} \mathrm{e}^{i(\mathbf{k}_2+\mathbf{k}_3-\mathbf{k}_4)\cdot\delta} \\
& + \sum_{\mathbf{k}_1 \ldots \mathbf{k}_4} b^\dagger_{\mathbf{k}_1} b^\dagger_{\mathbf{k}_2} b_{\mathbf{k}_3} a^\dagger_{\mathbf{k}_4} \mathrm{e}^{i(\mathbf{k}_1+\mathbf{k}_2+\mathbf{k}_4-\mathbf{k}_3)\cdot \mathbf{r}_i} \sum_\delta \nu_{i,i+\delta} \mathrm{e}^{i\mathbf{k}_4\cdot\delta} \Bigg] \Bigg\} \\
+ \frac{D}{2i} \sum_{i\in B} \frac{1}{(N/2)^2} \Bigg\{ -\frac{1}{2} \Bigg[& \sum_{\mathbf{k}_1 \ldots \mathbf{k}_4} b_{\mathbf{k}_1} a^\dagger_{\mathbf{k}_2} a_{\mathbf{k}_3} a_{\mathbf{k}_4} \mathrm{e}^{i(\mathbf{k}_2-\mathbf{k}_1-\mathbf{k}_3-\mathbf{k}_4)\cdot \mathbf{r}_i} \sum_\delta \nu_{i,i+\delta} \mathrm{e}^{i(\mathbf{k}_2-\mathbf{k}_3-\mathbf{k}_4)\cdot\delta} \\
& + \sum_{\mathbf{k}_1 \ldots \mathbf{k}_4} b^\dagger_{\mathbf{k}_1} b_{\mathbf{k}_2} b_{\mathbf{k}_3} a_{\mathbf{k}_4} \mathrm{e}^{i(\mathbf{k}_1-\mathbf{k}_2-\mathbf{k}_3-\mathbf{k}_4)\cdot \mathbf{r}_i} \sum_\delta \nu_{i,i+\delta} \mathrm{e}^{-i\mathbf{k}_4\cdot\delta} \Bigg] \\
+ \frac{1}{2} \Bigg[& \sum_{\mathbf{k}_1 \ldots \mathbf{k}_4} b^\dagger_{\mathbf{k}_1} a^\dagger_{\mathbf{k}_2} a^\dagger_{\mathbf{k}_3} a_{\mathbf{k}_4} \mathrm{e}^{i(\mathbf{k}_1+\mathbf{k}_2+\mathbf{k}_3-\mathbf{k}_4)\cdot \mathbf{r}_i} \sum_\delta \nu_{i,i+\delta} \mathrm{e}^{i(\mathbf{k}_2+\mathbf{k}_3-\mathbf{k}_4)\cdot\delta} \\
& + \sum_{\mathbf{k}_1 \ldots \mathbf{k}_4} b^\dagger_{\mathbf{k}_1} b^\dagger_{\mathbf{k}_2} b_{\mathbf{k}_3} a^\dagger_{\mathbf{k}_4} \mathrm{e}^{i(\mathbf{k}_1+\mathbf{k}_2+\mathbf{k}_4-\mathbf{k}_3)\cdot \mathbf{r}_i} \sum_\delta \nu_{i,i+\delta} \mathrm{e}^{i\mathbf{k}_4\cdot\delta} \Bigg] \Bigg\}.
\end{aligned} \tag{9.31}$$

As in the non-interacting part, $\nu_{i,j}$ keeps the sum of sines non-zero. By carrying out sums over i, one $\mathbf{k}_i$ and renaming, we obtain the following expression for the interaction part of the DMI

$$\begin{aligned}
H^4_{\mathrm{DMI}} = D \frac{1}{(N/2)} \sum_{\mathbf{k}\mathbf{q}\mathbf{q}'} \sin(k) \Big[& a^\dagger_{\mathbf{k}} b^\dagger_{\mathbf{q}} b^\dagger_{\mathbf{q}'} b_{\mathbf{k}+\mathbf{q}+\mathbf{q}'} + a_{\mathbf{k}} b^\dagger_{\mathbf{k}+\mathbf{q}+\mathbf{q}'} b_{\mathbf{q}} b_{\mathbf{q}'} \\
& - a^\dagger_{\mathbf{q}} a^\dagger_{\mathbf{q}'} a_{\mathbf{q}+\mathbf{q}'+\mathbf{k}} b^\dagger_{\mathbf{k}} - a^\dagger_{\mathbf{q}+\mathbf{q}'+\mathbf{k}} a_{\mathbf{q}} a_{\mathbf{q}'} b_{\mathbf{k}} \Big].
\end{aligned} \tag{9.32}$$

9.5 Total Hamiltonian

Having obtained the non-interacting and interaction Hamiltonian in momentum space for all interactions, we now add them together. To simplify the expressions, we define two new functions

$$\begin{aligned} f_2(k) &= J\,\cos(k) \\ f_3(k) &= D\,\sin(k). \end{aligned} \tag{9.33}$$

For the non-interacting Hamiltonian, we use the expression for H^2_{ex} in Eq. (9.11). For the magnetic anisotropy, H^2_{ani} from Eq. (9.17) will contribute. As the Zeeman coupling is purely non-interaction, we insert the entire H_{Zee} from Eq. (9.21). From DMI, H^2_{DMI} Eq. (9.29) will add to the total non-interacting Hamiltonian.

We thus obtain the following non-interacting, total Hamiltonian

$$\begin{aligned} H^2 &= H^2_{\text{ex}} + H^2_{\text{ani}} + H_{\text{Zee}} + H^2_{\text{DMI}} \\ &= SJ\sum_{\mathbf{k}} z[a^\dagger_{\mathbf{k}}a_{\mathbf{k}} + b^\dagger_{\mathbf{k}}b_{\mathbf{k}}] + 2SJ[a_{\mathbf{k}}b_{-\mathbf{k}} + a^\dagger_{\mathbf{k}}b^\dagger_{-\mathbf{k}}]\cos(k) \\ &+ 2SK_z\sum_{\mathbf{k}}\left[a^\dagger_{\mathbf{k}}a_{\mathbf{k}} + b^\dagger_{\mathbf{k}}b_{\mathbf{k}}\right] - \mu h\sum_{\mathbf{k}}\left[b^\dagger_{\mathbf{k}}b_{\mathbf{k}} - a^\dagger_{\mathbf{k}}a_{\mathbf{k}}\right] \\ &- D4S\sum_{\mathbf{k}}\left[a^\dagger_{\mathbf{k}}b^\dagger_{-\mathbf{k}} + a_{\mathbf{k}}b_{-\mathbf{k}}\right]\sin(k). \end{aligned} \tag{9.34}$$

We observe that there are no linear terms, $\mathcal{O}(\{a,b\})$. This is because we found the correct quantisation axis. Another important observation is that H^2 is not diagonal. H^2 contains terms that are off-diagonal such as e.g. $a^\dagger_{\mathbf{k}}b_{-\mathbf{k}}$. We will therefore, in the next chapter, perform a Bogoliubov transformation.

We collect the terms of the Hamiltonians for the total interacting Hamiltonian as well. We use H^4_{ex} in Eq. (9.14) for the direct exchange interaction. Magnetic anisotropy contributes with H^4_{ani} from Eq. (9.19). As mentioned above, the Zeeman coupling does not contribute to the interaction Hamiltonian. For DMI, H^4_{DMI} in Eq. (9.32) contributes. We thus obtain the following total interaction Hamiltonian

$$\begin{aligned} H^4 &= H^4_{\text{ex}} + H^4_{\text{ani}} + H^4_{\text{DMI}} \\ &= 4J(-\frac{1}{4})\frac{1}{(N/2)}\sum_{\mathbf{k},\mathbf{q},\mathbf{q}'}\cos(k)[a_{\mathbf{k}}b_{\mathbf{k}+\mathbf{q}+\mathbf{q}'}b_{\mathbf{q}}b_{\mathbf{q}'} + a_{\mathbf{k}+\mathbf{q}+\mathbf{q}'}a_{\mathbf{q}}b_{\mathbf{k}} + \text{h.c.} \\ &\qquad\qquad +4a^\dagger_{\mathbf{q}-\mathbf{k}}a_{\mathbf{q}}b^\dagger_{\mathbf{q}'+\mathbf{k}}b_{\mathbf{q}'}] \\ &- K_z\frac{1}{(N/2)}\sum_{\mathbf{k}\mathbf{q}\mathbf{q}'}\left[a^\dagger_{\mathbf{q}-\mathbf{k}}a_{\mathbf{q}}a^\dagger_{\mathbf{q}'+\mathbf{k}}a_{\mathbf{q}'} + b^\dagger_{\mathbf{q}-\mathbf{k}}b_{\mathbf{q}}b^\dagger_{\mathbf{q}'+\mathbf{k}}b_{\mathbf{q}'}\right] \\ &+ D\frac{1}{(N/2)}\sum_{\mathbf{k}\mathbf{q}\mathbf{q}'}\sin(k)\Big[a^\dagger_{\mathbf{k}}b^\dagger_{\mathbf{q}}b^\dagger_{\mathbf{q}'}b_{\mathbf{k}+\mathbf{q}+\mathbf{q}'} + a_{\mathbf{k}}b^\dagger_{\mathbf{k}+\mathbf{q}+\mathbf{q}'}b_{\mathbf{q}}b_{\mathbf{q}'} \\ &\qquad\qquad -a^\dagger_{\mathbf{q}}a^\dagger_{\mathbf{q}'}a_{\mathbf{q}+\mathbf{q}'+\mathbf{k}}b^\dagger_{\mathbf{k}} - a^\dagger_{\mathbf{q}+\mathbf{q}'+\mathbf{k}}a_{\mathbf{q}}a_{\mathbf{q}'}b_{\mathbf{k}}\Big]. \end{aligned} \tag{9.35}$$

In the next chapter, we will rewrite H^4 in terms of the Bogoliubov basis that we find through the diagonalisation.

Chapter 10

Stability Analysis of Antiferromagnetic System

We see that even in momentum space, the non-interacting Hamiltonian is still not diagonal. We thus need to perform a Bogoliubov transformation to diagonalise it. During the process of finding the appropriate Bogoliubov transformation, we will also find the dispersion relation for the clockwise and counter-clockwise magnons. We expect to find dispersion relations similar to Figure 3dI in ref. [50]. The next step in the stability analysis will then be to reduce the triple sum of the interaction Hamiltonian, to the specific momenta where the condensates exist. They exist at the minima of the dispersion relations. We will see that the condensations occur at $\mathbf{k} \pm \mathbf{Q}$.

After finding the interaction Hamiltonian at the momenta where the condensates exist, we insert the Bogoliubov transformation. Physically, this means that we find a basis that renders the non-interacting Hamiltonian diagonal, and treat the interacting Hamiltonian as a small perturbation. When we have obtained the Hamiltonian describing the interactions between the magnons, we insert the expectation value of the operators, known as a Madelung transformation. We then obtain the interaction potential. This is the potential that determines if the interactions are repulsive, and a condensate can exist, or if they are attractive, and a condensate cannot exist.

10.1 Bogoliubov transformation

We start by collecting the expanded non-interacting Hamiltonians, namely H^2_{ex} from Eq. (9.12) for the direct exchange interaction, H^2_{ani} from Eq. (9.18) for the magnetic anisotropy, H^2_{Zee} from Eq. (9.22) for the Zeeman coupling and H^2_{DMI} Eq. (9.30) for

the DMI. The expanded, non-interacting Hamiltonian is then

$$\begin{aligned} H^2 = SJ \sum_{\mathbf{k}} & \big[z[a^\dagger_{\mathbf{k}} a_{\mathbf{k}} + a_{\mathbf{k}} a^\dagger_{\mathbf{k}} + b^\dagger_{\mathbf{k}} b_{\mathbf{k}} + b_{\mathbf{k}} b^\dagger_{\mathbf{k}}] \\ & +2[a_{\mathbf{k}} b_{-\mathbf{k}} + b_{-\mathbf{k}} a_{\mathbf{k}} + a^\dagger_{\mathbf{k}} b^\dagger_{-\mathbf{k}} + b^\dagger_{-\mathbf{k}} a^\dagger_{\mathbf{k}}] \cos(k)\big] \\ +SK_z \sum_{\mathbf{k}} & \big[a^\dagger_{\mathbf{k}} a_{\mathbf{k}} + a_{\mathbf{k}} a^\dagger_{\mathbf{k}} + b^\dagger_{\mathbf{k}} b_{\mathbf{k}} + b_{\mathbf{k}} b^\dagger_{\mathbf{k}}\big] \\ -\frac{\mu h}{2} \sum_{\mathbf{k}} & \big[b^\dagger_{\mathbf{k}} b_{\mathbf{k}} + b_{\mathbf{k}} b^\dagger_{\mathbf{k}} - a^\dagger_{\mathbf{k}} a_{\mathbf{k}} - a_{\mathbf{k}} a^\dagger_{\mathbf{k}}\big] \\ -D2S \sum_{\mathbf{k}} & \big[a^\dagger_{\mathbf{k}} b^\dagger_{-\mathbf{k}} + a^\dagger_{\mathbf{k}} b^\dagger_{-\mathbf{k}} + a_{\mathbf{k}} b_{-\mathbf{k}} + a_{\mathbf{k}} b_{-\mathbf{k}}\big] \sin(k). \end{aligned} \tag{10.1}$$

To clean up the expressions, we define three new coefficients

$$\begin{aligned} \omega_E &= 2SJ \\ \omega_D &= 2DS \\ \omega_A &= SK_z \\ \omega_H &= \frac{1}{2}\mu h, \end{aligned} \tag{10.2}$$

where we have explicitly inserted $z = 2$ in the direct exchange interaction, as we consider a 1D spin chain.

We want to write the Hamiltonian in Eq. (10.1) on matrix form. When we have achieved that, we can start diagonalising it. The first step is to collect terms

$$\begin{aligned} H^2 = \sum_{\mathbf{k}} & \big[\omega_E + \omega_A + \omega_H\big] a^\dagger_{\mathbf{k}} a_{\mathbf{k}} + \big[\omega_E + \omega_A + \omega_H\big] a_{\mathbf{k}} a^\dagger_{\mathbf{k}} \\ & + \big[\omega_E + \omega_A - \omega_H\big] b^\dagger_{\mathbf{k}} b_{\mathbf{k}} + \big[\omega_E + \omega_A - \omega_H\big] b_{\mathbf{k}} b^\dagger_{\mathbf{k}} \\ & + \big[\omega_E \cos(k) - \omega_D \sin(k)\big] a_{\mathbf{k}} b_{-\mathbf{k}} + \big[\omega_E \cos(k) - \omega_D \sin(k)\big] b_{-\mathbf{k}} a_{\mathbf{k}} \\ & + \big[\omega_E \cos(k) - \omega_D \sin(k)\big] a^\dagger_{\mathbf{k}} b^\dagger_{-\mathbf{k}} + \big[\omega_E \cos(k) - \omega_D \sin(k)\big] b^\dagger_{-\mathbf{k}} a^\dagger_{\mathbf{k}}. \end{aligned} \tag{10.3}$$

We choose the basis such that our non-interacting Hamiltonian is block-diagonal. Achieving this form allows us to use the same diagonalisation procedure as in section 5.1. With a block-diagonal matrix, as shown in Eq. (10.5), we can solve the blocks independently, resulting in two separate systems of reduced dimensions

The basis for Eq. (10.3) is $\vec{\Phi} = (\vec{\Phi}^{\mathrm{I}}_{\mathbf{k}}\ \vec{\Phi}^{\mathrm{II}}_{\mathbf{k}})^\mathsf{T} = (a_{\mathbf{k}}\ b^\dagger_{-\mathbf{k}}\ a^\dagger_{-\mathbf{k}}\ b_{\mathbf{k}})^\mathsf{T}$. The Hermitian conjugate is then $\vec{\Phi}^\dagger_{\mathbf{k}} = (\vec{\Phi}^{\mathrm{I}}_{\mathbf{k}}\ \vec{\Phi}^{\mathrm{II}}_{\mathbf{k}})^\dagger = (a^\dagger_{\mathbf{k}}\ b_{-\mathbf{k}}\ a_{-\mathbf{k}}\ b^\dagger_{\mathbf{k}})$. We can thus rewrite Eq. (10.3) as

$$H^2 = \sum_{\mathbf{k}} \vec{\Phi}^\dagger_{\mathbf{k}} H_{\mathbf{k}} \vec{\Phi}_{\mathbf{k}}, \tag{10.4}$$

where $H_{\mathbf{k}}$ is defined as

$$H_{\mathbf{k}} = \begin{pmatrix} H^{\mathrm{I}}_{\mathbf{k}} & 0 \\ 0 & H^{\mathrm{II}}_{\mathbf{k}} \end{pmatrix}. \tag{10.5}$$

In order to write H^2 on the matrix form in Eq. (10.4), we utilise the fact that $\sum_{\mathbf{k}} a_{\mathbf{k}} b_{-\mathbf{k}} = \sum_{\mathbf{k}} a_{-\mathbf{k}} b_{\mathbf{k}}$, as the sum runs over 1BZ. The upper right and lower left blocks of $H_{\mathbf{k}}$ are 2x2-matrices of all zeros. We therefore obtained the desired form of $H_{\mathbf{k}}$, namely a 4x4 block-diagonal matrix. The other 2x2-matrices in Eq. (10.5) are

$$H_{\mathbf{k}}^{\mathrm{I}} = \begin{pmatrix} \omega_E + \omega_A + \omega_H & \omega_E \cos(k) - \omega_D \sin(k) \\ \omega_E \cos(k) - \omega_D \sin(k) & \omega_E + \omega_A - \omega_H \end{pmatrix}, \tag{10.6}$$

and

$$H_{\mathbf{k}}^{\mathrm{II}} = \begin{pmatrix} \omega_E + \omega_A + \omega_H & \omega_E \cos(k) + \omega_D \sin(k) \\ \omega_E \cos(k) + \omega_D \sin(k) & \omega_E + \omega_A - \omega_H \end{pmatrix}. \tag{10.7}$$

These Hamiltonians are Hermitian, as they should be. We also see that $H_{\mathbf{k}}^{\mathrm{II}}$ is equal to $H_{-\mathbf{k}}^{\mathrm{I}}$. We note that $\vec{\Phi}_{\mathbf{k}}^{\mathrm{II},T} = \vec{\Phi}_{-\mathbf{k}}^{\mathrm{I}\,\dagger}$. This means that the Bogoliubov coefficients are the same for subsystem I and II, when we let $\mathbf{k} \to -\mathbf{k}$. These properties, along with the block-diagonal form, allows us to consider just one sub-system.

We choose to look at sub-system I

$$H^{2,\mathrm{I}} = \sum_{\mathbf{k}} \vec{\Phi}_{\mathbf{k}}^{\mathrm{I}\,\dagger} H_{\mathbf{k}}^{\mathrm{I}} \vec{\Phi}_{k}^{\mathrm{I}}. \tag{10.8}$$

As in section 5.1, we now define a matrix U for the Bogoliubov transformation. This matrix defines new bosonic operators $\alpha_{\mathbf{k}}$ and $\beta_{\mathbf{k}}$. Since the inverse of matrix U also will be useful, we present both the matrix and its inverse

$$U_{\mathbf{k}} = \begin{pmatrix} u_{\mathbf{k}} & v_{\mathbf{k}}^* \\ v_{\mathbf{k}} & u_{\mathbf{k}} \end{pmatrix}, \quad U_{\mathbf{k}}^{-1} \begin{pmatrix} u_{\mathbf{k}} & -v_{\mathbf{k}}^* \\ -v_{\mathbf{k}} & u_{\mathbf{k}} \end{pmatrix}. \tag{10.9}$$

The u and v are the Bogoliubov coefficients and without loss of generality, we will assume these to be real [57]. This implies that $v^* = v$

Our new operators are defined such that they follow the same bosonic commutation relations as our current operators does, namely $[a_{\mathbf{k}}, a_{\mathbf{k}'}^\dagger] = \delta_{\mathbf{k}\mathbf{k}'}$, $[b_{\mathbf{k}}, b_{\mathbf{k}'}^\dagger] = \delta_{\mathbf{k}\mathbf{k}'}$, while all other commutators are zero. The new operators thus follow $[\alpha_{\mathbf{k}}, \alpha_{\mathbf{k}'}^\dagger] = \delta_{\mathbf{k}\mathbf{k}'}$, $[\beta_{\mathbf{k}}, \beta_{\mathbf{k}'}^\dagger] = \delta_{\mathbf{k}\mathbf{k}'}$ while all other commutators are zero. The new operator vector is $\vec{\tilde{\Phi}}_{\mathbf{k}}^1 = (\alpha_{\mathbf{k}}\ \beta_{-\mathbf{k}}^\dagger)^{\mathsf{T}}$. We refer to section 5.1 for details.

The Bogoliubov transformed operators are defined as

$$\vec{\tilde{\Phi}}_{\mathbf{k}}^{\mathrm{I}} = U_{\mathbf{k}} \vec{\Phi}_{\mathbf{k}}^{\mathrm{I}},$$

$$\begin{pmatrix} \alpha_{\mathbf{k}} \\ \beta_{-\mathbf{k}}^\dagger \end{pmatrix} = \begin{pmatrix} u_{\mathbf{k}} & v_{\mathbf{k}} \\ v_{\mathbf{k}} & u_{\mathbf{k}} \end{pmatrix} \begin{pmatrix} a_{\mathbf{k}} \\ b_{-\mathbf{k}}^\dagger \end{pmatrix}. \tag{10.10}$$

We will make more use of expressing $a_{\mathbf{k}}$, $b^{\dagger}_{-\mathbf{k}}$ in terms of $\alpha_{\mathbf{k}}$, $\beta^{\dagger}_{-\mathbf{k}}$. We therefore multiply with the inverse of matrix $U_{\mathbf{k}}$ from the left in Eq. (10.10)

$$\vec{\Phi}^{1}_{\mathbf{k}} = U^{-1}_{\mathbf{k}} \vec{\tilde{\Phi}}^{1}_{\mathbf{k}},$$

$$\begin{pmatrix} a_{\mathbf{k}} \\ b^{\dagger}_{-\mathbf{k}} \end{pmatrix} = \begin{pmatrix} u_{\mathbf{k}} & -v_{\mathbf{k}} \\ -v_{\mathbf{k}} & u_{\mathbf{k}} \end{pmatrix} \begin{pmatrix} \alpha_{\mathbf{k}} \\ \beta^{\dagger}_{-\mathbf{k}} \end{pmatrix}. \tag{10.11}$$

As we stated above, the Bogoliubov transformed operators $\alpha_{\mathbf{k}}$ and $\beta_{\mathbf{k}}$ should follow the same commutation relations as before. This imposes, as in section 5.1, the constraint

$$u^2_{\mathbf{k}} - v^2_{\mathbf{k}} = 1. \tag{10.12}$$

Following the same procedure as in Part II, we insert the expressions for $a_{\mathbf{k}}$ and $b_{\mathbf{k}}$ found in Eq. (10.11), into Eq. (10.8), and obtain

$$\begin{aligned} H^{2,\mathrm{I}} &= \sum_{\mathbf{k}} \vec{\tilde{\Phi}}_{\mathbf{k}} (U^{-1}_{\mathbf{k}})^{\dagger} \, H^{\mathrm{I}}_{\mathbf{k}} \, U^{-1}_{\mathbf{k}} \vec{\tilde{\Phi}}_{\mathbf{k}} \\ &= \sum_{\mathbf{k}} \vec{\tilde{\Phi}}_{\mathbf{k}} \tilde{H}^{\mathrm{I}}_{\mathbf{k}} \vec{\tilde{\Phi}}_{\mathbf{k}}. \end{aligned} \tag{10.13}$$

We have defined a new matrix, $\tilde{H}^{\mathrm{I}}_{\mathbf{k}}$ as

$$\tilde{H}^{\mathrm{I}}_{\mathbf{k}} = (U^{-1}_{\mathbf{k}})^{\dagger} \, H^{\mathrm{I}}_{\mathbf{k}} \, U^{-1}_{\mathbf{k}}. \tag{10.14}$$

Analogously to the ferromagnetic case, this is the matrix we diagonalise. The matrix reads

$$\tilde{H}^{\mathrm{I}}_{\mathbf{k}} = \begin{pmatrix} \tilde{H}^{\mathrm{I},(1,1)}_{\mathbf{k}} & \tilde{H}^{\mathrm{I},(1,2)}_{\mathbf{k}} \\ \tilde{H}^{\mathrm{I},(2,1)}_{\mathbf{k}} & \tilde{H}^{\mathrm{I},(2,2)}_{\mathbf{k}} \end{pmatrix}, \tag{10.15}$$

and its elements are

$$\begin{aligned} \tilde{H}^{\mathrm{I},(1,1)}_{\mathbf{k}} =& u_{\mathbf{k}} \big[(\omega_E + \omega_A + \omega_H) u_{\mathbf{k}} - (\omega_E \cos(k) - \omega_D \sin(k) v_{\mathbf{k}} \big] \\ & - v^{*}_{\mathbf{k}} \big[(\omega_E \cos(k) - \omega_D \sin(k)) u_{\mathbf{k}} - (\omega_E + \omega_A - \omega_H) v_{\mathbf{k}} \big] \\ \tilde{H}^{\mathrm{I},(1,2)}_{\mathbf{k}} =& u_{\mathbf{k}} \big[-(\omega_E + \omega_A + \omega_H) v^{*}_{\mathbf{k}} + (\omega_E \cos(k) - \omega_D \sin(k)) u_{\mathbf{k}} \big] \\ & - v^{*}_{\mathbf{k}} \big[-(\omega_E \cos(k) - \omega_D \sin(k)) v_{\mathbf{k}^*} + (\omega_E + \omega_A - \omega_H) u_{\mathbf{k}} \big] \\ \tilde{H}^{\mathrm{I},(2,1)}_{\mathbf{k}} =& - v_{\mathbf{k}} \big[(\omega_E + \omega_A + \omega_H) u_{\mathbf{k}} - (\omega_E \cos(k) - \omega_D \sin(k)) v_{\mathbf{k}} \big] \\ & + u_{\mathbf{k}} \big[(\omega_E \cos(k) - \omega_D \sin(k)) u_{\mathbf{k}} - (\omega_E + \omega_A - \omega_H) v_{\mathbf{k}} \big] \\ \tilde{H}^{\mathrm{I},(2,2)}_{\mathbf{k}} =& - v_{\mathbf{k}} \big[(\omega_E + \omega_A + \omega_H) v_{\mathbf{k}} + (\omega_E \cos(k) - \omega_D \sin(k)) u_{\mathbf{k}} \big] \\ & + u_{\mathbf{k}} \big[-(\omega_E \cos(k) - \omega_D \sin(k)) v^{*}_{\mathbf{k}} + (\omega_E + \omega_A + \omega_H) u_{\mathbf{k}} \big]. \end{aligned} \tag{10.16}$$

To obtain a diagonal Hamiltonian, we need the off-diagonal elements to be zero. Thus, we need $\tilde{H}^{\mathrm{I},(1,2)}_{\mathbf{k}}$ and $\tilde{H}^{\mathrm{I},(2,1)}_{\mathbf{k}}$ to vanish. We observe that the matrix is symmetric, i.e $\tilde{H}^{\mathrm{I},(2,1)}_{\mathbf{k}} = \tilde{H}^{\mathrm{I},(1,2)}_{\mathbf{k}}$. By also utilising the constraint in Eq. (10.12), we find the

expressions for $u_{\mathbf{k}}$ and $v_{\mathbf{k}}$.

We start by setting $\tilde{H}^{\mathrm{I},(2,1)}_{\mathbf{k}}$ equal to zero,

$$\begin{aligned} 0 =& v_{\mathbf{k}}\big[(\omega_E+\omega_A+\omega_H)u_{\mathbf{k}} - (\omega_E\cos(k)-\omega_D\sin(k))v_{\mathbf{k}}\big] \\ &+u_{\mathbf{k}}\big[(\omega_E\cos(k)-\omega_D\sin(k))u_{\mathbf{k}} - (\omega_E+\omega_A-\omega_H)v_{\mathbf{k}}\big]. \end{aligned} \tag{10.17}$$

Employing the constraint $u^2_{\mathbf{k}} - v^2_{\mathbf{k}} = 1$ presented earlier, we find the following expression for $u^2_{\mathbf{k}}$ and $v^2_{\mathbf{k}}$

$$\begin{aligned} u^2_{\mathbf{k}} &= \frac{1}{2}\sqrt{\frac{(\omega_E+\omega_A)^2}{(\omega_E+\omega_A)^2-(\omega_E\cos(k)-\omega_D\sin(k))^2}} + \frac{1}{2} \\ v^2_{\mathbf{k}} &= \frac{1}{2}\sqrt{\frac{(\omega_E+\omega_A)^2}{(\omega_E+\omega_A)^2-(\omega_E\cos(k)-\omega_D\sin(k))^2}} - \frac{1}{2}. \end{aligned} \tag{10.18}$$

The elements of the matrix $\tilde{H}^{\mathrm{I}}_{\mathbf{k}}$ have physical meaning. After inserting the Bogoliubov coefficients in Eq. (10.18), the Hamiltonian in Eq. (10.13) now reads

$$H^{2,\mathrm{I}} = \sum_{\mathbf{k}} \varepsilon^{\alpha}_{\mathbf{k}}\alpha^{\dagger}_{\mathbf{k}}\alpha_{\mathbf{k}} + \varepsilon^{\beta}_{\mathbf{k}}\beta_{-\mathbf{k}}\beta^{\dagger}_{-\mathbf{k}}, \tag{10.19}$$

where we have renamed $\tilde{H}^{\mathrm{I},(1,1)}_{\mathbf{k}}$ to $\varepsilon^{\alpha}_{\mathbf{k}}$ and $\tilde{H}^{\mathrm{I},(2,2)}_{\mathbf{k}}$ to $\varepsilon^{\beta}_{\mathbf{k}}$. To obtain the correct form, we need to let $-\mathbf{k}\to\mathbf{k}$ in the second term, thus changing $\varepsilon^{\beta}_{\mathbf{k}}\to\varepsilon^{\beta}_{-\mathbf{k}}$. During these changes we make use of the commutation relation, providing an extra term to the reference energy.

Inserting $u_{\mathbf{k}}$ and $v_{\mathbf{k}}$ back into $\varepsilon^{\alpha}_{\mathbf{k}}$ and $\varepsilon^{\beta}_{-\mathbf{k}}$ we obtain

$$\begin{aligned} \varepsilon^{\alpha}_{\mathbf{k}} &= \big[(\omega_E+\omega_A)^2-(\omega_E\cos(k)-\omega_D\sin(k))^2\big]^{1/2}+\omega_H \\ \varepsilon^{\beta}_{-\mathbf{k}} &= \big[(\omega_E+\omega_A)^2-(\omega_E\cos(k)+\omega_D\sin(k))^2\big]^{1/2}-\omega_H, \end{aligned} \tag{10.20}$$

where we have assumed ω_D not too large, see Eq. (10.21).

The quantity we are interested in is $\varepsilon^{\beta}_{-\mathbf{k}}$. For simplicity of notation, we thus redefine $\varepsilon^{\beta}_{-\mathbf{k}}$ to $\varepsilon^{\beta}_{\mathbf{k}}$, such that $\varepsilon^{\beta}_{\mathbf{k}} = \big[(\omega_E+\omega_A)^2-(\omega_E\cos(k)+\omega_D\sin(k))^2\big]^{1/2}-\omega_H$. We can observe the effect of non-reciprocity here, as $a_{-\mathbf{k}}\neq a_{\mathbf{k}}$ and thus $\alpha_{-\mathbf{k}}\neq\alpha_{\mathbf{k}}$. Explicitly, sine is not an even function. However, the sum is symmetric, so $\sum_{\mathbf{k}} a^{\dagger}_{-\mathbf{k}}a_{-\mathbf{k}} = \sum_{\mathbf{k}} a^{\dagger}_{\mathbf{k}}a_{\mathbf{k}}$.

10.2 Dispersion relations

We now analyse how the various interactions affect the dispersion relations, $\varepsilon^{\alpha}_{\mathbf{k}}$ and $\varepsilon^{\beta}_{\mathbf{k}}$.

Only direct exchange interaction

Turning off the external magnetic field, anisotropy and DMI, we see that the dispersion relations are degenerate. This is shown in Figure 10.1. Another important observation is that the gap is now closed, at $k = 0$. Since this is the Heisenberg model, which has rotational symmetry that is spontaneously broken in the ground state, gapless excitations are expected from the aforementioned Goldstone's theorem.

As expected from the Heisenberg model for antiferromagnetic ordering, the dispersion relations at small k are linear.

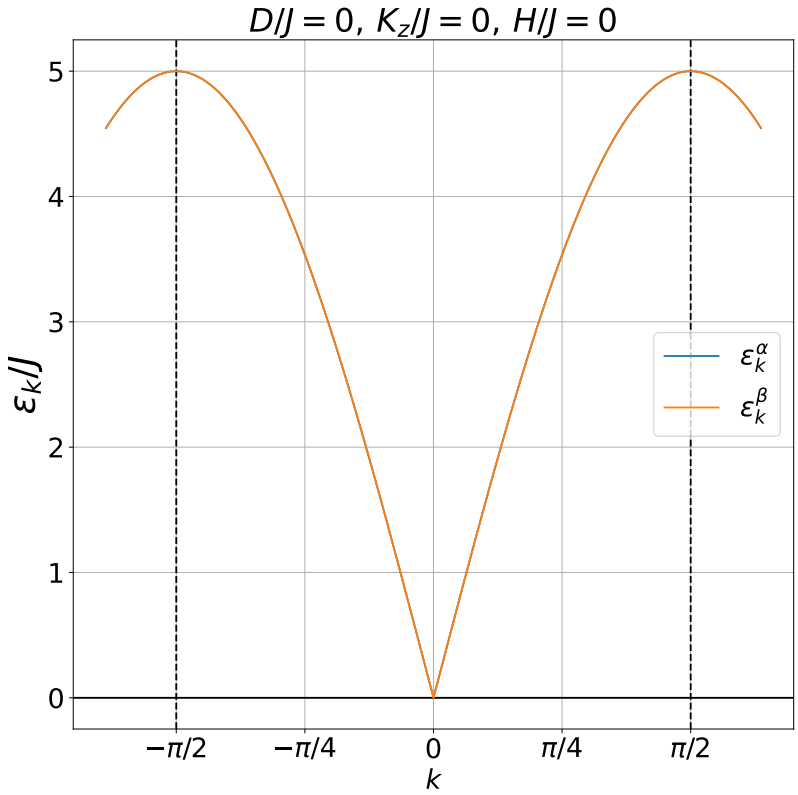

Figure 10.1: The dispersion relations for α- and β-magnons when external magnetic field, anisotropy and DMI is turned off. The dashed, vertical lines mark the boundaries of the 1BZ.

Anisotropy turned on, magnetic field and DMI turned off

The next interaction we want to investigate, is anisotropy. We thus leave the external magnetic field and DMI off, while turning on anisotropy. We see in Figure 10.2 that the dispersion relations are still degenerate, however, a gap has opened. Since anisotropy breaks the rotational symmetry, Goldstone's theorem no longer applies. We also see that the linear shape is not conserved. The dispersion relations are now quadratic at small k, as opposed to linear as in the previous case.

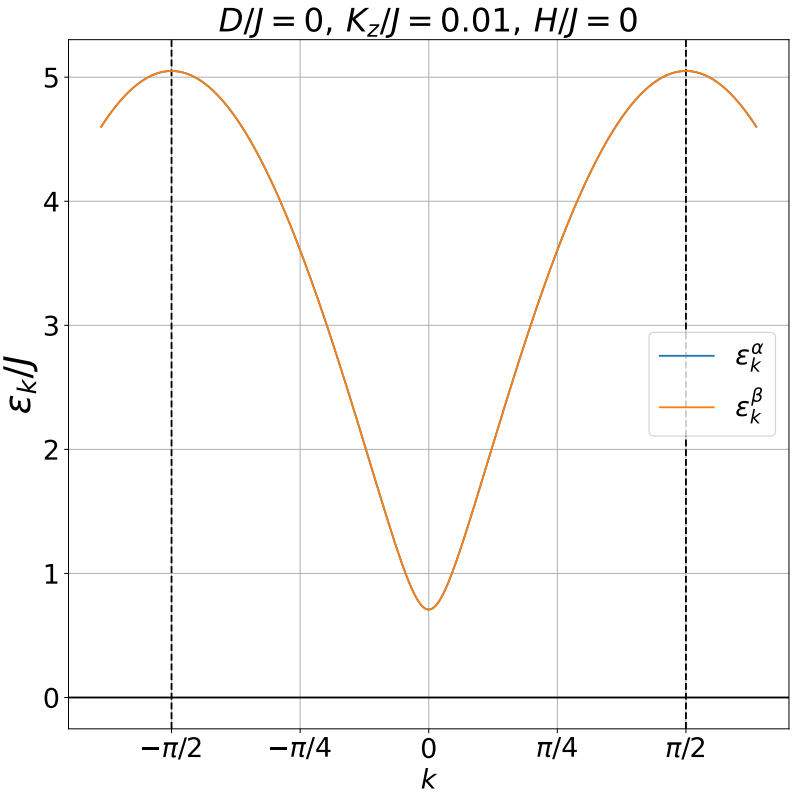

Figure 10.2: The dispersion relations for α- and β-magnons, when anisotropy is turned on while external magnetic field and DMI is turned off. The dashed, vertical lines mark the boundaries of the 1BZ.

Magnetic field and anisotropy turned on, DMI turned off

If we now turn on the magnetic field, we see in Figure 10.3 that the dispersion relations are non-degenerate. The external magnetic field has shifted the counter-clockwise dispersion relation, $\varepsilon^{\alpha}_{\mathbf{k}}$, upwards, while the clockwise, $\varepsilon^{\beta}_{\mathbf{k}}$, has been shifted downwards in energy. This result is easily understood when looking at the expressions in Eq. (10.20).

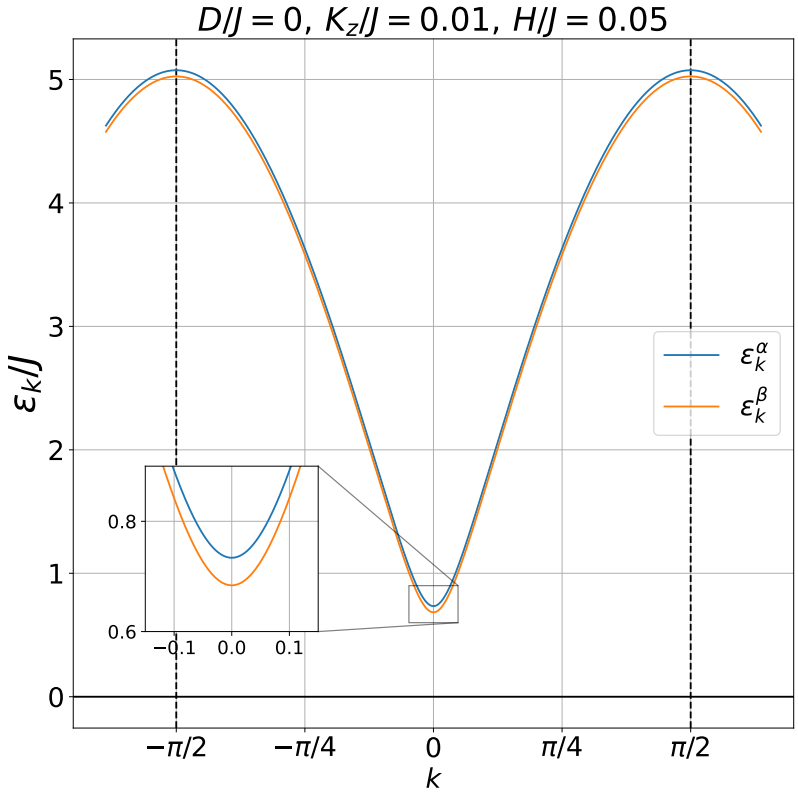

Figure 10.3: The dispersion relations for α- and β-magnons, when external magnetic field is turned on while anisotropy and DMI is turned off. The dashed, vertical lines mark the boundaries of the 1BZ.

We now want to turn on DMI. It is important to note that there is a constraint on the strength of the DMI, that follows from the dispersion relations [58]. We need

$$\omega_D \leq 4\sqrt{JK_z}. \tag{10.21}$$

All interactions

We observe that the dispersion relations are shifted horizontally, with equal offsets to the left and right from $k = 0$. We will see that this is due to the DMI. We also note that the dispersion relations are shifted vertically around a certain value.

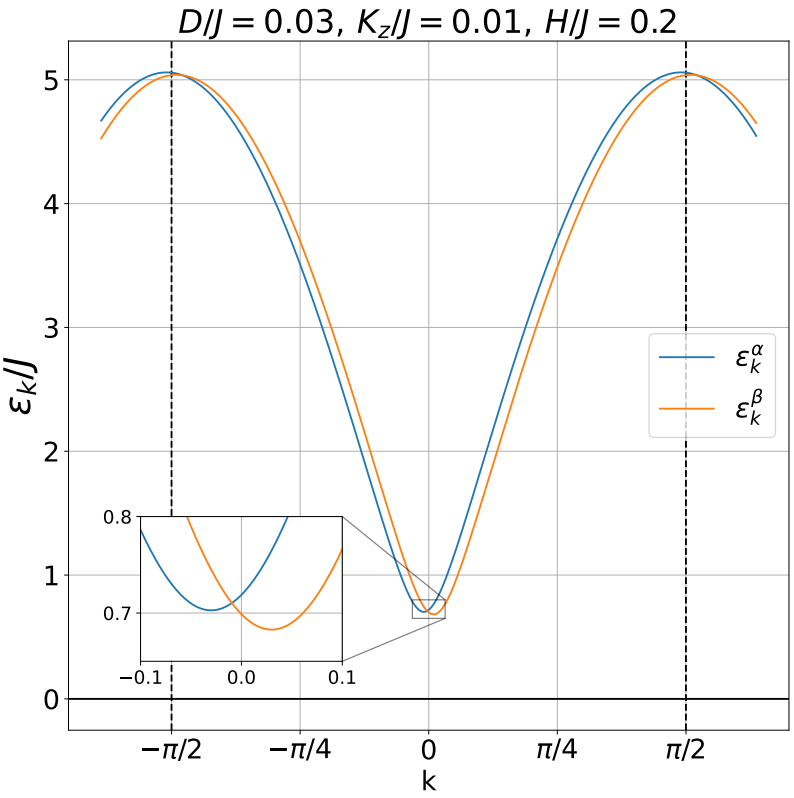

Figure 10.4: Dispersion relations for α- and β-magnons with $D/J = 0.03$, $K_z/J = 0.05$ and $H/J = 0.01$. The dashed, vertical lines mark the boundaries of the 1BZ.

Dispersion relations as functions of anisotropy

To see how the dispersion relations vary as functions of the anisotropy, we show $\varepsilon^{\alpha}_{\mathbf{k}}$ and $\varepsilon^{\beta}_{\mathbf{k}}$ for four different values of K_z in Figure 10.5. We observe that the shape of the dispersion relations changes. When K_z is increased, the minimum and maxima stay at the same k-value, while the amplitude is reduced.

The curvature of the dispersion relations is given by $\partial^2\varepsilon_k/\partial k^2$. From Figure 10.5, we see that the curvature is reduced when the anisotropy strength is increased. The reciprocal of the curvature is proportional to the effective mass [59]. Thus, we can deduce that the effective mass of the magnons is increased with increased anisotropy strength.

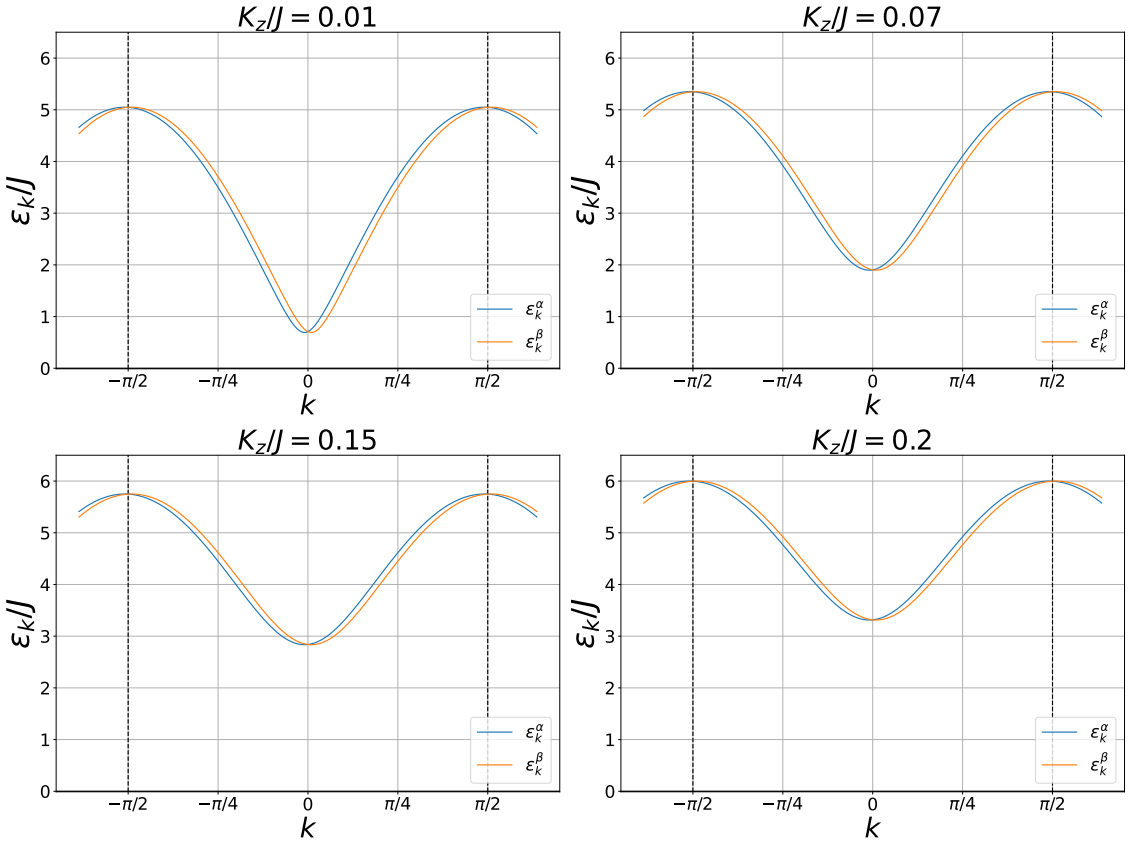

Figure 10.5: The dispersion relations for α- and β-magnons, when we vary K_z. Upper left, $K_z/J = 0.01$. Upper right, $K_z/J = 0.07$. Lower left, $K_z/J = 0.15$. Lower right, $K_z/J = 0.2$. Magnetic field is turned off, and $D/J = 0.03$. The dashed, vertical lines mark the boundaries of the 1BZ.

Dispersion relations as functions of DMI

We present the same analysis for the DMI. The four plots in Figure 10.6 show the dispersion relations with varying D. We observe that the dispersion relations are increasingly shifted horizontally with increasing D. The minima are thus shifted to larger k-values.

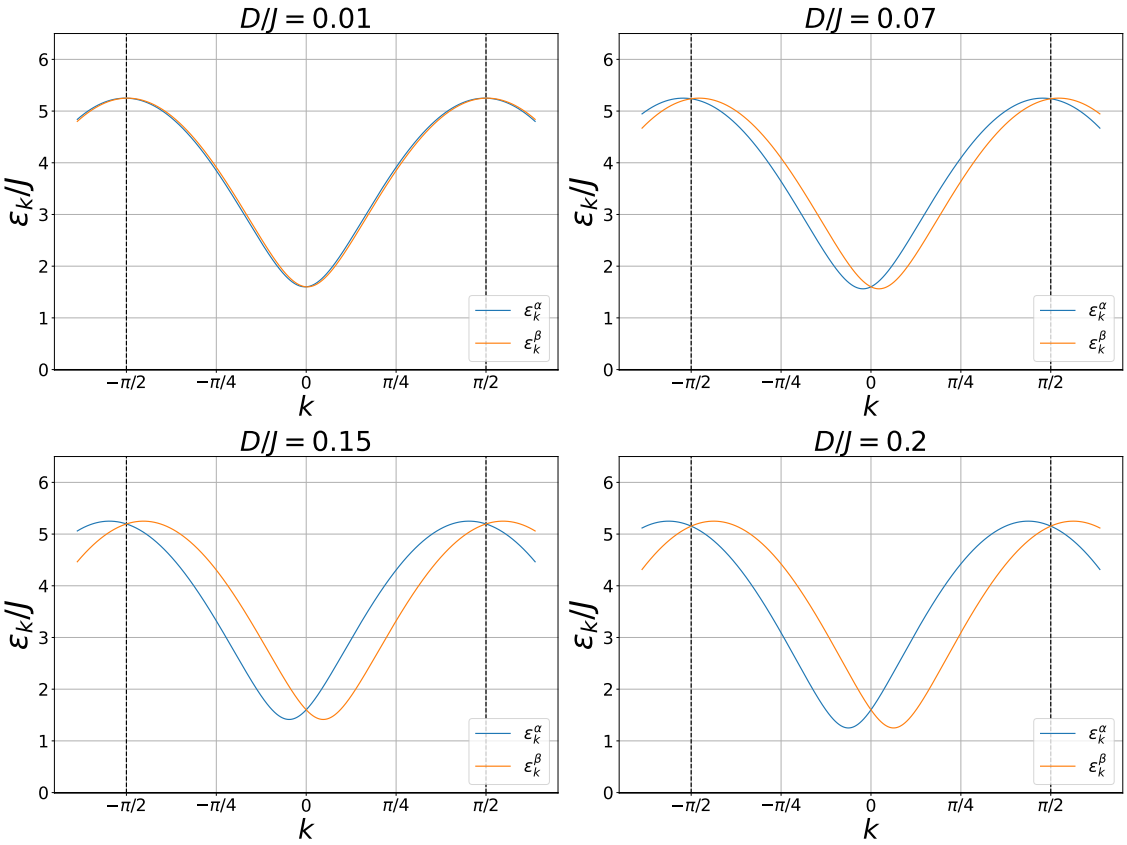

Figure 10.6: The dispersion relations for α- and β-magnons, when we vary D. Upper left, $D/J = 0.01$. Upper right, $D/J = 0.07$. Lower left, $D/J = 0.15$. Lower right, $D/J = 0.2$. Magnetic field is turned off, and $K_z/J = 0.05$. The dashed, vertical lines mark the boundaries of the 1BZ.

10.3 Interaction Hamiltonian

The main goal of this thesis is, as already mentioned, to find the effective of interactions between the magnons at the k-values that are candidates for condensates. The necessary condition is that the interactions are repulsive. To investigate this, we need to find an expression for the interaction potential. In the previous section, we found a Bogoliubov-transformation that diagonalised the non-interacting Hamiltonian. We view the interaction Hamiltonian as a small perturbation to the non-interacting Hamiltonian. The total interaction Hamiltonian was presented in Eq. (9.35).
Before inserting the Bogoliubov transformation, it is important to note that the sum

in Eq. (9.35) is a triple sum over all momenta. However, the only magnons that are interesting for us, are those in the condensate. From Figure 10.4, we see that these magnons lie in the minima of $\varepsilon_{\mathbf{k}}$ at $\mathbf{k} \pm \mathbf{Q}$. Therefore, we reduce the sum to consider only combinations that give $\alpha^{(\dagger)}_{-\mathbf{Q}}$ and $\beta^{(\dagger)}_{+\mathbf{Q}}$. To obtain that, we need to reduce the sum for the Hamiltonian in Eq. (9.35) first.

The resulting Hamiltonian, H_Q, is then

$$\begin{aligned}
H_Q = \frac{1}{(N/2)} \Big\{ \Big[& \big[-f_2(Q) - f_3(Q)\big]\big[a_{-\mathbf{Q}} b^\dagger_{\mathbf{Q}} b_{\mathbf{Q}} b_{\mathbf{Q}} + 2 a_{-\mathbf{Q}} b^\dagger_{-\mathbf{Q}} b_{-\mathbf{Q}} b_{\mathbf{Q}}\big] \\
& + \big[-f_2(Q) + f_3(Q)\big]\big[2 a_{\mathbf{Q}} b^\dagger_{\mathbf{Q}} b_{\mathbf{Q}} b_{-\mathbf{Q}} + a_{\mathbf{Q}} b^\dagger_{-\mathbf{Q}} b_{-\mathbf{Q}} b_{-\mathbf{Q}}\big] + \text{h.c.}\Big] \\
& + \Big[\big[-f_2(Q) - f_3(Q)\big]\big[a^\dagger_{-\mathbf{Q}} a_{-\mathbf{Q}} a_{-\mathbf{Q}} b_{\mathbf{Q}} + 2 a^\dagger_{\mathbf{Q}} a_{\mathbf{Q}} a_{-\mathbf{Q}} b_{\mathbf{Q}}\big] \\
& + \big[-f_2(Q) + f_3(Q)\big]\big[a^\dagger_{\mathbf{Q}} a_{\mathbf{Q}} a_{\mathbf{Q}} b_{-\mathbf{Q}} + 2 a^\dagger_{-\mathbf{Q}} a_{-\mathbf{Q}} a_{\mathbf{Q}} b_{-\mathbf{Q}}\big] + \text{h.c.}\Big] \\
& - 4J\big[a^\dagger_{\mathbf{Q}} a_{\mathbf{Q}} b^\dagger_{\mathbf{Q}} b_{\mathbf{Q}} + a^\dagger_{-\mathbf{Q}} a_{-\mathbf{Q}} b^\dagger_{-\mathbf{Q}} b_{-\mathbf{Q}} + a^\dagger_{\mathbf{Q}} a_{\mathbf{Q}} b^\dagger_{-\mathbf{Q}} b_{-\mathbf{Q}} + a^\dagger_{-\mathbf{Q}} a_{-\mathbf{Q}} b^\dagger_{\mathbf{Q}} b_{\mathbf{Q}} \\
& \qquad + \cos(Q)\big[a^\dagger_{\mathbf{Q}} a_{-\mathbf{Q}} b^\dagger_{-\mathbf{Q}} b_{\mathbf{Q}} + a^\dagger_{-\mathbf{Q}} a_{\mathbf{Q}} b^\dagger_{\mathbf{Q}} b_{-\mathbf{Q}}\big]\big] \\
& - (K_z/2)\big[a^\dagger_{\mathbf{Q}} a_{\mathbf{Q}} a^\dagger_{\mathbf{Q}} a_{\mathbf{Q}} + a^\dagger_{-\mathbf{Q}} a_{-\mathbf{Q}} a^\dagger_{-\mathbf{Q}} a_{-\mathbf{Q}} + 4 a^\dagger_{\mathbf{Q}} a_{\mathbf{Q}} a^\dagger_{-\mathbf{Q}} a_{-\mathbf{Q}} \\
& \qquad + b^\dagger_{\mathbf{Q}} b_{\mathbf{Q}} b^\dagger_{\mathbf{Q}} b_{\mathbf{Q}} + b^\dagger_{-\mathbf{Q}} b_{-\mathbf{Q}} b^\dagger_{-\mathbf{Q}} b_{-\mathbf{Q}} + 4 b^\dagger_{\mathbf{Q}} b_{\mathbf{Q}} b^\dagger_{-\mathbf{Q}} b_{-\mathbf{Q}} + \text{h.c.}\big] \Big\}. \qquad (10.22)
\end{aligned}$$

To find this Hamiltonian in the diagonal basis, we insert the (inverse) Bogoliubov transformation in Eq. (10.11). When collecting terms after the insertion, we omit terms that include operators $\alpha^{(\dagger)}_{+\mathbf{Q}}$, $\beta^{(\dagger)}_{-\mathbf{Q}}$ as these are not part of the condensates. The condensates form at the minima of the dispersion relations. At $\mathbf{k} = +\mathbf{Q}$ α-magnons are not in a minimum. The same applies for β-magnons at $\mathbf{k} = -\mathbf{Q}$. As in the ferromagnetic case, in section 5.2, we can use the commutation relations $[\alpha_{\mathbf{k}}, \alpha^\dagger_{\mathbf{k}'}] = [\beta_{\mathbf{k}}, \beta^\dagger_{\mathbf{k}'}] = \delta_{\mathbf{k}\mathbf{k}'}$ and neglect terms emerging from the $\delta_{\mathbf{k}\mathbf{k}'}$ as those are of one order of magnitude smaller than H^2 in Eq. (10.19). The final result is then

$$\begin{aligned}
H_Q = & A\big[\alpha_{-\mathbf{Q}} \beta^\dagger_{\mathbf{Q}} \beta_{\mathbf{Q}} \beta_{\mathbf{Q}} + \beta^\dagger_{\mathbf{Q}} \alpha_{-\mathbf{Q}} \alpha^\dagger_{-\mathbf{Q}} \alpha^\dagger_{-\mathbf{Q}} + \alpha_{-\mathbf{Q}} \alpha_{-\mathbf{Q}} \beta_{\mathbf{Q}} \alpha^\dagger_{-\mathbf{Q}} + \beta^\dagger_{\mathbf{Q}} \beta^\dagger_{\mathbf{Q}} \beta_{\mathbf{Q}} \alpha^\dagger_{-\mathbf{Q}}\big] \\
& + B\big[\alpha_{-\mathbf{Q}} \alpha_{-\mathbf{Q}} \beta_{\mathbf{Q}} \beta_{\mathbf{Q}} + \beta^\dagger_{\mathbf{Q}} \beta^\dagger_{\mathbf{Q}} \alpha^\dagger_{-\mathbf{Q}} \alpha^\dagger_{-\mathbf{Q}}\big] \\
& + C\big[\alpha_{-\mathbf{Q}} \alpha_{-\mathbf{Q}} \alpha^\dagger_{-\mathbf{Q}} \alpha^\dagger_{-\mathbf{Q}} + \beta^\dagger_{\mathbf{Q}} \beta^\dagger_{\mathbf{Q}} \beta_{\mathbf{Q}} \beta_{\mathbf{Q}}\big] \\
& + D \alpha_{-\mathbf{Q}} \beta^\dagger_{\mathbf{Q}} \beta_{\mathbf{Q}} \alpha^\dagger_{-\mathbf{Q}}, \qquad (10.23)
\end{aligned}$$

where we defined coefficients A, B, C and D as

$$\begin{aligned}
A &= \big[-f_2(Q) - f_3(Q)\big]\big[\alpha^1_Q + \alpha^2_Q\big] - 4J\big[\alpha^3_Q\big] - K_z\big[2\alpha^3_Q\big] \\
B &= \big[-f_2(Q) - f_3(Q)\big]\big[2\alpha^3_Q\big] - 4J\big[(1/2)\alpha^2_Q\big] - K_z\big[\alpha^2_Q\big] \\
C &= \big[-f_2(Q) - f_3(Q)\big]\big[2\alpha^3_Q\big] - 4J\big[(1/2)\alpha^2_Q\big] - K_z\big[\alpha^1_Q - 2\alpha^2_Q\big] \\
D &= \big[-f_2(Q) - f_3(Q)\big]\big[8\alpha^3_Q\big] - 4J\big[\alpha^1_Q - \alpha^2_Q\big] - K_z\big[4\alpha^2_Q\big]. \qquad (10.24)
\end{aligned}$$

Additionally, we have defined three new functions in Eq. (10.24),

$$\begin{aligned}\alpha_Q^1 &= u_{-Q}^4 + v_{-Q}^4 + 4u_{-Q}^2 v_{-Q}^2 \\ \alpha_Q^2 &= 2u_{-Q}^2 v_{-Q}^2 \\ \alpha_Q^3 &= -u_{-Q}v_{-Q}(u_{-Q}^2 + v_{-Q}^2).\end{aligned} \tag{10.25}$$

In Eq. (10.23), we observe that the terms in the third line only include one type of magnons. These terms thus represent intravalley scattering, as they only consist of either operators at the minimum for α- or β-magnons. The other terms includes both α- and β-operators, and thus representing intervalley scattering. We define two Hamiltonians, H_{intra} and H_{inter} for, respectively, intravalley scattering and intervalley scattering

$$\begin{aligned}H_{\text{intra}} &= C\big[\alpha_{-\mathbf{Q}}\alpha_{-\mathbf{Q}}\alpha^\dagger_{-\mathbf{Q}}\alpha^\dagger_{-\mathbf{Q}} + \beta^\dagger_{\mathbf{Q}}\beta^\dagger_{\mathbf{Q}}\beta_{\mathbf{Q}}\beta_{\mathbf{Q}}\big] \\ H_{\text{inter}} &= A\big[\alpha_{-\mathbf{Q}}\beta^\dagger_{\mathbf{Q}}\beta_{\mathbf{Q}}\beta_{\mathbf{Q}} + \beta^\dagger_{\mathbf{Q}}\alpha_{-\mathbf{Q}}\alpha^\dagger_{-\mathbf{Q}}\alpha^\dagger_{-\mathbf{Q}} + \alpha_{-\mathbf{Q}}\alpha_{-\mathbf{Q}}\beta_{\mathbf{Q}}\alpha^\dagger_{-\mathbf{Q}} + \beta^\dagger_{\mathbf{Q}}\beta^\dagger_{\mathbf{Q}}\beta_{\mathbf{Q}}\alpha^\dagger_{-\mathbf{Q}}\big] \\ &\quad + B\big[\alpha_{-\mathbf{Q}}\alpha_{-\mathbf{Q}}\beta_{\mathbf{Q}}\beta_{\mathbf{Q}} + \beta^\dagger_{\mathbf{Q}}\beta^\dagger_{\mathbf{Q}}\alpha^\dagger_{-\mathbf{Q}}\alpha^\dagger_{-\mathbf{Q}}\big] \\ &\quad + D\alpha_{-\mathbf{Q}}\beta^\dagger_{\mathbf{Q}}\beta_{\mathbf{Q}}\alpha^\dagger_{-\mathbf{Q}}.\end{aligned} \tag{10.26}$$

The coefficient C can be interpreted as the amplitude of intravalley scattering within the two condensates. Coefficients A, B and D can be interpreted as the amplitude of various types of intervalley scattering between the two condensates.

10.4 Interaction potential

We have now obtained our Hamiltonian in the desired basis. Following the procedure of section 5.3, we now insert the Madelung transformation to find the interaction potential. This amounts to inserting the expectation value of the operators. The transformations in the antiferromagnetic case are

$$\begin{aligned}\langle\alpha_{-\mathbf{Q}}\rangle &= \sqrt{N^\alpha}\,\mathrm{e}^{i\phi^\alpha} \\ \langle\beta_{\mathbf{Q}}\rangle &= \sqrt{N^\beta}\,\mathrm{e}^{i\phi^\beta}\end{aligned} \tag{10.27}$$

The interaction potential is now

$$\begin{aligned}\mathcal{V}_4 =& AN_\alpha^{1/2}N_\beta^{1/2}[N_\alpha + N_\beta]2\cos(\phi_\alpha + \phi_\beta) + BN_\alpha N_\beta 2\cos(2(\phi_\alpha + \phi_\beta)) \\ &+ C(N_\alpha^2 + N_\beta^2) + DN_\alpha N_\beta.\end{aligned} \tag{10.28}$$

We once again assume that we can keep the number of magnons in the condensate constant, with pumping. We also assume that scattering processes, including spin-orbit coupling, cause the magnon number in each condensate to vary. Unlike the ferromagnetic case, where there was only one species of magnons, scattering from one species of magnons to the other includes a change in angular momentum. This can happen through spin-orbit coupling. As for the FMI, we also introduce the total

phase, adding the phases in the two condensates. Introducing the same parameters as in the ferromagnetic case, the total number of magnons in both condensates $N_c = N_\beta + N_\alpha$, the difference in numbers of magnons in the condensates $\delta = N_\beta - N_\alpha$ and the total phase $\Phi = \phi_\beta + \phi_\alpha$. Observing the definition of δ, we can refer to this parameter as the polarisation of the condensate system. If $\delta \neq 0$, we have more of one species of magnons, and thus more of one type of angular momentum.

Writing the interaction potential $\mathcal{V}_4$ in terms of N_c, δ and Φ gives

$$\mathcal{V}_4 = \frac{N_c^2}{2}\Big[(C + \frac{D}{2}) - (\frac{D}{2} + B\,\cos(2\Phi) - C)(\delta/N_c)^2 + B\,\cos(2\Phi) \\ +2A\,\sqrt{1-(\delta/N_c)^2}\,\cos(\Phi)\Big]. \tag{10.29}$$

An interesting remark at this point, is that the interaction potential of the antiferromagnetic system, in Eq. (10.29), has the same form as the ferromagnetic system, in Eq. (5.10) with different coefficients.

We define two interaction potentials, $\mathcal{V}_{4,\text{intra}}$ and $\mathcal{V}_{4,\text{inter}}$, for the intravalley scattering and intervalley scattering, respectively.

$$\mathcal{V}_{4,\text{intra}} = \frac{N_c^2}{2}C\big[1-(\delta/N_c)^2\big] \\ \mathcal{V}_{4,\text{inter}} = \frac{N_c^2}{2}\Big[\frac{D}{2} - (\frac{D}{2} + B\,\cos(2\Phi))(\delta/N_c)^2 + B\,\cos(2\Phi) + 2A\,\sqrt{1-(\delta/N_c)^2}\,\cos(\Phi)\Big]. \tag{10.30}$$

In Figure 11.1 we show the value of $\mathcal{V}_{4,\text{intra}}$ and $\mathcal{V}_{4,\text{inter}}$ as functions of the strengths of DMI and anisotropy.

Since the ferromagnetic and antiferromagnetic potentials have the same form and variables, we already have an expression for the second derivatives in Eq. (5.13). In our antiferromagnetic system, we find that extremum points v) and vi) from Eq. (5.12) are not valid. We thus have four extrema,

$$\begin{aligned} &\text{i) } (\delta/N_c)^2 = 0, \Phi = 0 \\ &\text{ii) } (\delta/N_c)^2 = 0, \Phi = \pi \\ &\text{iii) } (\delta/N_c)^2 = 1 - \left[\frac{A\,\cos(\Phi)}{C - D/2 - B\,\cos(2\Phi)}\right]^2, \Phi = 0 \\ &\text{iv) } (\delta/N_c)^2 = 1 - \left[\frac{A\,\cos(\Phi)}{C - D/2 - B\,\cos(2\Phi)}\right]^2, \Phi = \pi. \end{aligned} \tag{10.31}$$

10.5 Phase diagrams

As the goal of this work is to determine if a BEC of magnons can exist in an AFMI, we need to investigate if the potential is repulsive. We thus consider the signs of the second derivatives of $\mathcal{V}_4$, and of $\mathcal{V}_4$ itself. An adequate way to inspect this is by drawing phase diagrams. As first done in section 5.3, we present once again the criteria for an extremum point to be a minimum, via the second derivative test

$$\begin{aligned} &\text{a) } \partial^2\mathcal{V}_4/\partial\delta^2 > 0, \\ &\text{b) } \partial^2\mathcal{V}_4/\partial\Phi^2 > 0 \\ &\text{c) } (\partial^2\mathcal{V}_4/\partial\delta^2)\,(\partial^2\mathcal{V}_4/\partial\Phi^2) - (\partial^2\mathcal{V}_4/\partial\delta\partial\Phi)^2 > 0. \end{aligned} \tag{10.32}$$

A useful observation here is that, as we can see from Eq. (5.13), $\partial^2\mathcal{V}_4/\partial\delta\Phi$ is a function of $\sin(\Phi)$, which is zero in all extrema. We thus focus on a) and b).

In our antiferromagnetic case, the coefficients *A, B, C* and *D* are functions of the direct exchange interaction strength J, the anisotropy strength K_z, and the DMI strength D. The value of J is hard to change experimentally, so we choose to look at how the coefficients *A, B, C* and *D* vary as functions of K_z and D.

We show the phase diagrams in units of J.

Extremum point i)

The values of the second derivatives of $\mathcal{V}_4$, are shown in Figures 10.7, with $\partial^2\mathcal{V}_4/\partial\delta^2$ in 10.7(a) and with $\partial^2\mathcal{V}_4/\partial\Phi^2$ in 10.7(b). In Figure 10.7(c) we show the value of $\mathcal{V}_4$ in units of J.

In Figure 10.7, the red regions indicate positive values, while blue shows negative values. We see that for $\partial^2\mathcal{V}_4/\partial\Phi^2$ there is no region where it is positive. Thus, this extremum point is not a minimum and there cannot exist a BEC with these values of δ and Φ.

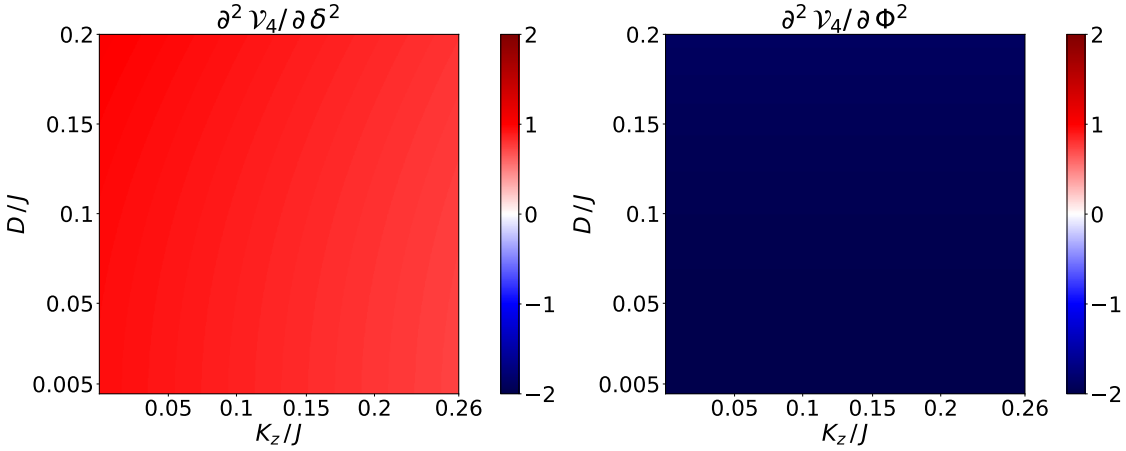

(a) (b)

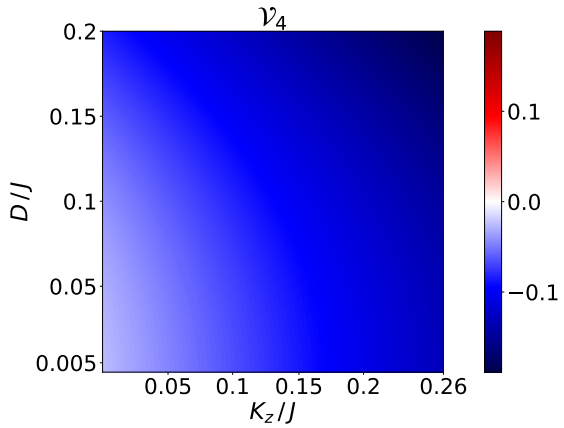

(c)

Figure 10.7: (a) and (b) The second derivatives of $\mathcal{V}_4$, as functions of K_z and D, in extremum point i) from Eq. (10.31). (c) $\mathcal{V}_4$ as a function of K_z and D in extremum point i).

Extremum point ii)

In Figures 10.8(a) and 10.8(b) we see that the entire diagram for $\partial^2\mathcal{V}_4/\partial\delta^2$ and $\partial^2\mathcal{V}_4/\partial\Phi^2$ are positive. For $\mathcal{V}_4$ in Figure 10.8(c) the entire diagram is negative. We can thus conclude that this extremum point is a minimum, and that the interaction potential is repulsive. Thus, there can exist a condensate with $\delta = 0$ and $\Phi = \pi$.

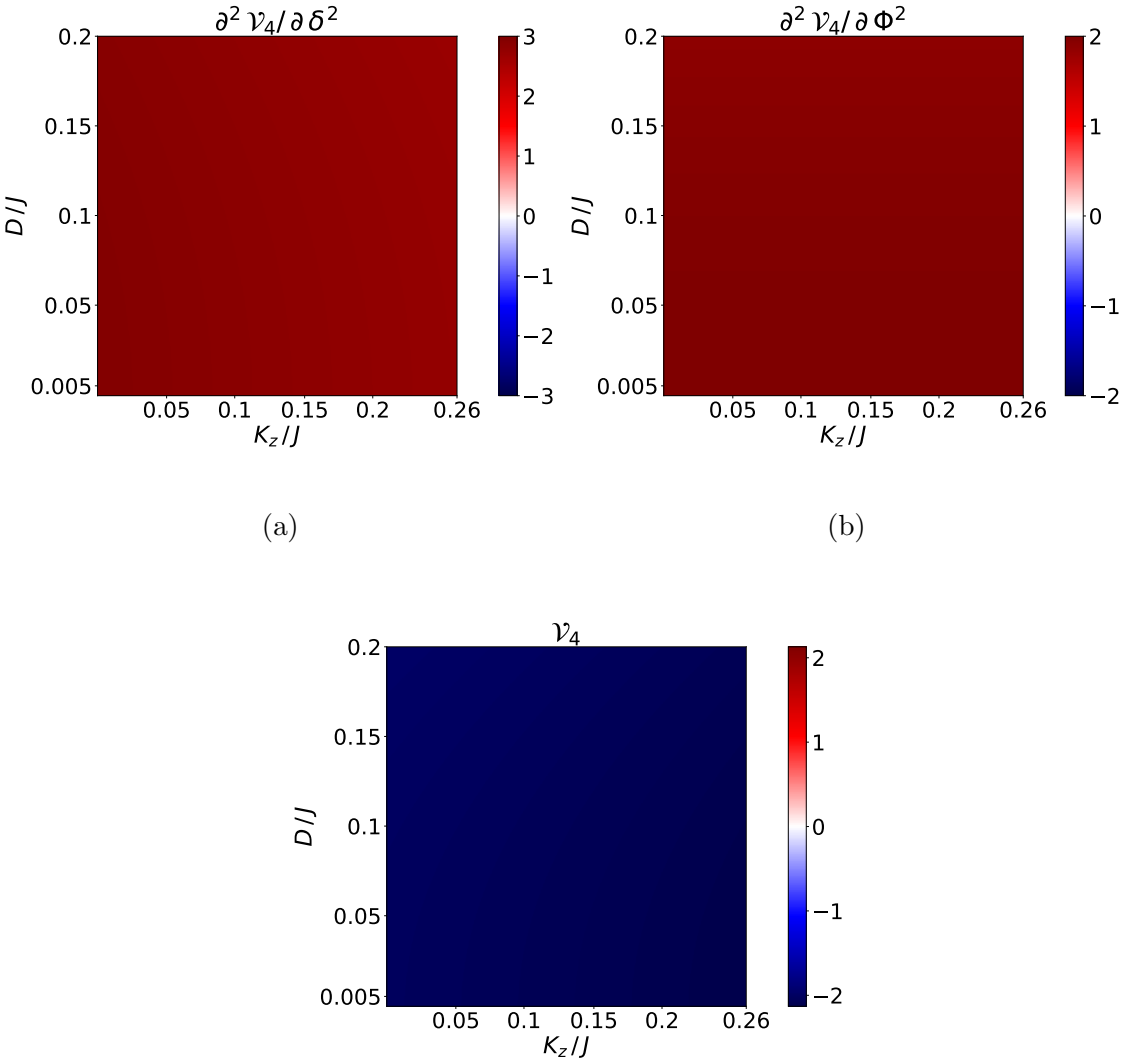

(a)

(b)

(c)

Figure 10.8: (a) and (b) The signs of the second derivatives of $\mathcal{V}_4$, as functions of K_z and D, in extremum point ii) from Eq. (10.31). (c) $\mathcal{V}_4$ as a function of K_z and D in extremum point ii).

Extremum point iii)

We show the value of $\partial^2\mathcal{V}_4/\partial\delta^2$ and $\partial^2\mathcal{V}_4/\partial\Phi^2$ in Figure 10.9(a) and 10.9(b). Similarly to extremum point i), we have no overlapping regions where both second derivatives are positive. From Figure 10.9(c) we see that almost the whole of the plot for $\mathcal{V}_4$ is positive, except for a small region in the upper right corner. This shows that we cannot have a condensate with these values for δ and Φ.

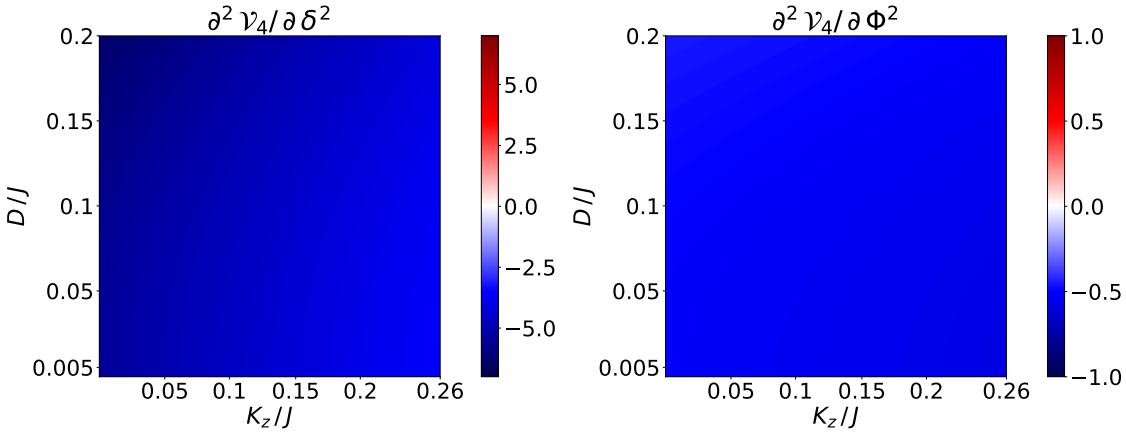

(a) (b)

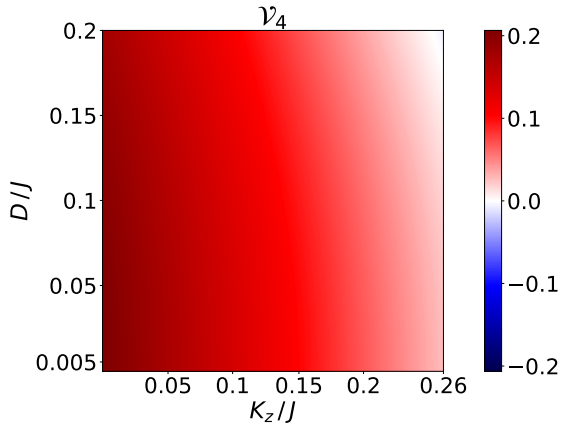

(c)

Figure 10.9: (a) and (b) The second derivatives of $\mathcal{V}_4$, $\partial^2\mathcal{V}_4/\partial\delta^2$ and $\partial^2\mathcal{V}_4/\partial\Phi^2$ shown as functions of K_z and D, in extremum point iii) where δ and Φ are as in Eq. (10.31). (c) $\mathcal{V}_4$ as a function of K_z and D in extremum point iii).

Extremum point iv)

Figures 10.10(a) and 10.10(b), respectively, show $\partial^2\mathcal{V}_4/\partial\delta^2$ and $\partial^2\mathcal{V}_4/\partial\Phi^2$ as functions of K_z and D. The red colour shows the regions where the second derivatives are positive. We see that the whole plot of both second derivatives are positive. Looking at $\mathcal{V}_4$ in Figure 10.10(c), we see that the entire plot is negative. We therefore conclude that for these values of δ and Φ a condensate can form.

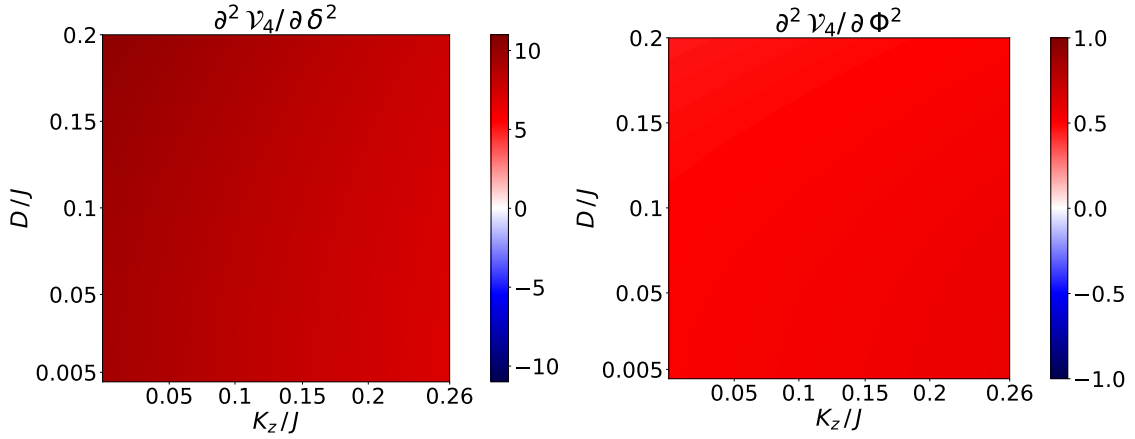

(a)

(b)

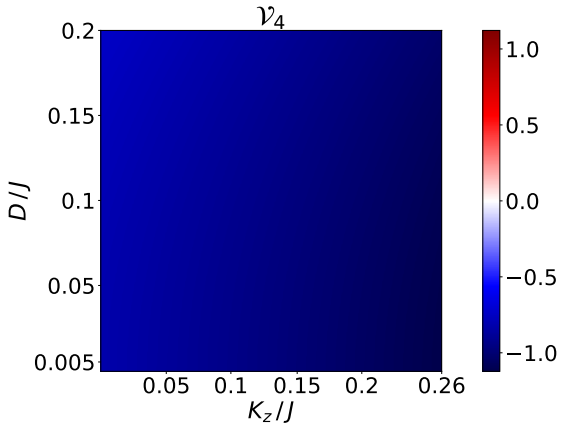

(c)

Figure 10.10: (a) and (b) $\partial^2\mathcal{V}_4/\partial\delta^2$ and $\partial^2\mathcal{V}_4/\partial\Phi^2$ as functions of K_z and D, in extremum point iv) where δ and Φ are as in Eq. (10.31). (c) $\mathcal{V}_4$ as a function of K_z and D in extremum point iv)

Chapter 11

Discussion

As stated previously, a necessary criterion for BECs to exist, is that the effective interactions between the constituents are repulsive. We observe from the phase diagrams in section 10.5 that this criterion can be met.

11.1 Degenerate condensates

As we saw in section 10.5, there are more than one combination of δ and Φ that allow a condensate of magnons. This implies that degenerate condensates can coexist with the same system parameters. At higher temperatures, we can assume that the combination of δ and Φ with the lowest energy will be occupied. However, at low temperatures the magnons might not be able to escape local minima, and condensates can be degenerate.

As mentioned, we include DMI as it is present in the system we decided to investigate [50]. As we saw in Figure 10.6, the strength of the DMI determines the k values at which the condensates form. If the condensates form at finite k, it is easier to observe them and thus the experiments are easier to conduct. [51].

In Figure 11.1 we observe that the value of $\mathcal{V}_4$ is dominated by $\mathcal{V}_{4,\text{intra}}$ at extremum point i) and iii), while in extremum point ii) and iv) the value of $\mathcal{V}_4$ is dominated by $\mathcal{V}_{4,\text{inter}}$. In Appendix B we have included plots similar to those in Figure B.1, for a specific non-zero value of the DM-strength. We observe that in extremum points ii) and iv), $\mathcal{V}_4$ is still dominated by $\mathcal{V}_{4,\text{inter}}$.

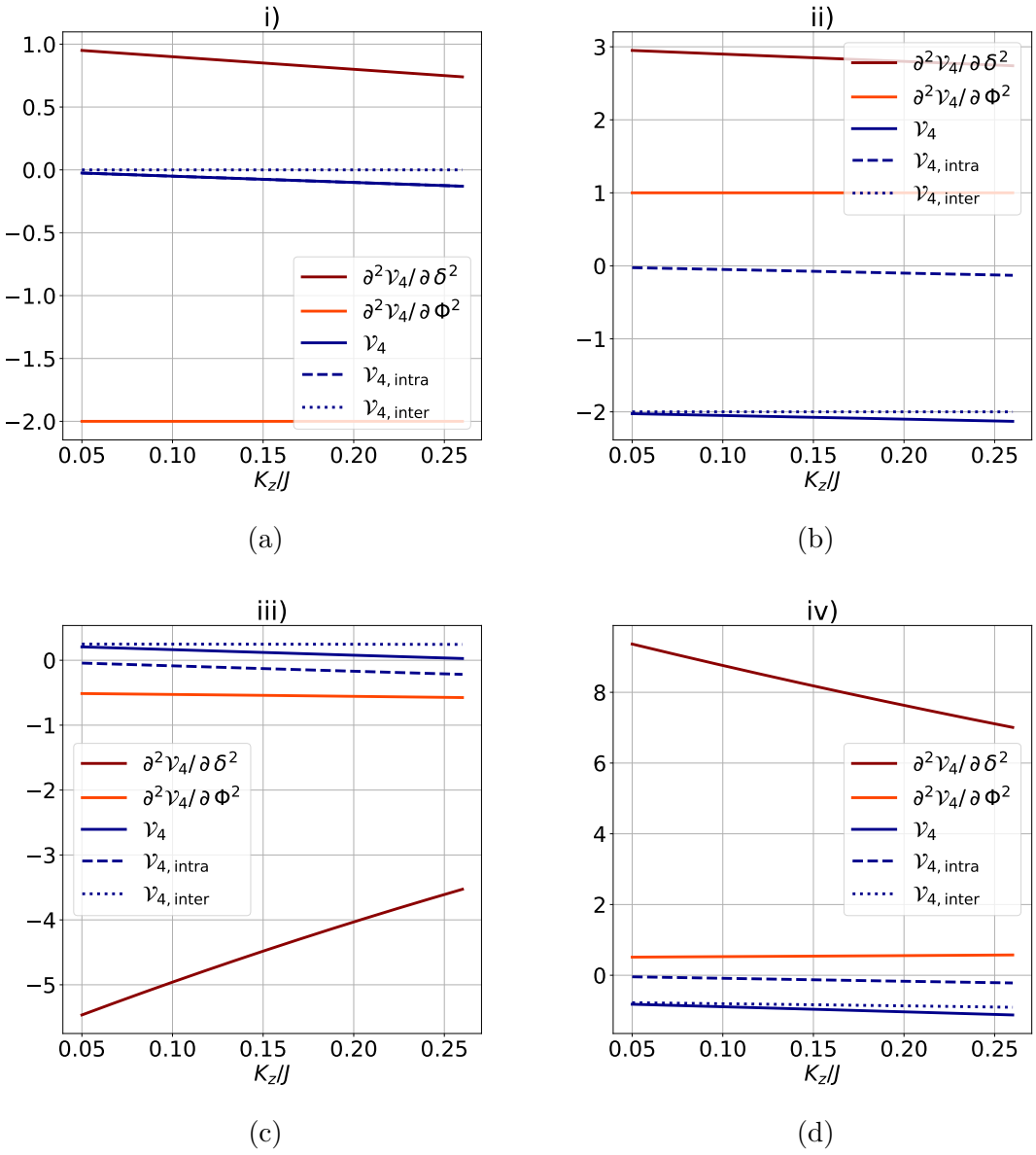

(a) (b)

(c) (d)

Figure 11.1: The value of $\mathcal{V}_4$ and its second derivatives, $\partial^2\mathcal{V}_4/\partial\delta^2$ and $\partial^2\mathcal{V}_4/\partial\Phi^2$ when DMI is turned off are shown in (a) for extremum point i), (b) for extremum point ii), (c) for extremum point iii) and (d) for extremum point iv). We also included $\mathcal{V}_{4,\text{intra}}$ and $\mathcal{V}_{4,\text{inter}}$ in the figures.

We see that even without DMI, extremum point ii) and iv) can accommodate a BEC of magnons in an AFMI.

11.2 Intravalley and intervalley scattering

In Figure 11.2 we show how the coefficients A, B, C and D vary as functions of K_z and D. The coefficients are defined in Eq. (10.24) and stem from Eq. (10.23). We can interpret them as the amplitude of the different scatterings. Coefficient C can be interpreted as amplitude of intervalley scattering. Coefficient A, B and D can be interpreted as the amplitude of various forms of intervalley scattering.

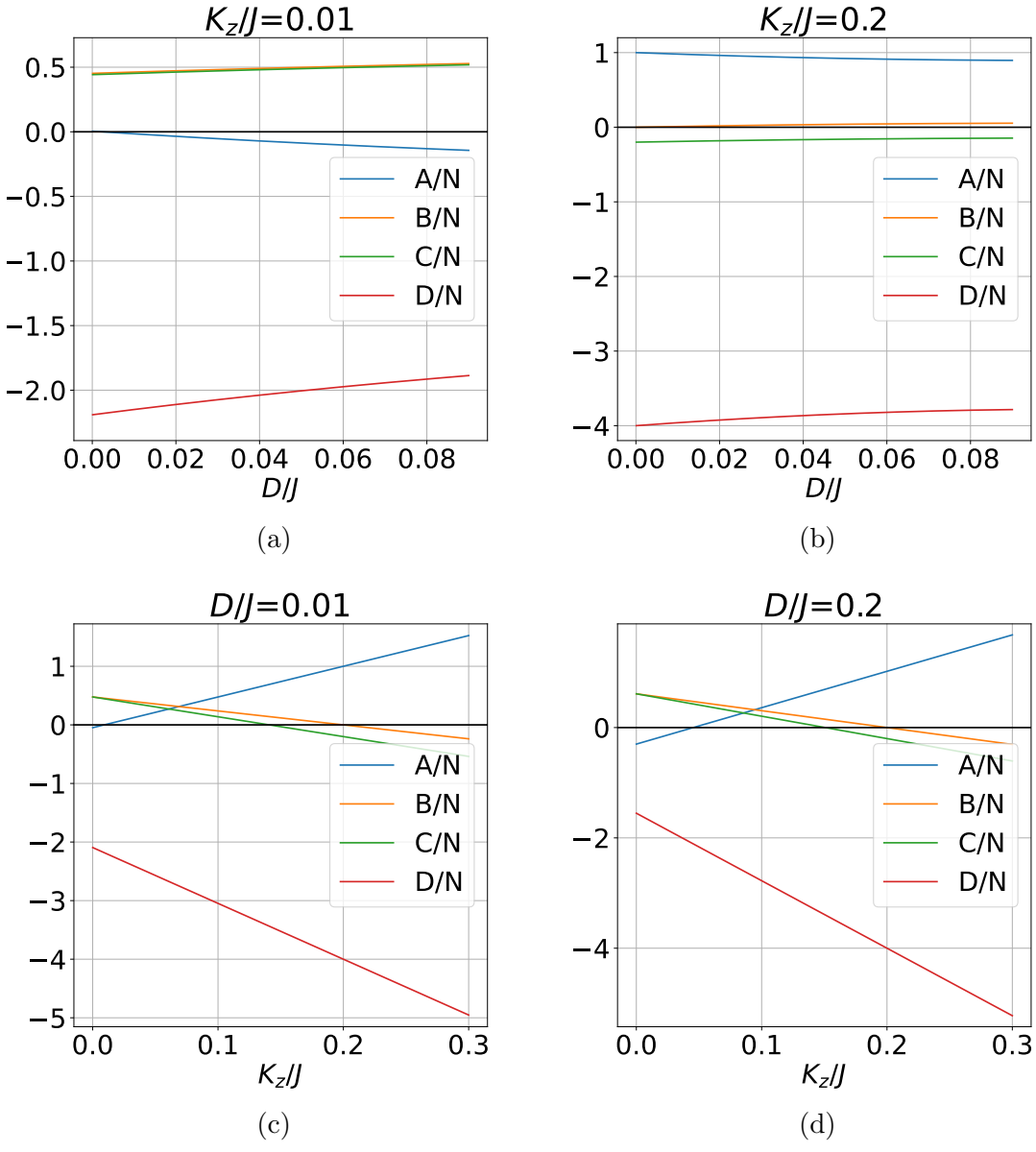

Figure 11.2: The plots illustrate $A/N, B/N, C/N$ and D/N vary as functions of (a) K_z/J for a small DM-strength, $D/J = 0.01$. (b) K_z/J for a large DM-strength, $D/J = 0.2$. (c) D/J for a small anisotropy-strength, $K_z/J = 0.01$. (d) D/J for a large anisotropy-strength, $K_z/J = 0.2$.

We observe in Figures 11.2(a) and 11.2(b) that increasing the anisotropy strength, changes the sign of coefficient C. This means that the sign of the amplitude of intravalley scattering is changed.

As far as the authors are aware, only one previous study has carrioud out a similar analysis, Arakawa in ref. [60]. In this paper, Arakawa studies $MnFe_2$, where DMI is negligible. As previously discussed, the DMI makes experiments easier to conduct. Arakawa employs the Hartree-Fock method for mean-field. We believe the Madelung transformation is a more suitable choice of mean-field theory. The Hartree-Fock method outputs an effective non-interacting Hamiltonian for the particles, however because of the nature of BEC, we question whether this holds for these calculations.

During the calculations in ref. [60], they also disregard the contribution from the anisotropy. However, as we can see in Figure 11.2, the sign of C changes as a function of the anisotropy strength. Recall that C is the amplitude of intravalley scattering. Thus, we believe that it is important to include the anisotropy.

In our calculations we also included all types of scattering, A, B, C and D. As we see in Figure 11.1, the intervalley scattering is dominant for extremum point ii) and iv), which are the two combinations of δ and Φ that we found suitable for condensation. Thus, we also question the omission of the intervalley scattering in ref. [60].

Chapter 12

Conclusion

We have presented an analysis of the stability of BEC in AFMIs, where anisotropy and DMI was included in addition to the direct exchange interaction and external magnetic field. The external magnetic field was out of plane, parallel to the quantisation axis. DMI was uniform, in order to obtain the desired dispersion relation. The magnetic anisotropy was easy-axis and on-site.

After performing various transformations to obtain the interaction potential between the magnons, we found its extremum points. The potential as a function of the difference in magnon population in the valleys, and the total phase of the condensates, was presented in section 10.5. There we observed that two of the extremum points were minima. By pumping in magnons to obtain a finite chemical potential, we have found necessary and sufficient conditions for a theoretical prediction of magnon condensation in AMFIs.

We found that there were two types of scattering in the condensates, intravalley and intervalley. In the two extremum points that gives rise to condensation, the contribution from intervalley scattering dominated.

We found two minima for the interaction potential, thus predicting degenerate condensates. From the phase diagrams in section 10.5, we see that extremum point ii) has lower value for the potential. Thus we can conclude that for systems with appropriate temperatures, extremum point ii) will dominate the degenerate state.

Chapter 13

Outlook

In our system, we vary the magnetic anisotropy-strength K_z and the DM-strength D. However, experimentally it is easier to vary the strength of the external magnetic field. It would be interesting to investigate a system with external magnetic field in the plane, as opposed to ours, which is out of plane. We expect the in-plane magnetic field to appear in the interaction Hamiltonian, and thus be present in the interaction potential $\mathcal{V}_4$.

An intriguing modification of our system would be to instead use an easy-plane magnetic anisotropy. Thus, having both easy-axis and hard-axis anisotropy [61].

In our bosonisation procedure, we utilised the Holstein-Primakoff transformation. The advantages of this choice of bosonisation is that the transformation is Hermitian. Thus, the Hamiltonian is also Hermitian. However, this transformation includes an approximation, and is therefore not exact. In contrast, the Dyson-Maleev transformation is exact. Although this bosonisation is exact, it is, however, not consistently Hermitian [62, 63, 64]. Calculations have shown that the non-interacting Hamiltonian is the same for the Dyson-Maleev and Holstein-Primakoff regime. The interaction Hamiltonian, however, is not. It would be interesting to see if the conclusions differ for the two procedures.

As mentioned, our antiferromagnetic system is collinear. However, by using a triangular lattice, the system could be non-collinear. Alternatively, we also obtain the non-collinearity by assuming a strong DMI. We assumed the DMI to be not too strong, in order to preserve the assumed ordering of the spins.

Appendix

A Derivation of $\mathcal{V}_4$*

A more detailed calculations that obtained the extra term in eq. (5.8) is presented here. Writing out the Hamiltonian again, just for convenience

$$\begin{aligned} H_Q = & A\big[\alpha^\dagger_{\boldsymbol{Q}}\alpha^\dagger_{\boldsymbol{Q}}\alpha_{\boldsymbol{Q}}\alpha_{\boldsymbol{Q}} + \alpha^\dagger_{-\boldsymbol{Q}}\alpha^\dagger_{-\boldsymbol{Q}}\alpha_{-\boldsymbol{Q}}\alpha_{-\boldsymbol{Q}}\big] \\ & + 2B\,\alpha^\dagger_{\boldsymbol{Q}}\alpha^\dagger_{-\boldsymbol{Q}}\alpha_{\boldsymbol{Q}}\alpha_{-\boldsymbol{Q}} \\ & + C\big[\alpha^\dagger_{\boldsymbol{Q}}\alpha_{\boldsymbol{Q}}\alpha_{\boldsymbol{Q}}\alpha_{-\boldsymbol{Q}} + \alpha^\dagger_{-\boldsymbol{Q}}\alpha_{-\boldsymbol{Q}}\alpha_{-\boldsymbol{Q}}\alpha_{\boldsymbol{Q}} + \text{h.c.}\big] \\ & + D\big[\alpha_{-\boldsymbol{Q}}\alpha_{\boldsymbol{Q}}\alpha_{\boldsymbol{Q}}\alpha_{-\boldsymbol{Q}} + \text{h.c.}\big]. \end{aligned} \tag{A.1}$$

We now insert $\langle\alpha_{\pm\boldsymbol{Q}}\rangle = \sqrt{N_{\pm\boldsymbol{Q}}}\exp(i\phi_\pm)$ into eq. (A.1). This results in

$$\begin{aligned} \mathcal{V}_4 = & A\big[\sqrt{N_{+\boldsymbol{Q}}}\exp(-i\phi_+)\sqrt{N_{+\boldsymbol{Q}}}\exp(-i\phi_+)\sqrt{N_{+\boldsymbol{Q}}}\exp(i\phi_+)\sqrt{N_{+\boldsymbol{Q}}}\exp(i\phi_+) + \\ & \quad \sqrt{N_{-\boldsymbol{Q}}}\exp(-i\phi_-)\sqrt{N_{-\boldsymbol{Q}}}\exp(-i\phi_-)\sqrt{N_{-\boldsymbol{Q}}}\exp(i\phi_-)\sqrt{N_{-\boldsymbol{Q}}}\exp(i\phi_-)\big] \\ & + 2B\,\sqrt{N_{+\boldsymbol{Q}}}\exp(-i\phi_+)\sqrt{N_{-\boldsymbol{Q}}}\exp(-i\phi_-)\sqrt{N_{+\boldsymbol{Q}}}\exp(i\phi_+)\sqrt{N_{-\boldsymbol{Q}}}\exp(i\phi_-) \\ & + C\big[\sqrt{N_{+\boldsymbol{Q}}}\exp(-i\phi_+)\sqrt{N_{+\boldsymbol{Q}}}\exp(i\phi_+)\sqrt{N_{+\boldsymbol{Q}}}\exp(i\phi_+)\sqrt{N_{-\boldsymbol{Q}}}\exp(i\phi_-) + \\ & \quad \sqrt{N_{-\boldsymbol{Q}}}\exp(-i\phi_-)\sqrt{N_{-\boldsymbol{Q}}}\exp(i\phi_-)\sqrt{N_{-\boldsymbol{Q}}}\exp(i\phi_-)\sqrt{N_{+\boldsymbol{Q}}}\exp(i\phi_+) + \text{h.c.}\big] \\ & + D\big[\sqrt{N_{-\boldsymbol{Q}}}\exp(i\phi_-)\sqrt{N_{+\boldsymbol{Q}}}\exp(i\phi_+)\sqrt{N_{+\boldsymbol{Q}}}\exp(i\phi_+)\sqrt{N_{-\boldsymbol{Q}}}\exp(i\phi_-) + \text{h.c.}\big]. \end{aligned} \tag{A.2}$$

Collecting terms gives us

$$\begin{aligned} \mathcal{V}_4 = & A\big[N^2_{+\boldsymbol{Q}}\exp(-2i\phi_+ + 2i\phi_+) + N^2_{-\boldsymbol{Q}}\exp(-2i\phi_- + 2i\phi_-)\big] \\ & + 2B\,N_{+\boldsymbol{Q}}N_{-\boldsymbol{Q}}\exp(-i\phi_+ + i\phi_+)\exp(-i\phi_- + i\phi_-) \\ & + C\big[\sqrt{N_{+\boldsymbol{Q}}}^3\sqrt{N_{-\boldsymbol{Q}}}\exp(-i\phi_+ + i\phi_+)\exp(i\phi_+ + i\phi_-) + \\ & \quad \sqrt{N_{-\boldsymbol{Q}}}^3\sqrt{N_{+\boldsymbol{Q}}}\exp(-i\phi_- + i\phi_-)\exp(i\phi_- + i\phi_+) + \text{h.c.}\big] \\ & + D\big[N_{-\boldsymbol{Q}}\sqrt{N_{+\boldsymbol{Q}}}\exp(2i\phi_-)\exp(2i\phi_+) + \text{h.c.}\big]. \end{aligned} \tag{A.3}$$

Writing the Hermitian conjugates explicitly in the last three lines and combining terms results in

$$\begin{aligned} \mathcal{V}_4 = & A\big[N^2_{+\boldsymbol{Q}} + N^2_{-\boldsymbol{Q}}\big] \\ & + 2B\,N_{+\boldsymbol{Q}}N_{-\boldsymbol{Q}} \\ & + C\big[\sqrt{N_{+\boldsymbol{Q}}}^3\sqrt{N_{-\boldsymbol{Q}}}2\cos(\Phi) + \sqrt{N_{-\boldsymbol{Q}}}^3\sqrt{N_{+\boldsymbol{Q}}}2\cos(\Phi)\big] \\ & + D\big[N_{-\boldsymbol{Q}}N_{+\boldsymbol{Q}}2\cos(2\Phi)\big]. \end{aligned} \tag{A.4}$$

We now choose to represent $N_{+\boldsymbol{Q}}, N_{-\boldsymbol{Q}}, \phi_+$ and ϕ_- in terms of N_c, δ and Φ. Since $N_{+\boldsymbol{Q}} = \frac{N_c+\delta}{2}, N_{-\boldsymbol{Q}} = \frac{N_c-\delta}{2}$, this means that $N_{+\boldsymbol{Q}}^2 + N_{-\boldsymbol{Q}}^2 = [N_c^2 + \delta^2]/2$, $N_{+\boldsymbol{Q}} N_{-\boldsymbol{Q}} = [N_c^2 - \delta^2]/4$, $\sqrt{N_{+\boldsymbol{Q}}}\sqrt{N_{-\boldsymbol{Q}}}(N_{+\boldsymbol{Q}} + N_{-\boldsymbol{Q}}) = [N_c\sqrt{N_c^2 - \delta^2}]/2$.

Inserting this into eq. (A.4), we obtain

$$\begin{aligned}
\mathcal{V}_4 =& A\frac{1}{2}\big[N_c^2 + \delta^2\big] + 2B\,\frac{1}{4}\big[N_c^2 - \delta^2\big] + \\
& C\frac{1}{2}\big[N_c\sqrt{N_c^2 - \delta^2}\big]2\cos(\Phi) + D\frac{1}{4}\big[N_c^2 - \delta^2\big]2\cos(2\Phi) \\
=& A\frac{1}{2}N_c^2\big[1 + (\delta/N_c)^2\big] + B\,\frac{1}{2}N_c^2\big[1 - (\delta/N_c)^2\big] + \\
& C\frac{1}{2}N_c^2\sqrt{1 - (\delta/N_c)^2}2\cos(\Phi) + D\frac{1}{2}N_c^2\big[1 - (\delta/N_c^2)^2\big]\cos(2\Phi). \qquad \text{(A.5)}
\end{aligned}$$

Moving terms around, we see that eq. (A.5) is eq. (5.10). In comparison with [23], we see that we have an extra term, namely $D\cos 2\Phi$.

B Additional Figures

In this Appendix, we place additional figures referenced in section 11.

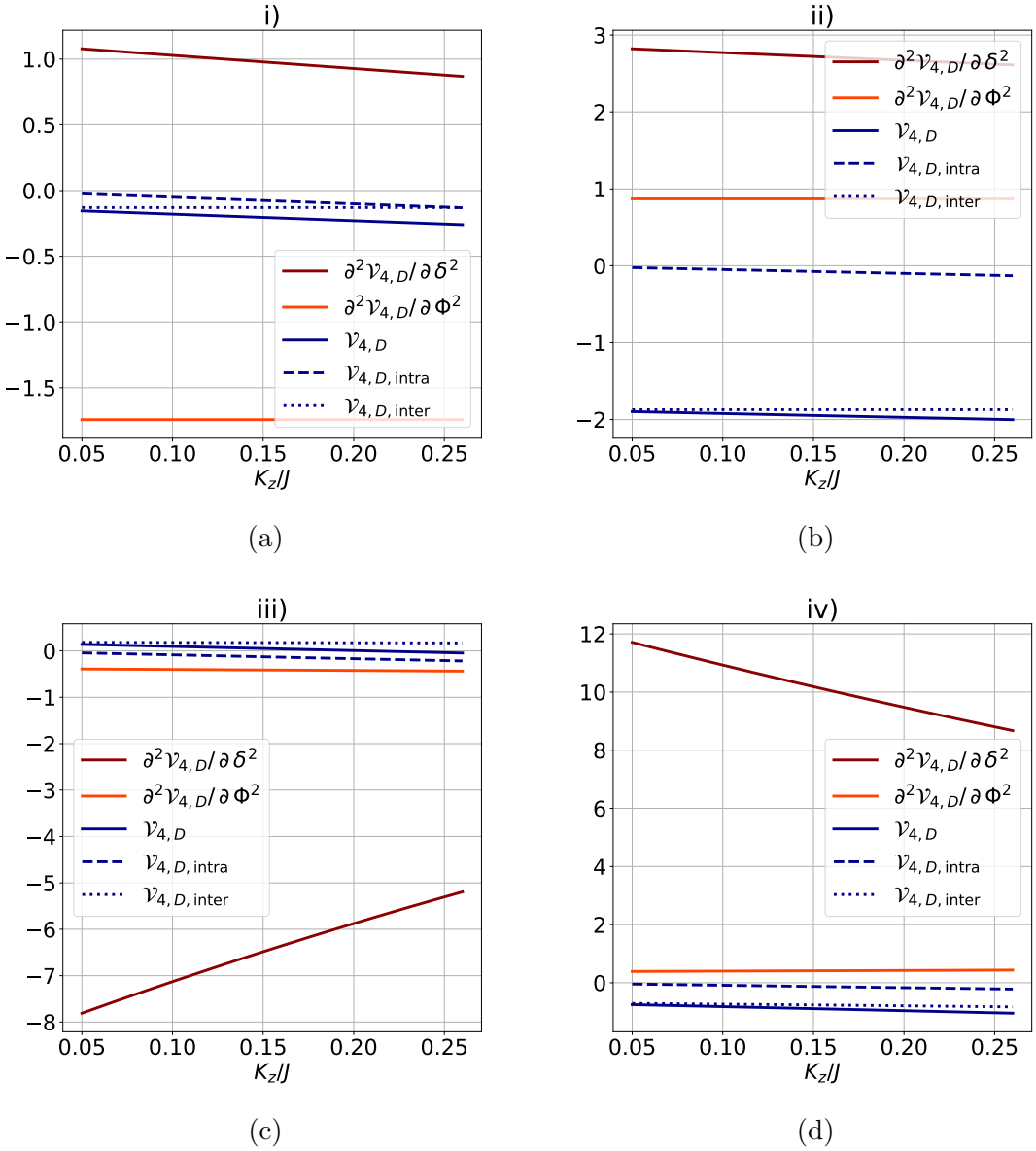

(a) (b)

(c) (d)

Figure B.1: The value of $\mathcal{V}_4$ and its second derivatives, $\partial^2\mathcal{V}_4/\partial\delta^2$ and $\partial^2\mathcal{V}_4/\partial\Phi^2$ when DMI is turned on for a specific value are shown in (a) for extremum point i), (b) for extremum point ii), (c) for extremum point iii) and (d) for extremum point iv). We also included $\mathcal{V}_{4,\text{intra}}$ and $\mathcal{V}_{4,\text{inter}}$ in the figures.

Bibliography

[1] D. J. Griffiths and Darrell F. Schroeter. *Introduction to quantum mechanics*. 3. Cambridge university press, 2018. ISBN: 978-1-107-18963-8.

[2] K. Huang. *Statistical Mechanics*. 2. New York: Wiley, 1987.

[3] W. Ketterle. 'Nobel lecture: When atoms behave as waves: Bose-Einstein condensation and the atom laser'. In: *Reviews of Modern Physics* 74.4 (2002), pp. 1131–1151. ISSN: 0034-6861. DOI: 10.1103/revmodphys.74.1131.

[4] V. Zapf, M. Jaime and C. D Batista. 'Bose-Einstein condensation in quantum magnets'. In: *Reviews of Modern Physics* 86.2 (2014), pp. 563–614. ISSN: 0034-6861. DOI: 10.1103/revmodphys.86.563.

[5] P. Gorroochurn. 'The End of Statistical Independence: The Story of Bose–Einstein Statistics'. In: *The Mathematical Intelligencer* 40.3 (2018), pp. 12–17. ISSN: 0343-6993. DOI: 10.1007/s00283-017-9772-4.

[6] A. Einstein. 'Quantentheorie des einatomigen idealen Gases. 2. Abhandlung'. In: *Sitzungsberichte der Preussischen Akademie der Wissenschaften* (1925), pp. 3–14.

[7] M.H. Anderson, J.R. Ensher, M.R. Matthews and E.A. Cornell. 'Observation of Bose-Einstein Condensation in a Dilute Atomic Vapor'. In: *Science* 269 (1995), pp. 198–201. DOI: 10.1126/science.269.5221.198.

[8] E. A. Cornell and C. E. Wieman. 'Nobel Lecture: Bose-Einstein condensation in a dilute gas, the first 70 years and some recent experiments'. In: *Reviews of Modern Physics* 74.3 (2002), pp. 875–893. ISSN: 0034-6861. DOI: 10.1103/revmodphys.74.875.

[9] K. B. Davis, M. O. Mewes, M. R. Andrews, N. J. Van Druten, D. S. Durfee, D. M. Kurn and W. Ketterle. 'Bose-Einstein Condensation in a Gas of Sodium Atoms'. In: *Physical Review Letters* 75.22 (1995), pp. 3969–3973. ISSN: 0031-9007. DOI: 10.1103/physrevlett.75.3969.

[10] F. Bloch. 'Zur Theorie des Ferromagnetismus'. In: *Zeitschrift für Physik* 61.3-4 (1930), pp. 206–219. ISSN: 1434-6001. DOI: 10.1007/bf01339661.

[11] V. L. Safonov. *Nonequilibrium Magnons: Theory, Experiment, and Applications*. 2013.

[12] R. Skomski. 'Magnetic Exchange Interactions'. In: *Handbook of Magnetism and Magnetic Materials*. Ed. by M. Coey and S. S. P. Parkin. Springer, 2021. DOI: https://doi.org/10.1007/978-3-030-63101-7.

[13] S. M. Girvin and K. Yang. *Modern Condensed Matter Physics*. Cambridge university press, 2019. ISBN: 978-1-107-13739-4.

[14] J. Klaers, J. Schmitt, F. Vewinger and M. Weitz. 'Bose–Einstein condensation of photons in an optical microcavity'. In: *Nature* 468.7323 (2010), pp. 545–548. ISSN: 0028-0836. DOI: 10.1038/nature09567.

[15] L. V. Butov, A. L. Ivanov, A. Imamoglu, P. B. Littlewood, A. A. Shashkin, V. T. Dolgopolov, K. L. Campman and A. C. Gossard. 'Stimulated Scattering of Indirect Excitons in Coupled Quantum Wells: Signature of a Degenerate Bose-Gas of Excitons'. In: *Physical Review Letters* 86.24 (2001), pp. 5608–5611. ISSN: 0031-9007. DOI: 10.1103/physrevlett.86.5608.

[16] Ko. Yoshioka, E. Chae and M. Kuwata-Gonokami. 'Transition to a Bose–Einstein condensate and relaxation explosion of excitons at sub-Kelvin temperatures'. In: *Nature Communications* 2.1 (2011), p. 328. ISSN: 2041-1723. DOI: 10.1038/ncomms1335. URL: https://dx.doi.org/10.1038/ncomms1335.

[17] J. Kasprzak, M. Richard, S. Kundermann, A. Baas, P. Jeambrun, J. M. J. Keeling, F. M. Marchetti, M. H. Szymańska, R. André, J. L. Staehli, V. Savona, P. B. Littlewood, B. Deveaud and Le Si Dang. 'Bose–Einstein condensation of exciton polaritons'. In: *Nature* 443.7110 (2006), pp. 409–414. ISSN: 0028-0836. DOI: 10.1038/nature05131. URL: https://dx.doi.org/10.1038/nature05131.

[18] S. O. Demokritov, V. E. Demidov, O. Dzyapko, G. A. Melkov, A. A. Serga, B. Hillebrands and A. N. Slavin. 'Bose–Einstein condensation of quasi-equilibrium magnons at room temperature under pumping'. In: *Nature* 443.7110 (2006), pp. 430–433. ISSN: 0028-0836. DOI: 10.1038/nature05117.

[19] C. Sun, T. Nattermann and V. L. Pokrovsky. 'Bose–Einstein condensation and superfluidity of magnons in yttrium iron garnet films'. In: *Journal of Physics D: Applied Physics* (2017). DOI: 10.1088/1361-6463/aa5.

[20] SN Andrianov and SA Moiseev. 'Magnon qubit and quantum computing on magnon Bose-Einstein condensates'. In: *Physical Review A* 90.4 (2014), p. 042303.

[21] J. Kasprzak, M. Richard, S. Kundermann, A. Baas, P. Jeambrun, J. M. J. Keeling, F. M. Marchetti, M. H. Szymańska, R. André, J. L. Staehli, V. Savona, P. B. Littlewood, B. Deveaud and Le Si Dang. 'Bose–Einstein condensation of exciton polaritons'. In: *Nature* 443.7110 (2006), pp. 409–414. ISSN: 0028-0836. DOI: 10.1038/nature05131. URL: https://dx.doi.org/10.1038/nature05131.

[22] L. D. Landau and E. M. Lifshitz. *Statistical Physics*. Vol. 5. Course of Theoretical Physics. Pergamon Press, 1969.

[23] H. Salman, N. G. Berloff and S. O. Demokritov. 'Microscopic Theory of Bose-Einstein Condensation of Magnons at Room Temperature'. In: *Universal Themes of Bose-Einstein Condensation*. Ed. by David W. Snoke, Nick P. Proukakis and Peter B. Littlewood. Cambridge University Press, 2017, pp. 493–504. ISBN: 9781316084366.

[24] P. C. Hemmer. *Kvantemekanikk*. Tapir Akademisk Forlag, 2005. ISBN: 9788251920285.

[25] M. F. Reid. 'Theory of Rare-Earth Electronic Structure and Spectroscopy'. In: *Handbook on the Physics and Chemistry of Rare Earths*. Ed. by J.-C. G. Bünzli and V. K. Pecharsky. Vol. 50. Elsevier, 2016. ISBN: 0168-1273. DOI: https://doi.org/10.1016/bs.hpcre.2016.09.001.

[26] R. Sharpe, J. Munarriz, T. Lim, Y. Jiao, J. W. Niemantsverdriet, V. Polo and J. Gracia. 'Orbital Physics of Perovskites for the Oxygen Evolution Reaction'. In: *Topics in Catalysis* 61.3 (2018), pp. 267–275. ISSN: 1572-9028. DOI: 10.1007/s11244-018-0895-4.

[27] R. Skomski. *Simple models of magnetism*. Oxford university press, 2008. ISBN: 9780198570752.

[28] A. Bonanni, T. Dietl and H. Ohno. 'Dilute Magnetic Materials'. In: *Handbook of Magnetism and Magnetic Materials*. Ed. by J. M. D. Coey and S. S. P. Parkin. Springer, 2021.

[29] J. M. D. Coey. 'History of Magnetism and Basic Concepts'. In: *Handbook of Magnetism and Magnetic Materials*. Ed. by J. M. D. Coey and S. S. P. Parkin. Springer, 2021.

[30] J. Hick, F. Salui, A. Kreisel and P. Kopietz. 'Bose-Einstein condensation at finite momentum and magnon condensation in thin film ferromagnets'. In: *The European physical journal B* (2010). DOI: http://dx.doi.org/10.1140/epjb/e2010-10596-7.

[31] A. Kreisel, F. Sauli, L. Bartosch and P. Kopietz. 'Microscopic spin-wave theory for yttrium-iron garnet films'. In: *The European physical journal B* (2009). DOI: http://dx.doi.org/10.1140/epjb/e2009-00279-y.

[32] M. G. Cottam. *Linear And Nonlinear Spin Waves In Magnetic Films And Superlattices*. Singapore: World Scientific, 1994. ISBN: 9789810210069 9789814343121.

[33] M. Shiranzaei, R. E. Troncoso, J. Fransson, A. Brataas and A. Qaiumzadeh. 'Thermal squeezing and nonlinear spectral shift of magnons in antiferromagnetic insulators'. In: *New Journal of Physics* 24.10 (2022), p. 103009. ISSN: 1367-2630. DOI: 10.1088/1367-2630/ac94f0. URL: https://dx.doi.org/10.1088/1367-2630/ac94f0.

[34] M. E. Fisher and D. R. Nelson. 'Spin Flop, Supersolids, and Bicritical and Tetracritical Points'. In: *Physical Review Letters* 32.24 (1974), pp. 1350–1353. DOI: 10.1103/PhysRevLett.32.1350. URL: https://link.aps.org/doi/10.1103/PhysRevLett.32.1350.

[35] S. M. Rezende, A. Azevedo and R. L. Rodríguez-Suárez. 'Introduction to antiferromagnetic magnons'. In: *Journal of Applied Physics* 126.15 (2019), p. 151101. ISSN: 0021-8979. DOI: 10.1063/1.5109132. URL: https://doi.org/10.1063/1.5109132.

[36] T. Moriya. 'Anisotropic Superexchange Interaction and Weak Ferromagnetism'. In: *Physical Review* 120.1 (1960), pp. 91–98. ISSN: 0031-899X. DOI: 10.1103/physrev.120.91.

[37] T. Moriya. 'New Mechanism of Anisotropic Superexchange Interaction'. In: *Physical Review Letters* 4.5 (1960), pp. 228–230. ISSN: 0031-9007. DOI: 10.1103/physrevlett.4.228.

[38] A. Fert, V. Cros and J. Sampaio. 'Skyrmions on the track'. In: *Nature Nanotechnology* 8.3 (2013), pp. 152–156. ISSN: 1748-3387. DOI: 10.1038/nnano.2013.29.

[39] F. Li. 'On the magnon Bose Einstein condensation in ferromagnetic film'. Thesis. 2014. URL: https://hdl.handle.net/1969.1/153964.

[40] Y. Yamamoto. *Chapter 4 Bogoliubov theory of the weakly interacting Bose gas*. Web Page. URL: https://www.nii.ac.jp/qis/first-quantum/e/forStudents/lecture/pdf/qis385/QIS385_chap4.pdf.

[41] N. Bogoliubov. 'On the theory of superfluidity'. In: *Journal of Physics* 11 (1947), pp. 23–32.

[42] I. V. Borisenko, B. Divinskiy, V. E. Demidov, G. Li, T. Nattermann, V. L. Pokrovsky and S. O. Demokritov. 'Direct evidence of spatial stability of Bose-Einstein condensate of magnons'. In: *Nature communications* 11.1 (2020), pp. 1–7. ISSN: 2041-1723.

[43] P. Nowik-Boltyk, O. Dzyapko, V. E. Demidov, N. G. Berloff and S. O. Demokritov. 'Spatially non-uniform ground state and quantized vortices in a two-component Bose-Einstein condensate of magnons'. In: *Scientific Reports* 2.1 (2012). ISSN: 2045-2322. DOI: 10.1038/srep00482.

[44] A. A. Serga, C. W. Sandweg, V. I. Vasyuchka, M. B. Jungfleisch, B. Hillebrands, A. Kreisel, P. Kopietz and M. P. Kostylev. 'Brillouin light scattering spectroscopy of parametrically excited dipole-exchange magnons'. In: *Physical Review B* 86.13 (2012). ISSN: 1098-0121. DOI: 10.1103/physrevb.86.134403.

[45] T. Frostad, H. L. Skarsvåg, A. Qaiumzadeh and A. Brataas. 'Spin-transfer-assisted parametric pumping of magnons in yttrium iron garnet'. In: *Physical Review B* 106.2 (2022), p. 024423. DOI: 10.1103/PhysRevB.106.024423.

[46] J. L. Van Hemmen. 'A note on the diagonalization of quadratic boson and fermion hamiltonians'. In: *Zeitschrift für Physik B Condensed Matter* 38.3 (1980), pp. 271–277. ISSN: 0722-3277. DOI: 10.1007/bf01315667.

[47] Ronald L. Lipsman and Jonathan M. Rosenberg. *Multivariable Calculus with MATLAB: With Applications to Geometry and Physics*. Cham: Cham: Springer International Publishing AG, 2017. ISBN: 9783319650692 3319650696.

[48] K. Nakata, K. A. Van Hoogdalem, P. Simon and D. Loss. 'Josephson and persistent spin currents in Bose-Einstein condensates of magnons'. In: *Physical Review B* 90.14 (2014). ISSN: 1098-0121. DOI: 10.1103/physrevb.90.144419.

[49] G. Gitgeatpong, Y. Zhao, P. Piyawongwatthana, Y. Qiu, L. W Harriger, N. P Butch, T. J Sato and K. Matan. 'Nonreciprocal Magnons and Symmetry-Breaking in the Noncentrosymmetric Antiferromagnet'. In: *Physical Review Letters* 119.4 (2017). ISSN: 0031-9007. DOI: 10.1103/physrevlett.119.047201. URL: https://dx.doi.org/10.1103/physrevlett.119.047201.

[50] M. Kawano, Y. Onose and C. Hotta. 'Designing Rashba–Dresselhaus effect in magnetic insulators'. In: *Communications Physics* 2.1 (2019). ISSN: 2399-3650. DOI: 10.1038/s42005-019-0128-6. URL: https://dx.doi.org/10.1038/s42005-019-0128-6.

[51] S. O. Demokritov. 'Comment on "Bose–Einstein Condensation and Spin Superfluidity of Magnons in a Perpendicularly Magnetized Yttrium Iron Garnet Film" (JETP Letters 112, 299 (2020))'. In: *JETP Letters* 115.11 (2022), pp. 691–693. ISSN: 1090-6487. DOI: 10.1134/S0021364022600719. URL: https://doi.org/10.1134/S0021364022600719.

[52] G. Gitgeatpong, Y. Zhao, P. Piyawongwatthana, Y. Qiu, L. W. Harriger, N. P. Butch, T. J. Sato and K. Matan. 'Nonreciprocal Magnons and Symmetry-Breaking in the Noncentrosymmetric Antiferromagnet [Supplemental Material]'. In: *Physical Review Letters* 119.4 (2017). ISSN: 0031-9007. DOI: 10.1103/physrevlett.119.047201. URL: https://dx.doi.org/10.1103/physrevlett.119.047201.

[53] M. D. Schwartz. *Quantum Field Theory and the Standard Model*. Cambridge: Cambridge University Press, 2013. ISBN: 9781107034730. DOI: DOI:10.1017/9781139540940. URL: https://www.cambridge.org/core/books/quantum-field-theory-and-the-standard-model/A4CD66B998F2C696DCC75B984A7D5799.

[54] N. D. Mermin and H. Wagner. 'Absence of Ferromagnetism or Antiferromagnetism in One- or Two-Dimensional Isotropic Heisenberg Models'. In: *Physical Review Letters* 17.22 (1966), pp. 1133–1136. DOI: 10.1103/PhysRevLett.17.1133. URL: https://link.aps.org/doi/10.1103/PhysRevLett.17.1133.

[55] M. Powalski, K. P. Schmidt and G. Uhrig. 'Mutually attracting spin waves in the square-lattice quantum antiferromagnet'. In: *SciPost Physics* 4.1 (2018). ISSN: 2542-4653. DOI: 10.21468/scipostphys.4.1.001. URL: https://dx.doi.org/10.21468/scipostphys.4.1.001.

[56] J. Goldstone, A. Salam and S. Weinberg. 'Broken Symmetries'. In: *Physical Review* 127.3 (1962), pp. 965–970. DOI: 10.1103/PhysRev.127.965. URL: https://link.aps.org/doi/10.1103/PhysRev.127.965.

[57] M. H. A. Kalthoff. 'Nonequilibrium materials engineering in correlated systems via light-matter coupling'. Thesis. 2022. URL: https://hdl.handle.net/21.11116/0000-000A-DD0D-0.

[58] R. Khoshlahni, A. Qaiumzadeh, A. Bergman and A. Brataas. 'Ultrafast generation and dynamics of isolated skyrmions in antiferromagnetic insulators'. In: *Physical Review B* 99.5 (2019), p. 054423. DOI: 10.1103/PhysRevB.99.054423. URL: https://link.aps.org/doi/10.1103/PhysRevB.99.054423.

[59] C Kittel. *Introduction to solid state physics*. 2004.

[60] N. Arakawa. 'Controlling stability of Bose-Einstein condensation of interacting magnons in an antiferromagnet by an external magnetic field'. In: *Physical Review B* 99.1 (2019). ISSN: 2469-9950. DOI: 10.1103/physrevb.99.014405. URL: https://dx.doi.org/10.1103/physrevb.99.014405.

[61] V. Brehm, O. Gomonay, S. Lepadatu, M. Kläui, J. Sinova, A. Brataas and A. Qaiumzadeh. 'Micromagnetic study of spin transport in easy-plane antiferromagnetic insulators'. In: *Physical Review B* 107.18 (2023), p. 184404. DOI: 10.1103/PhysRevB.107.184404. URL: https://link.aps.org/doi/10.1103/PhysRevB.107.184404.

[62] A. Klein and E. R. Marshalek. 'Boson realizations of Lie algebras with applications to nuclear physics'. In: *Reviews of Modern Physics* 63.2 (1991), pp. 375–558. DOI: 10.1103/RevModPhys.63.375. URL: https://link.aps.org/doi/10.1103/RevModPhys.63.375.

[63] F. J. Dyson. 'General Theory of Spin-Wave Interactions'. In: *Physical Review* 102.5 (1956), pp. 1217–1230. DOI: 10.1103/PhysRev.102.1217. URL: https://link.aps.org/doi/10.1103/PhysRev.102.1217.

[64] SV Maleev. 'Scattering of slow neutrons in ferromagnets'. In: *Sov. Phys. JETP* 6.4 (1958), p. 776.

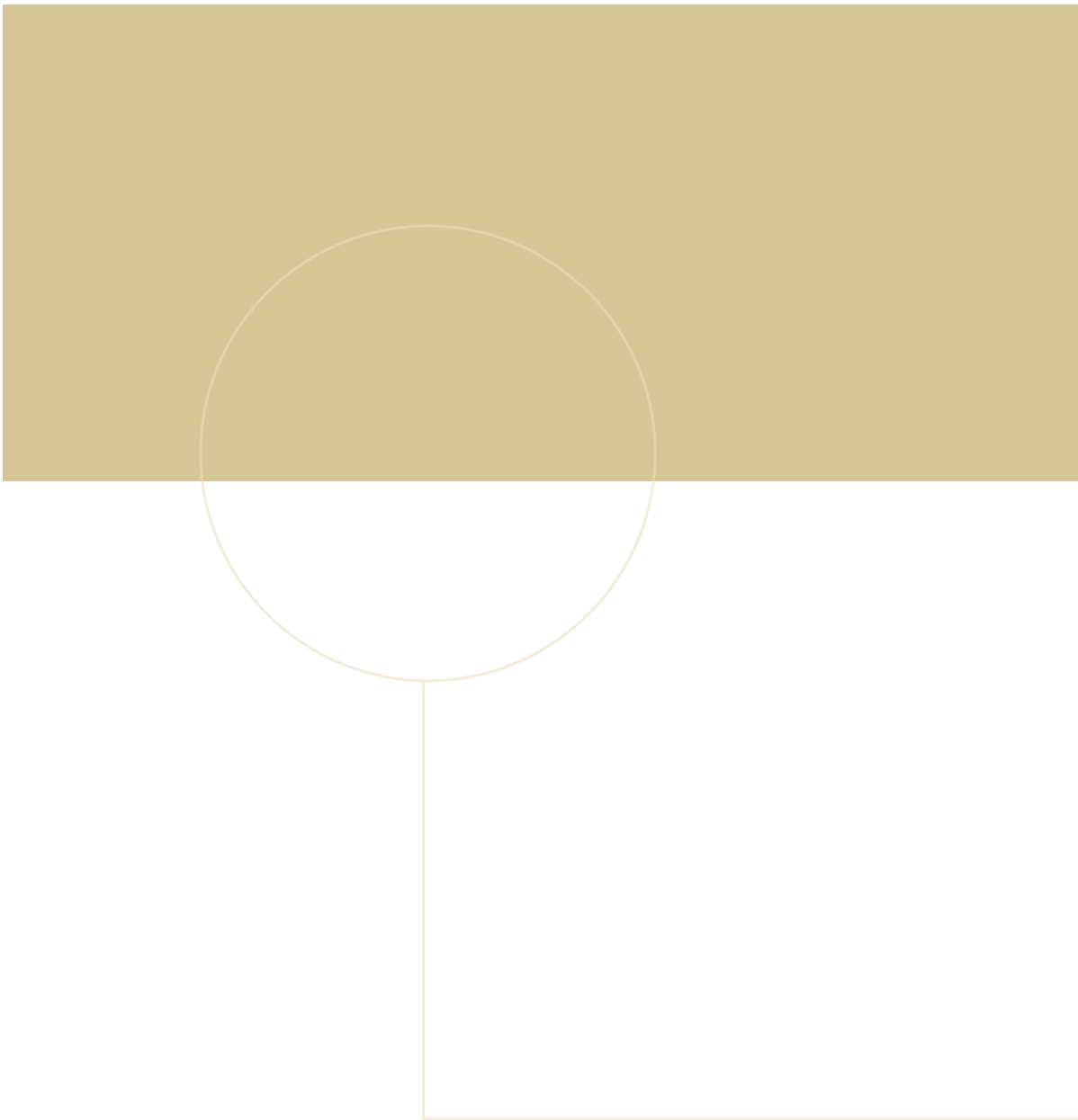

NTNU
Norwegian University of
Science and Technology

QuSpin